

DISS. ETH NO. 24031

**Development of a strategy for structural determination of α_2C and β_3
adrenergic receptors**

A thesis submitted to attain the degree of

Doctor of Science at ETH ZÜRICH

(Dr. Sc. ETH Zürich)

Presented by

ŽIVA VUČKOVIČ MÜLLER

Univ. Dipl. Biochem., University of Ljubljana, Faculty of Chemistry and Chemical
Technology, Slovenia

Born on 30. 07. 1987

Citizen of Republic of Slovenia

Accepted on the recommendation of:

Prof. Gebhard Schertler, examiner

Dr. Dmitry Veprintsev, scientific supervisor

Prof. Gerhard Wider, co-examiner

Dr. Roger Dawson, co-examiner

2017

CONTENTS

| | |
|---|------|
| ACKNOWLEDGEMENTS | v |
| ABBREVIATIONS | vi |
| SUMMARY | viii |
| RÉSUMÉ | x |
| PUBLICATIONS..... | xii |
| 1. INTRODUCTION | 1 |
| 1. 1. G-protein coupled receptors (GPCRs) | 1 |
| 1. 2. Adrenergic receptors (ARs) | 3 |
| 1. 3. Crystallisation of membrane proteins and GPCRs..... | 6 |
| 1. 3. 1. Expression systems for GPCRs..... | 7 |
| 1. 3. 2. Modifications of GPCRs | 8 |
| 1. 3. 3. Use of ligands for the crystallisation..... | 9 |
| 1. 3. 4. Use of detergents and new methods for crystallisation..... | 10 |
| 1. 4. The aim of the thesis | 11 |
| 2. MATERIALS AND METHODS..... | 12 |
| 2. 1. Protein constructs..... | 12 |
| 2. 2. Transient transfection of mammalian cells | 12 |
| 2. 3. Cell harvesting | 12 |
| 2. 4. Crude protein extract analysis..... | 13 |
| 2. 5. In gel thermostability assay of crude extracts..... | 13 |
| 2. 6. Preparation of stable cell lines and clonal selection..... | 13 |
| 2. 7. Expression of protein in shaker flasks | 14 |
| 2. 8. CPM assay of purified proteins..... | 15 |
| 2. 9. 1D4 resin preparation and regeneration | 16 |
| 2. 9. 1. 1D4 resin preparation..... | 16 |
| 2. 9. 2. 1D4 resin regeneration | 16 |
| 2. 10. Preparation of cell membranes..... | 16 |
| 2. 11. Protein purification | 17 |
| 2. 11. 1. Initial protein purification | 17 |
| 2. 11. 2. Further improvements to the purification protocol | 19 |
| 2. 12. Adjusting parameters for the purification | 19 |
| 2. 12. 1. Optimisation of solubilisation conditions | 19 |
| 2. 12. 2. Determination of the right amount of washing and elution buffer of the resin..... | 20 |

| | |
|--|----|
| 2. 12. 3. Determination of the right amount of the 3C protease for protein cleavage | 20 |
| 2. 12. 4. Deglycosylation tests | 20 |
| 2. 12. 5. Dephosphorylation tests | 20 |
| 2. 12. 6. Determination of the stability of a purified protein in detergent using FSEC | 20 |
| 2. 13. Crystallisation | 21 |
| 2. 13. 1. Vapour diffusion set up | 21 |
| 2. 13. 2. Lipidic cubic phase set up | 21 |
| 2. 14. SAXS and WAXS experiments | 21 |
| 3. RESULTS | 24 |
| 3. 1. Constructs design | 24 |
| 3. 1. 1. Design of $\alpha 2C$ and $\beta 3$ AR constructs with transferred mutations | 25 |
| 3. 2. Constructs test | 26 |
| 3. 2. 1. Expression tests | 26 |
| 3. 2. 2. In gel thermostability assays with crude protein samples | 29 |
| 3. 3. Stable cell line production and selection, protein production | 30 |
| 3. 4. Testing the temperature stabilisation by ligands | 34 |
| 3. 4. 1. Optimisation of the CPM assay | 34 |
| 3. 4. 2. Ligand-induced stabilisation of $\alpha 2C$ -T4L AR | 36 |
| 3. 4. 3. Ligand-induced stabilisation of $\beta 3$ -T4L AR | 38 |
| 3. 4. 4. Comparison of stability between the non-mutated and mutated human $\beta 3$ -T4L AR | 40 |
| 3. 5. Protein purification | 42 |
| 3. 5. 1. Adjusting the parameters for the purification | 42 |
| 3. 6. Purification of $\beta 3$ -T4L AR | 46 |
| 3. 6. 1. Detergent tests for crystallisation trials of $\beta 3$ -T4L AR | 46 |
| 3. 6. 2. Stability of $\beta 3$ -T4L AR in different detergents | 47 |
| 3. 7. Purification of m $\beta 3$ -T4L AR | 49 |
| 3. 7. 1. Optimisation of the purification protocol | 51 |
| 3. 8. Purification of $\alpha 2C$ -T4L AR | 57 |
| 3. 9. Crystallisation tests | 59 |
| 3. 10. SAXS and WAXS experiments | 63 |
| 4. DISCUSSION | 65 |
| 4. 1. Choice of the construct | 65 |
| 4. 1. 1. In plate screening of cells | 65 |
| 4. 1. 2. In gel fluorescence assays | 65 |
| 4. 1. 3. FSEC tests of receptor constructs in solubilised crude samples | 66 |
| 4. 1. 4. In gel thermostability assays | 66 |

| | |
|--|----|
| 4. 2. Clonal selection and protein expression..... | 67 |
| 4. 3. Temperature stabilisation of crystallisation constructs by ligands..... | 68 |
| 4. 3. 1. Optimisation of the method..... | 68 |
| 4. 3. 2. Stabilisation of α 2C-T4L and β 3-T4L AR by ligands | 69 |
| 4. 3. 3. Comparison between the non-mutated and mutated human β 3-T4L AR..... | 69 |
| 4. 4. Protein purification | 70 |
| 4. 4. 1. Optimisation of the purification protocol..... | 70 |
| 4. 4. 2. Purification of β 3-T4L and m β 3-T4L AR..... | 72 |
| 4. 4. 3. Purification of α 2C-T4L AR..... | 73 |
| 4. 5. Crystallisation of α 2C-T4L, β 3-T4L and m β 3-T4L ARs..... | 74 |
| 4. 6. SAXS/WAXS experiments | 74 |
| 5. CONCLUSIONS AND OUTLOOK..... | 75 |
| APPENDIX..... | 78 |
| REFERENCES | 85 |

ACKNOWLEDGEMENTS

No one can be a lonely island and I was lucky enough that I had a lot of people around myself that I was always able to ask for an advice and that have greatly contributed to this project. I would like to take this opportunity to officially thank them.

To my supervisors: prof. Gebhard Schertler and Dr. Dmitry Veprintsev. You gave me the opportunity to work on this project even though I had no previous lab experience with crystallography. I appreciated that I was always able to get an advice when needed and that you showed me the right path when I felt lost.

To my committee members: prof. Gerhard Wider and Dr. Roger Dawson. I appreciate the time you took from your busy schedules to come to PSI and discuss my project. I was also always able to contact you in case I got stuck and I really appreciate that you were always prepared to help.

To the members of my group. To Dalibor, who sat with me at the initial beamtimes and who showed me how to practically work on a crystallography project. I will always appreciate all the time you invested in me. Daniel and Tamara deserve a special mentioning as well. Without you, I would not be able to produce the results I did. I knew that I have an amazing support in you two. Thank you!

To Robert. Thank you for sharing your knowledge with me. I appreciated discussions we had and I hope I will be able to transfer everything I learnt into my future projects.

To the ones that were there to discuss science as well as general life issues: Kathrin, Ching-Ju, Jonas, Pikyee, Elena, Thomas, Niranjana, Wenting, Sandra and Dragana. Special thanks go to Miloš and Xavi who were always prepared to discuss difficult data. I appreciated the time you spent with me explaining things to me and trying to come to conclusions.

To Francine, Ulla, Antonietta, Jose, Laura and May for providing the most amazing support one can wish for.

Lastly, there are some people without whom all this would definitely not be possible. Thanks to my family for supporting me financially and morally through all these years of studying. I will always be grateful for your support. Special thanks to my husband who went with me through this during the last 4 years. You know the best how much work it was put into this and I was lucky to have such an amazing person by my side who understood all cancelled holidays when the beamtimes came in between and was waiting for me with cooked dinner when I arrived home late at night. Thanks also to my husband's family for supporting us during these last years.

ABBREVIATIONS

| | |
|-----------------------------|---|
| A80426 | <i>N</i> -Methyl- <i>N</i> -[[<i>(1R)</i> -1,2,3,4-tetrahydro-5-methoxy-1-naphthalenyl]methyl]-6-benzofuranethanamine mesylate |
| AA | amino acid |
| alprenolol | 1-[(1-Methylethyl)amino]-3-[2-(2-propenyl)phenoxy]-2-propanol hydrochloride |
| apo protein | protein without ligand |
| AR | adrenergic receptor |
| AUC | analytical ultracentrifugation |
| b ₅₆₂ RIL (BRIL) | apocytochrome b ₅₆₂ RIL |
| carvedilol | 1-(9 <i>H</i> -Carbazol-4-yloxy)-3-[[2-(2-methoxyphenoxy)ethyl]amino]-2-propanol |
| CGP 12177 | 4-[3-[(1,1-Dimethylethyl)amino]2-hydroxypropoxy]-1,3-dihydro-2 <i>H</i> -benzimidazol-2-one hydrochloride |
| CGP 20712 | 1-[2-((3-Carbamoyl-4-hydroxy)phenoxy)ethylamino]-3-[4-(1-methyl-4-trifluoromethyl-2-imidazolyl)phenoxy]-2-propanol dihydrochloride |
| CHAPSO | 3-[(3-Cholamidopropyl]dimethylammonio)-2-hydroxy-1-propanesulfonate |
| CHS | cholesterol hemisuccinate |
| CIP | calf intestinal phosphatase |
| CL 316243 | 5-[(2 <i>R</i>)-2-[[<i>(2R)</i> -2-(3-Chlorophenyl)-2-hydroxyethyl]amino]propyl]-1,3-benzodioxole-2,2-dicarboxylic acid disodium salt |
| CMC | critical micelle concentration |
| CPM | <i>N</i> -[4-(7-diethylamino-4-methyl-3-coumarinyl) phenyl]maleimide |
| CV | column volume |
| cyanopindolol | 4-[3- <i>tert</i> -Butylamino]-2-hydroxypropoxy]-1 <i>H</i> -indole-2-carbonitrile hemifumarate |
| Da | dalton |
| DDM | <i>n</i> -dodecyl β- <i>D</i> -maltopyranoside |
| DM | <i>n</i> -decyl-β- <i>D</i> -maltopyranoside |
| DMEM | Dulbecco's Modified Eagle Medium |
| DMPC | 1,2-dimyristoyl- <i>sn</i> -glycero-3-phosphocholine |
| EDTA | ethylenediamine tetra-acetic acid |
| efaroxan | 2-(2-Ethyl-2,3-dihydro-2-benzofuranyl)-4,5-dihydro-1 <i>H</i> -imidazole hydrochloride |
| FBS | Foetal bovine serum |
| formoterol | (±)-(<i>R,R</i>)- <i>N</i> -[2-Hydroxy-5-[1-hydroxy-2-[[2-(4-methoxyphenyl)-1-methylethyl]amino]ethyl]phenyl] formamide hemifumarate |
| FSEC | fluorescence-detection size exclusion chromatography |
| GFP | green fluorescent protein |
| GF SEC | gel filtration size exclusion chromatography |
| GPCR | G-protein coupled receptor |
| Hega-10 | <i>n</i> -decanoyl- <i>N</i> -hydroxyethylglucamide |
| HEK 293 GnTi- cells | Human embryonic kidney cells deficient in <i>N</i> -acetylglucosaminyltransferase I activity |
| HEPES | <i>N</i> -(2-hydroxyethyl)-piperazine- <i>N'</i> -2-ethanesulfonic acid |
| ICI 215,001 | (<i>S</i>)-4-[2-Hydroxy-3-phenoxypropylaminoethoxy]phenoxyacetic acid hydrochloride |
| imiloxan | 2-(1-Ethyl-2-indazolyl)methyl-1,4-benzodioxan hydrochloride |
| isoproterenol | 4-[1-Hydroxy-2-[(1-methylethyl)amino]ethyl]-1,2-benzenediol hydrochloride |
| JP 1302 | <i>N</i> -[4-(4-Methyl-1-piperazinyl)phenyl]-9-acridinamine dihydrochloride |

| | |
|--------------------------|--|
| LCP | lipidic cubic phase |
| LMNG | Lauryl Maltose Neopentyl Glycol |
| L 755507 | 4-[[[(Hexylamino)carbonyl]amino]- <i>N</i> -[4-[2-[[[(2 <i>S</i>)-2-hydroxy-3-(4-hydroxyphenoxy)propyl]amino]ethyl]phenyl]-benzenesulfonamide |
| MAG | monoacylglycerol |
| M | marker |
| min | minute |
| nitrobiphenylene oxalate | (<i>R</i>)-2-[1-(3'-Nitrobiphenyl-2-yloxy)ethyl]-4,5-dihydro-1 <i>H</i> -imidazole oxalate |
| O/N | over night |
| PBS | phosphate-buffered saline |
| PDB | protein data bank |
| PEG | polyethylene glycol |
| PEI | polyethylenimine |
| PEM | protein expression medium |
| PTMs | post-translational modifications |
| PS | penicillin streptomycin |
| PSF | penicillin streptomycin fungizone |
| rauwolscine | 17 α -Hydroxy-20 α -yohimban-16 β -carboxylic acid,methyl ester hydrochloride |
| RFU | relative fluorescence unit |
| roxindole | 3-[4-(3,6-Dihydro-4-phenyl-1(2 <i>H</i>)-pyridinyl)butyl]-1 <i>H</i> -indol-5-ol hydrochloride |
| RS79948 | (8 <i>aR</i> ,12 <i>aS</i> ,13 <i>aS</i>)-5,8,8 <i>a</i> ,9,10,11,12,12 <i>a</i> ,13,13 <i>a</i> -dehydro-3-methoxy-12-(ethylsulfonyl)-6 <i>H</i> -isoquino[2,1- <i>g</i>][1,6]naphthyridine hydrochloride |
| RT | room temperature |
| S32212 | 1,2-Dihydro- <i>N</i> -[4-methoxy-3-(4-methyl-1-piperazinyl)phenyl]-3 <i>H</i> -benz[e]indole-3-carboxamide hydrochloride |
| salbutamol | α^1 -[[[(1,1-Dimethylethyl)amino]methyl]-4-hydroxy-1,3-benzenedimethanol hemisulfate |
| salmeterol | 4-Hydroxy- α 1-[[[6-(4-phenylbutoxy)hexyl]amino]methyl]-1,3-benzenedimethanol 1-hydroxy-2-naphthalenecarboxylic acid salt |
| SKF86466 | 6-Chloro- <i>N</i> -methyl-2,3,4,5-tetrahydro-1- <i>H</i> -3-benzazepine hydrochloride |
| spiroxatrine | 8-[(2,3-Dihydro-1,4-benzodioxin-2-yl)methyl]-1-phenyl-1,3,8-triazaspiro[4,5]decan-4-one |
| S-propranolol | (<i>S</i>)-(-)-1-[(1-methylethyl)amino]-3-(1-naphthalenyloxy)-2-propanol hydrochloride |
| SR 58611A | [[[(7 <i>S</i>)-7-[[[(2 <i>R</i>)-2-(3-chlorophenyl)-2-hydroxyethyl]amino]-5,6,7,8-tetrahydro-2-naphthalenyl]ox]yacetic acid ethyl ester hydrochloride |
| SR 59230A | 1-(2-Ethylphenoxy)-3-[[[(1 <i>S</i>)-1,2,3,4-tetrahydro-1-naphthalenyl]amino]-2(<i>S</i>)-2-propanol hydrochloride |
| ST91 | <i>N</i> -(2,6-Diethylphenyl)-4,5-dihydro-1 <i>H</i> -imidazol-2-amine hydrochloride |
| T _m | melting temperature |
| TM | transmembrane |
| Trp | tryptophan |
| VD | vapour diffusion |
| ZD 2079 | 4-[2-[[[(2 <i>R</i>)-2-Hydroxy-2-phenylethyl]amino]ethoxy]-benzeneacetic acid hydrochloride |
| W | wash |
| WB 4101 | 2-(2,6-Dimethoxyphenoxyethyl)aminomethyl-1,4-benzodioxane hydrochloride |
| 3CP | human rhinovirus 3C protease |

SUMMARY

G-protein coupled receptors (GPCRs) play an important role in physiological processes by transmitting the signal from the extracellular side into the cell. They are targeted by 30-50% of all available drugs on the market [1, 2]. However, many of these drugs are unspecific, leading to several side effects that are affecting the quality of life of patients. Determining the structure of the receptors might give us a better understanding in how these drugs are acting on the receptors and allow the design of medicines with fewer side effects. Crystal structures of several members of GPCRs have been determined in the last few years following the first structure of β_2 adrenergic receptor in 2007 [3, 4]. Even though there has been a huge development in protein engineering that led to an increase in the number of structures solved, crystallisation is still mainly a “trial and error” process that requires several years and sufficient funds to succeed.

In this thesis I present the efforts done towards the structural determination of α_2C and β_3 adrenergic receptors. All members of adrenergic receptors have been transiently expressed and assessed for the protein expression, localisation and thermostability by using in plate cell screening of live cells, analysis of samples for GFP fluorescence and fluorescence size exclusion chromatography (FSEC). I have proven that these methods provide quick and efficient assays in order to determine the expression and monodispersity of the initial constructs. I have also shown that the thermostability of the proteins can be determined using crude extracts by connecting the heating of the protein with the remaining GFP fluorescence after loading the protein on a gel. I have shown that one round of the clonal selection of stable cell lines of HEK 293 GnTi- cells is sufficient in order to pick out the best clone. Stable cell lines expressed the protein in the range of 1-4 mg of protein/L of cell suspension. I have developed an improved receptor purification protocol that minimised the concentration step required and led to an improved sample quality, as judged by the sharp, monodisperse peak on the gel filtration elution profile.

To determine the additional thermostabilisation by ligands 30 ligands have been tested. Two most-stabilising antagonists have been found for each receptor: cyanopindolol and carvedilol for β_3 AR and rauwolsicne and RS 79948 for α_2C AR. I have shown that mutations that were transferred from turkey β_1 AR, had an effect on the additional thermostabilisation by ligands, but not on the thermostabilisation of the apo form of the protein. Vapour diffusion and lipidic cubic phase crystallisation have been set up with both receptors. Even though that several hits were observed, they were either salt crystals or they have been too small to obtain any diffraction. Additionally SAXS and WAXS data showed that upon the binding of ligands, the conformation of the β_3 -T4L adrenergic receptor changed from a state or an ensemble of states when the receptor does not have a ligand bound to active (agonist bound) or inactive (antagonist bound) form.

Despite extensive crystallisation experiments with both vapour diffusion and lipidic cubic phase techniques, I did not obtain diffracting crystals. Both receptors have been proven to be difficult crystallisation targets [http://gpcr.usc.edu/tracking_status.htm] and several more constructs would need to be tested to determine the structure. Although I did not manage to solve the structures of the chosen adrenergic receptors, I have established the pipeline that allows fast and efficient way for the choice of promising constructs and I managed to improve the purification protocol leading to sufficient amounts and purity of the protein for the crystallisation.

RÉSUMÉ

Les récepteurs couplés aux protéines G (RCPG) jouent un rôle important dans les processus physiologiques en transmettant le signal du côté extracellulaire dans la cellule. Ils sont ciblés par 30-50% de tous les médicaments disponibles sur le marché. Cependant, beaucoup de ces médicaments sont non spécifiques, conduisant à plusieurs effets secondaires qui affectent la qualité de vie des patients. La détermination de la structure des récepteurs pourrait nous permettre de mieux comprendre comment ces médicaments agissent sur les récepteurs et de prévoir la conception de médicaments avec des effets secondaires plus faibles. Les structures cristallines de plusieurs membres de RCPG ont été déterminées au cours des dernières années après la première structure du récepteur β_2 adrénergique en 2007. Bien qu'il y ait eu un énorme développement en génie des protéines qui a conduit à une augmentation du nombre de structures résolues, la cristallisation est encore essentiellement un processus d'essais et d'erreurs qui nécessite plusieurs années de recherche et des fonds suffisants pour réussir.

Dans cette thèse, je présente les efforts déployés pour déterminer la structure des récepteurs adrénergiques α_2C et β_3 . Tous les membres des récepteurs adrénergiques ont été exprimés de manière transitoire et évalués pour l'expression, la localisation et la thermostabilité de la protéine en utilisant dans le criblage de cellules sur plaque des cellules vivantes, l'analyse d'échantillons pour la fluorescence GFP et la chromatographie d'exclusion de taille de fluorescence (FSEC). J'ai montré que ces méthodes fournissent des essais rapides et efficaces pour déterminer l'expression et la monodispersité des constructions initiales. J'ai également démontré que la thermostabilité des protéines peut être déterminée à l'aide d'extraits bruts en reliant le chauffage de la protéine à la fluorescence GFP restante après chargement de la protéine sur un gel. J'ai montré qu'un tour de la sélection clonale des lignées cellulaires stables des cellules HEK 293 GnTi est suffisant pour choisir le meilleur clone. Des lignées cellulaires stables ont exprimé la protéine de l'ordre de 1 à 4 mg de protéine / L de suspension cellulaire. J'ai développé un protocole amélioré de purification des récepteurs qui minimise les étapes de concentration requises et conduit à une qualité d'échantillon améliorée, comme en témoigne le pic pointu et monodispersé sur le profil d'élution par filtration sur gel.

Pour déterminer la thermostabilisation supplémentaire par les ligands, 30 ligands ont été testés. Deux antagonistes les plus stabilisants ont été trouvés pour chaque récepteur: cyanopindolol et carvedilol pour β_3 AR et rauwolsicne et RS 79948 pour α_2C AR. Nous avons montré que les mutations ajoutées qui ont été transférées de la β_1 AR de la dinde avaient un effet sur la thermostabilisation supplémentaire par des ligands, mais pas sur la thermostabilisation de la forme apo de la protéine. La diffusion de vapeur et la cristallisation de la phase cubique lipidique ont été mises en place avec les

deux récepteurs. Même si plusieurs impacts ont été observés il s'agissait soit de cristaux de sel, soit ils étaient trop petits pour obtenir une diffraction. De plus, les données SAXS et WAXS ont montré que lors de la liaison des ligands, la conformation du récepteur adrénergique β 3-T4L changeait d'état ou d'ensemble d'états occupés lorsque le récepteur ne possédait pas de ligand lié à la forme active (agoniste lié) ou inactive (antagoniste lié).

Malgré des expériences de cristallisation poussées à l'aide de techniques de diffusion de vapeur et de phase cubique lipidique, je n'ai pas obtenu de cristaux diffractants. Les deux récepteurs se sont révélés être des cibles de cristallisation difficiles [http://gpcr.usc.edu/tracking_status.htm] et plusieurs autres constructions devraient être testées pour en déterminer la structure. Bien que je n'aie pas réussi à résoudre les structures des récepteurs adrénergiques choisis, j'ai établi le pipeline qui permet de choisir, de façon rapide et efficace, des constructions prometteuses et je suis parvenue à améliorer le protocole de purification aboutissant à des quantités suffisantes et à la pureté de la protéine pour la cristallisation.

PUBLICATIONS

Heydenreich FM*, Vuckovic Z*, Matkovic M and Veprintsev DB (2015) Stabilisation of G protein-coupled receptors by point mutations. *Front. Pharmacol.* **6**:82. doi: 10.3389/fphar.2015.00082

* These authors have contributed equally to this work.

Vuckovic Z, Kaeppler J, Mayer D and Veprintsev D (2016) Determination of ligand specificity by their stabilisation of α_2C and β_3 adrenergic receptors (in preparation)

1. INTRODUCTION

1. 1. G-protein coupled receptors (GPCRs)

G protein-coupled receptors (GPCRs) are physiologically important membrane proteins serving as critical eukaryotic signal transduction gatekeepers [1, 5, 6]. With over 800 members they represent one of the largest families of membrane proteins. They recognise a wide variety of extracellular stimuli and transmit these signals across the membrane to elicit intracellular responses through the activation of complex cytosolic signalling networks [1, 5, 6]. Upon ligand binding, GPCRs bind and activate intracellular heterotrimeric G proteins (consisting of α and $\beta\gamma$ subunits) which results in an increase of second messengers (for example Ca^{2+} and cAMP). GPCRs are also able to activate the mitogen-activated protein kinase (MAPK) pathway through a G-protein independent mechanism [7, 8]. Approximately half of the GPCRs have sensory functions, mediating olfaction, taste, light perception and pheromone signalling. The rest are targeted by ligands that range from small molecules to peptides and proteins [9]. GPCRs are, based on their sequence similarity, divided into five major families. Rhodopsin family or class A GPCRs represent the biggest family including 719 members that are targeted by a wide variety of different ligands. The majority of crystal structures solved so far belong to this family, including members of adrenergic receptors. This family is then followed by class B or secretin receptor family including 15 members, class C or glutamate family containing 22 members, adhesion family with 33 members and frizzled family with 11 members [10]. With approximately 30% (and according to some other estimations up to 50%) of all modern drugs on the market targeting GPCRs, they are also an important target in pharmacy and not only an interesting research field in the area of molecular signalling [2, 11, 12].

The structure of any GPCR can be divided into three parts: the extracellular, the transmembrane and the intracellular region. The extracellular region consists of N-terminal part of the receptor and 3 extracellular loops (ECL 1-3). There is a wide variety in the length and sequence composition of the extracellular parts with only 6% sequence identity when the comparison of primary structures is done [5, 6]. The transmembrane region consists of an anticlockwise bundle of seven α -helices (TM 1-7) when viewed from the extracellular side and represents the structural core of the receptor (figure 1.1.). This is the most conserved region in the GPCRs including all highly conserved residues. The intracellular part of the receptor is more conserved than the extracellular part with 26% sequence identity. Higher sequence identity in the intracellular part reflects the fact that the intracellular interface mediates G-protein coupling. The intracellular part consists of three intracellular loops (ICL 1-3), an intracellular amphipathic helix (H8) and C-terminus [1, 5, 6].

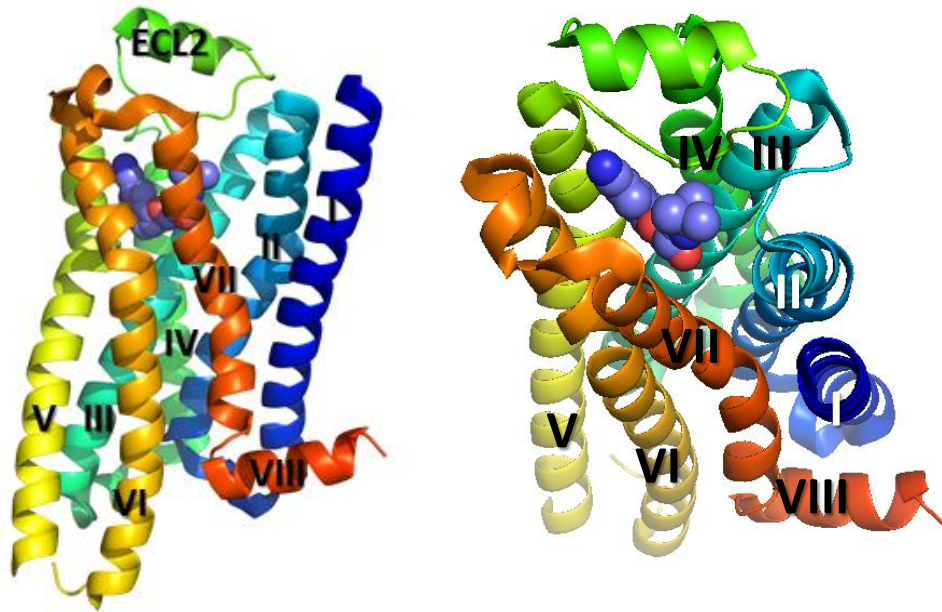


Figure 1.1.: A graphical representation of a general structure of GPCRs. The structure was modelled with PyMOL using the turkey β 1 AR structure as a template (PDB code: 4BVN). The helices are numbered using roman numbers (I-VIII), the majority of the intra- and extra-cellular part is missing, except ECL2 that is labelled. A ligand (cyanopindolol) is represented in spheres. On the right the top view of the receptor is shown, clearly showing the ligand binding in the receptor.

The extracellular part of the protein, especially the ECL2, is important in the first steps of ligand recognition and selectivity. It shapes the route for ligand entry into the binding pocket and is important for ligand-binding kinetics [13-16]. Two distinct types of extracellular region can be found: one that occludes the ligand-binding pocket and the second that leaves the ligand-binding pocket accessible. Rhodopsin, for example, belongs to the first group, where the N-terminus and ECL2 fold into a β -hairpin and form a “lid” on top of the ligand-binding pocket. Receptors belonging to this group presumably bind the hydrophobic ligands that may enter the receptor through the lipid bilayer [6, 17]. In receptors that bind water-soluble ligands, ECL2 can differ between subfamilies and can contain helices (for example in certain aminergic receptors) or sheets. An important conserved feature is a disulphide bridge between Cys^{3,25} and ECL2 that anchors the extracellular side and limits the extent of the conformational changes in this region during receptor activation [6].

The transmembrane region shows a consensus network of 24 inter-transmembrane (TM) contacts that are mediated by 36 topologically equivalent amino acids and seem to provide an evolutionary conserved structural scaffold for GPCRs [6]. Mutations of 14 of these amino acids resulted either in an increase or loss of receptor activity [17]. TM1 and TM2 do not undergo any major movement after receptor activation. Instead, they are considered to have an important role in membrane insertion,

folding and topogenesis of GPCRs [6]. TM3, on the other hand, is considered to be a structural and functional hub since the majority of the positions in this helix seem to be important for the maintenance of the structure and/or function of the protein [6]. Mutations in several positions on this helix cause either receptor inactivation or constitutive activation. The extracellular part of TM3 forms already mentioned disulphide bond with ECL2, while, in several receptors, the cytoplasmic end interacts with the ICL2 [6]. Residues in this helix also mediate extensive contacts with the ligand and participate in the formation of the “ligand-binding cradle” [6]. The receptor activation includes rearrangements in TM3, TM5, TM6 and TM7 leading to the opening of the cleft for the binding of the G-protein [6, 18, 19].

The intracellular parts, especially the ICL3 and the C-terminal tail, are long and probably intrinsically disordered in many GPCRs [20]. The C-terminal tail has key roles in receptor activation [21]. The polybasic motif proximal to H8 has been shown to facilitate G-protein pre-coupling and influences the rate of the activation of the receptor [22]. Besides that, several residues in the C-terminal tail of many receptors are extensively post-translationally modified. This might support the existence of a signalling “bar code” where diverse receptor-specific kinases phosphorylate the receptor. Different phosphorylated forms of the receptor can lead to unique signalling outputs through β -arrestins, influencing the receptor activity and internalisation from the membrane [6, 23].

1. 2. Adrenergic receptors (ARs)

Adrenergic receptors belong to the class A family of GPCRs. They are present on peripheral tissues and on neural populations within the central and sympathetic nervous system [24]. They mediate the actions of catecholamines (agonists adrenaline and noradrenaline) and are involved in a wide variety of physiological processes: blood pressure control, myocardial contractility, pulmonary function, metabolism, activities in the central nervous system and several others [24, 25]. The existence of two classes of ARs was described already in 1948 when the receptors were initially classified as α and β ARs, depending on the effect of different catecholamines. In 1967 the research suggested that there are more members than just two, so the β AR group was divided into β 1 and β 2 AR [26]. The division of α ARs into subgroups started in 1977 [27, 28]. Since then, with the development of pharmacology and the use of radioligand binding assays, three major families have been determined based on the pharmacology of AR agonists and antagonists: α 1, α 2 and β AR with three subtypes in each family: α 1A, α 1B, α 1D, α 2A, α 2B, α 2C, β 1, β 2 and β 3 AR (figure 1.2.) [29]. All, except α 2C AR, contain a palmitoylation on the C-terminus and, except α 2B AR, they all contain at least one asparagine-linked complex carbohydrate on their N-terminus [30].

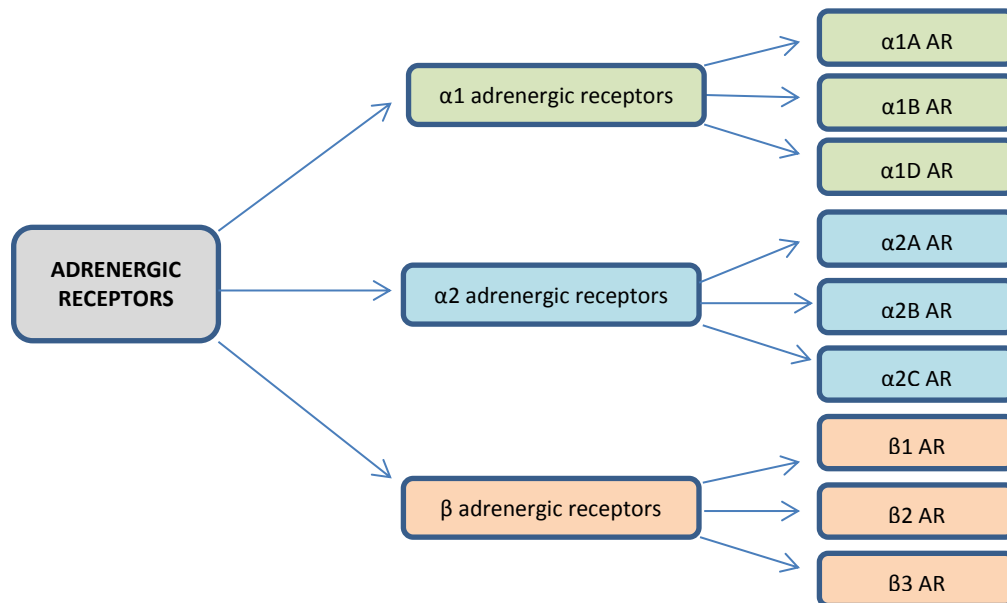


Figure 1. 2.: division of adrenergic receptor in subfamilies. ARs are divided into three families: $\alpha 1$, $\alpha 2$ and β ARs. Each family consists of three members: $\alpha 1$ ARs include $\alpha 1A$, $\alpha 1B$ and $\alpha 1D$ AR, $\alpha 2$ ARs include $\alpha 2A$, $\alpha 2B$ and $\alpha 2C$ AR and β ARs include $\beta 1$, $\beta 2$ and $\beta 3$ AR.

All adrenergic receptors are capable of binding a number of common ligands and signal via G proteins, but the downstream signalling differs between receptors (figure 1. 3.).

The $\alpha 1$ AR family members transduce the binding of catecholamines into the activation of $G_{q/11}$ which activates phospholipase C- β and generates inositol phosphates and diacylglycerol (elevating intracellular $[Ca^{2+}]$ and protein kinase C). Agonists can also activate voltage-gated Ca^{2+} channels. The tissue response is smooth-muscle contraction. $\alpha 2$ ARs signal through G_i and G_o proteins, thus inhibiting adenylyl cyclases and voltage-gated Ca^{2+} and activating Ca^{2+} -dependent K^+ channels. Tissue responses include sedation, analgesia, hypotension and vasoconstriction. Agonist stimulation of β ARs activates adenylyl cyclase via G_s leading to an increased heart rate and force of contraction in the case of $\beta 1$ AR activation and smooth-muscle relaxation in case of $\beta 2$ AR activation [25].

Since many cells express several members of AR simultaneously, a ligand (for example adrenaline) can activate multiple G proteins, coupled to diverse effectors with the potential for conflicting effects [25]. G protein-independent signalling was also observed [31].

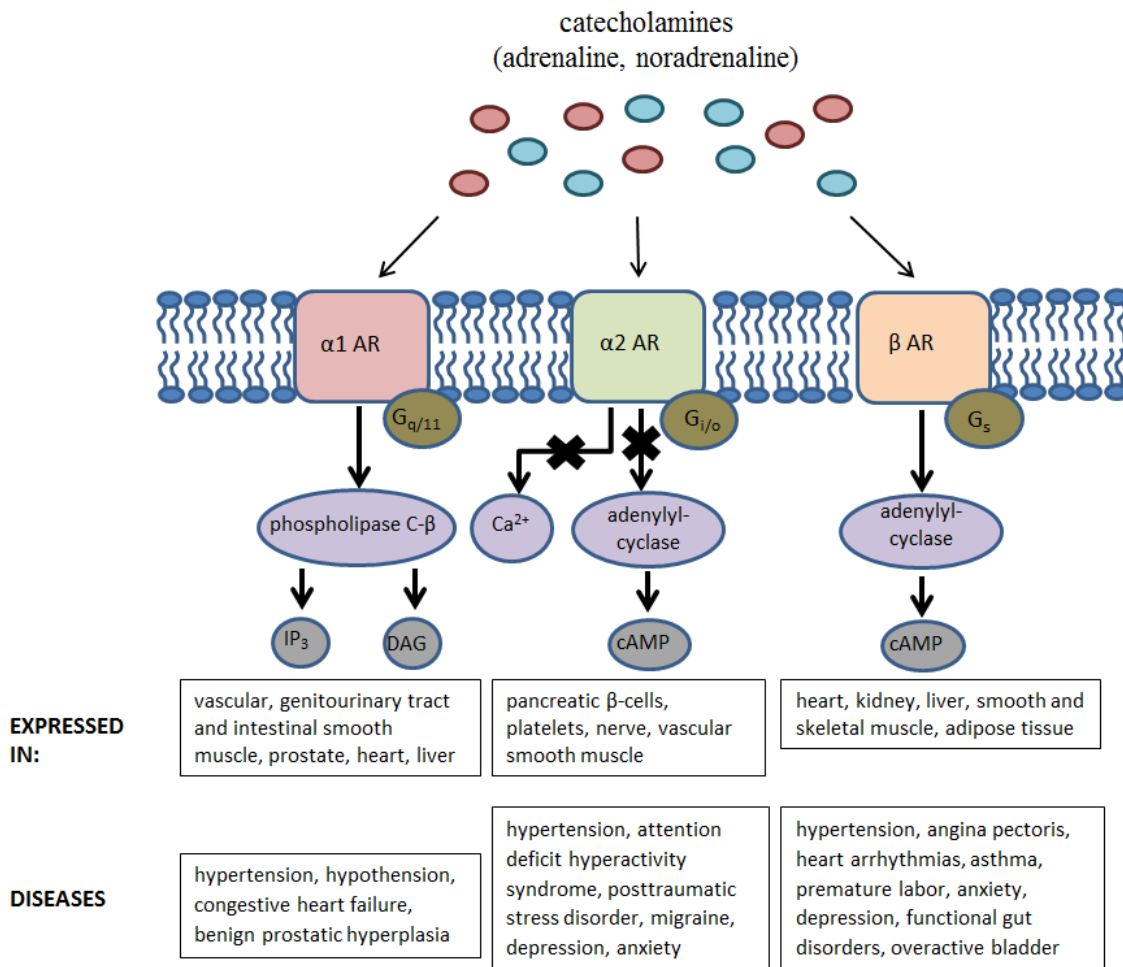


Figure 1.3.: the effect of catecholamines on different families of adrenergic receptors ($\alpha 1$, $\alpha 2$, β AR). $\alpha 1$ ARs couple to $G_{q/11}$ that activate phospholipase C- β which in turn leads to the increase in inositol triphosphate (IP_3) and diacylglycerol (DAG). This leads to the increase of Ca^{2+} and results in smooth muscle contraction. $\alpha 2$ ARs couple to $G_{i/o}$ which inhibits adenylyl cyclase and result in cAMP decrease. β ARs couple to G_s which activates adenylyl cyclase and increases the concentration of cAMP. The scheme is simplified since the intracellular response is much more complicated than shown in the figure. Inappropriate activation of these receptors leads to several diseases that are listed below the graphics. The figure is adapted by [32].

As adrenergic receptors are involved in many diseases, there are several drugs on the market that target specifically certain subfamilies of these receptors. Examples are β -blockers (β ARs inverse agonists and antagonists) that are used in the treatment of hypertension and ischemic heart disease presumably through their actions on β_1 AR [33-35]. However, some studies show that the beneficial actions of these medicines may occur via the β_2 AR since in heart failure the β_2 ARs comprise 36% of the total population of β ARs, while in the healthy heart β_1 AR represent 82% [33, 36]. β_2 AR agonists, on the other hand, are important anti-asthma medicines [24]. Determining the crystal

structures of different members of adrenergic receptors might give us a better insight into how these receptors work. Designing specific drugs that will only activate one specific group of receptors will help to produce medicines with fewer side effects than the ones that are currently on the market. However, it also seems that better understanding of the signal transduction will be important for achieving this goal.

1. 3. Crystallisation of membrane proteins and GPCRs

Although membrane proteins represent one third of the cell's proteome, the number of known 3-dimensional structures represents a minority in the protein data bank (PDB). High resolution 3D structures have proven to be fundamental for a better understanding of biological processes as well as an important tool capable of delivering detailed structural information on atomic level [37-39]. Since the first structure of the membrane protein in 1985, several hundreds of structures have been determined. However, the vast majority still remains to be solved.

A number of obstacles have at least partially, been overcome in the recent years leading to the increased number of membrane protein structures, though membrane protein crystallisation is still in its "log" phase. The number of GPCR structures solved has increased exponentially in recent years due to progress in the understanding of how to crystallise these proteins. These include: overexpression of recombinant proteins in different hosts, thermostabilisation of GPCRs by alanine scanning [40-42] or other engineering techniques, truncation of flexible domains, the creation of receptor-T4 lysozyme [3, 43], receptor-BRIL [44] and receptor-apocytochrome [45] chimeras (figure 1.4.), co-crystallisation of receptors with monoclonal antibody fragments [4, 18, 46, 47], removal of post-translational modifications, development of new detergents and lipids for more efficient solubilisation and crystallisation (for example the use of lipidic cubic phase [48]), and developments in automation, miniaturisation and synchrotron developments that allowed the work with very small and fragile crystals including the reduction in background scattering and artefacts from radiation damage [6, 37, 49, 50].

The first structure of a GPCR, rhodopsin, has been determined in 2000. In 2007 the first structure of non-rhodopsin GPCR was published, the structure of human β_2 AR [3, 4] followed by the structures of turkey β_1 AR [40] and human A_{2A} R [51] in 2008. Until 2016, over 30 structures of unique GPCRs have been published in the PDB database, including members of class B (glucagon receptor [52] and corticotrophin-releasing factor 1 receptor [53]), class C (glutamate receptor [54, 55]) and class F (smoothed receptor [56]) GPCRs.

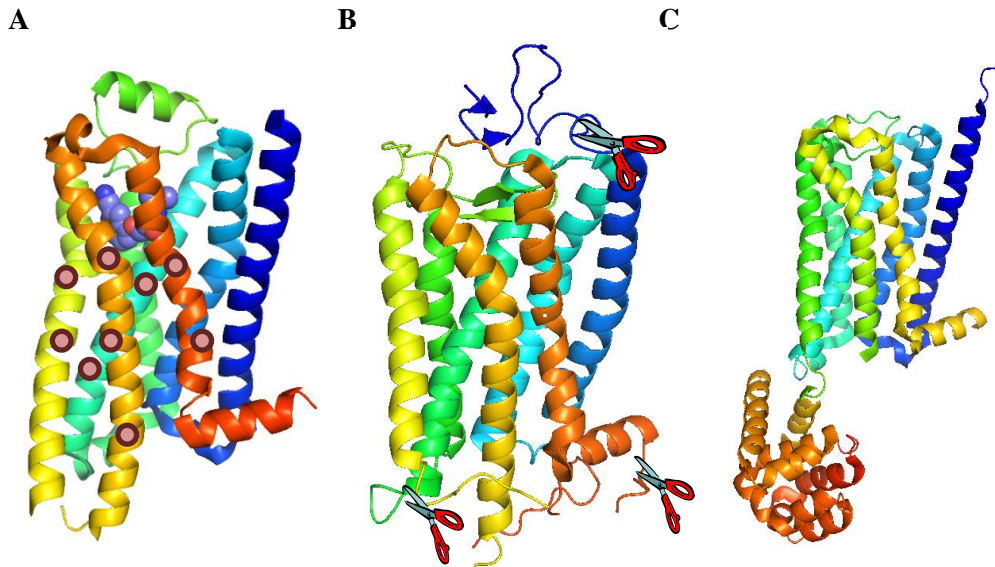


Figure 1. 4.: modifications of receptors increased the chances for successful crystallisation. Receptors can be thermostabilised (figure A), thermostabilised amino acids are represented by red circles (the majority of the thermostabilising mutations have been found on helices 3, 5, 6 and 7). The receptor on the figure is turkey $\beta 1$ AR (PDB code: 4BVN). Additionally, parts of the receptor can be cut (figure B) in order to remove the flexible parts that can cause problems in the crystallisation. As presented on the picture these include especially the N- and C-termini and ICL3. The receptor on the figure is bovine rhodopsin (PDB code: 1L9H). In order to increase the area involved in the crystallisation, ICL3 can be replaced with a fusion partner (figure C). In this case the M4 muscarinic acetylcholine receptor includes the minimal T4L fusion (PDB code: 5DSG).

1. 3. 1. Expression systems for GPCRs

Since the expression of GPCRs is very low in natural sources, all proteins have to be recombinantly expressed in order to reach high enough amounts required for crystallisation. GPCRs could generally not be expressed in *E. coli*, the expression system that represents the easiest, fastest and cheapest system to produce high quantities of functional protein [57]. So far only two receptors were expressed in *E. coli* BL21(DE3) expression system: human chemokine CXCR1 receptor and rat NTS₁ receptor [58-60]. Eukaryotic expression systems have more appropriate machinery for the proper expression and folding of membrane proteins and for the posttranslational modifications that have important roles in maintaining the receptor functions [12, 23, 61, 62]. The majority of proteins were therefore expressed in insect cells (*Sf9*, *Sf21* and High Five expression systems) with a few of the receptors expressed in yeast (*P. pastoris*) and mammalian cells (HEK 293 GnTi-) [58, 63].

1. 3. 2. Modifications of GPCRs

Long and disordered extra- and intracellular parts of the receptor impair crystallisation. It has been shown already 20 years ago that removal of the turkey $\beta 1$ AR C-terminal increases the expression [64] and it is nowadays a standard practice to remove the C-terminal tail. The N-terminus is also often removed, especially in class B, C and F that possess large N-terminal extracellular domains. The C- and N-terminal parts of crystallised GPCRs have generally been shorter than 40 residues [12]. Affinity tags for the purification as well as fluorescence proteins (for example green fluorescent protein, GFP) are added to the N- and C- terminus in order to be able to purify the protein and to monitor the expression and purification. The addition of GFP allows monodispersity screening by fluorescence size-exclusion screening (FSEC) using crude detergent solubilised extracts before purification [65-70]. This allows fast screening of many constructs which is useful in the initial stages of the crystallisation process. Samples that do not show a monodisperse peak can be excluded from the pipeline in the early stage. Truncations of N- and C-terminals often remove post-translational modifications (glycosylations, palmitoylations and phosphorylations) as well as cysteine residues that might form disulphide bonds. While the removal of certain post-translational modifications (PTMs) might be beneficial for crystallisation, it might also lead to lower stability and different effect of ligands on receptors. Significant modifications in these regions might have a major influence on ligand binding and especially on coupling with intracellular effector proteins. If the removal of PTMs has a major influence on the expression and stability of the receptor, they can also be removed enzymatically during purification [12]. There is no general truncation scheme so far. Structures solved by now have showed that cutting the C-terminal at 5-10 residues after the end of helix 8 might be important for the crystallisation [71]. More solved structures will be useful as guides in designing proper truncations.

ICL3 of class A GPCRs is often unstructured and is thus normally shortened and/or substituted with a fusion partner [58]. A fusion partner can provide additional polar surface that can aid in the crystallisation. A perfect fusion partner is compact, stable and easily crystallised [12]. Before fusing additional partners, the ends of the ICL3 need to be carefully assessed in order to not disturb the GPCR fold. Initially, the fusion partner used was T4L and 50% of all structures determined with fusion partners have been crystallised with this protein either in the ICL3, ICL2 or at the N-terminus. Additionally, almost 40% of proteins were crystallised with b₅₆₂RIL (BRIL) either in ICL3 or at the N-terminus. Other fusion partners used were minimal T4L, rubredoxin and the catalytic domain of *Pyrococcus abyssi* glycogen synthase [12, 44, 72-81].

Systematic mutagenesis has also been proven to increase the thermostability and “lock” the receptor in a single conformation, thus allowing the crystallisation of the receptor [40-42, 82, 83]. Another way

to facilitate crystallisation is the use of antibodies to stabilise the receptor in a specific conformation and increase the size of soluble domain. This has been successful in solving the structures of β 2 AR and human A_{2A}R [4, 18, 46, 47, 84].

1. 3. 3. Use of ligands for the crystallisation

Until 2007 the only solved crystal structure of any known GPCR was rhodopsin. Rhodopsin can be isolated from natural source and shows very low basal activity [85, 86]. Crystallisation of other members has been more difficult due to their highly dynamic nature. In the absence of ligands GPCRs exist in an equilibrium between several conformational states including the conformations R and R* that are defined as states that are unable (R state) or able (R* state) to activate G proteins and thus need to be stabilised in order to be crystallised [85, 87]. Rhodopsin, on the other hand, has a large activation energy barrier between R and R* which keeps the receptor mostly in the inactive state in the dark [7]. Ligands bind to the binding pocket of the GPCR, which can promote folding of the correct conformation as well as locking the receptor in a stable state. Interaction of a receptor with a ligand may also act as a chemical chaperone to aid GPCR expression [71]. Even though that the ligands have been usually only used during the purification of the receptors, recent studies have shown that supplementing small molecule ligands during expression can improve the membrane surface expression of GPCRs [71]. The crystallisation propensity is correlated to the extent of ligand-induced thermostabilisation of the receptor. Several methods have been developed for a high throughput assessment of the melting temperature, including the microscale fluorescent thermal-stability assay using CPM dye (CPM assay) [88]. A study by Zhang et al. has shown that a T_m higher than 55°C is usually required for successful crystallisation [71]. However, this is not the only requirement. Several properties of the ligands including the weight, binding affinity, hydrogen bonding and solubility also affect crystallisation propensity. The molecular weight and the size of the ligands matter since larger ligands might not easily gain access to the binding pocket, while smaller ligands may not be engaged in an extensive molecular interaction network and thus would not be able to lock the receptor in a well-folded state [71]. Since the interactions between the ligand and GPCR are dynamic, ideal ligands should have a high affinity and a slow dissociation rate. From the data obtained so far, a single-digit nM range is usually helpful in crystallisation. Additionally, a covalent bond-forming group could potentially make a covalent bond with the receptor thus improving the stability of the protein. However, for the majority of the ligands, little is known about the kinetics of binding [71]. In regards to the solubility, the ligands need to be reasonably soluble in water in order to manipulate them in high concentration during purification. Hydrogen bonds are important as well as they may contribute to the stable interactions in the ligand-binding pocket. In many of the solved structures so far, the ligand forms at least two hydrogen bonds with the receptor [71]. Therefore the choice of the ligand that can constrict the receptor in one state is crucial and this is also the reason

while the majority of the receptors until now has been crystallised in the inactive conformation with bound inverse agonists that reduce the basal activity or neutral antagonists that maintain basal activity [6, 89]. However, plenty of research has to be done in order to understand how ligands bind into binding pockets of receptors and thus help in the crystallisation of proteins.

1. 3. 4. Use of detergents and new methods for crystallisation

Since membrane proteins firstly need to be extracted from the cell membrane, methods used for soluble proteins generally cannot be applied for the crystallisation of these proteins. The development of new detergents, that are able to keep the protein intact during the process of solubilisation, purification and crystallisation, increased the success rate of membrane protein structure determination [37]. When detergent is used, it is extremely important that it efficiently solubilises the protein from the membrane, while being mild enough not to deteriorate the native structure and functionality of the protein [58]. The most commonly used system for extracting GPCRs from cell membrane is the mixed micelle system of DDM and CHS [12]. When using the traditional *in surfo* methods, the detergents with smaller micelles might be useful since the exposed part of the protein is big enough to still form crystal contacts, however since they barely cover the hydrophobic part of the protein, this often leads to protein aggregation. Examples of GPCRs crystallised using the *in surfo* method are bovine and squid rhodopsin [19, 90-99], turkey $\beta 1$ AR [40, 100-102] and human A_{2A} receptor [42, 103].

The majority of membrane proteins and GPCRs have been crystallised with *in meso* methods using either bicelles [104] or lipidic mesophases [105]. Bicelles are disk-like lipidic bilayer patches surrounded and stabilised by amphiphilic molecules. They provide an almost native environment for membrane proteins, but have a disadvantage because of their relative large size [58]. An example of successful crystallisation using this method is human $\beta 2$ AR in complex with a monoclonal antibody Fab fragment that was crystallised in bicelles made from a mixture of DMPC and CHAPSO in DDM [4]. The most used systems for GPCR crystallisation are lipidic mesophases, the bicontinuous liquid crystals composed of a curved lipidic bilayer that separates two continuous channels filled with water medium [58]. Contrary to the *in surfo* method, where micelles surround the receptor, in LCP the molecules can move freely and interact with each other. Crystal lattice contact can therefore form from hydrophilic and hydrophobic part of the receptor [12]. The concept of the crystallisation in LCP was initially validated by the crystallisation of bacteriorhodopsin and halorhodopsin [106-108]. Since these initial experiments, the number of structures solved in LCP has increased drastically and the LCP systems have been studied extensively [48, 109-111]. Monoacylglycerols (MAGs) are used as a lipid component of the LCP, the most commonly used one in GPCR crystallisation is monoolein (MAG 9.9). LCP is formed by mixing the MAG with water solution containing protein in the ratio of

3:2 (w/w) at 20°C. In the process of mixing, the protein is incorporated into the lipid bilayer that forms a stabilising, native-like environment. The vast majority of GPCRs has been crystallised in a mixture of monoolein and cholesterol in the ratio of 9:1 (w/w). Cholesterol makes the GPCR more stable and less conformationally flexible which might increase the ability of the protein to crystallise [111, 112].

LCP developments were an important part of the progress in the GPCR crystallisation. There is a number of reviews that allow researchers to grasp the recent advances in reconstitution, setting up the crystallisation, harvesting and cryocooling of the crystals grown in LCP [112-115].

1. 4. The aim of the thesis

Adrenergic receptors are targets of several drugs on the market. However, these are very unspecific, most probably affecting several receptors at the same time, causing different side effects. Good examples are certain beta blockers that act on β_1 adrenergic receptor, but need to be taken with caution when patients have pulmonary diseases. Knowing the differences in the structures of these, closely related, receptors might give us an insight into how these drugs act on each of them and will help in the design of more subtype specific medicines allowing patients to have a better quality of life. Two structures have already been solved (human β_2 AR and turkey β_1 AR), therefore the primary aim of the thesis was to expand the functional and structural information of this family of GPCRs.

All members of adrenergic receptors were assessed for the expression and thermostability in order to choose the most promising constructs for the crystallisation. Stable cell lines were produced and the purification protocol was established and modified in order to produce pure protein for crystallisation. Vapour diffusion as well as lipidic cubic phase crystallisations were tested. Additionally, an extensive test of 30 ligands has been performed in order to determine the effect of the ligands on the non-mutated and mutated receptors as well as to choose the ligand(s) that can additionally stabilise the receptors. SAXS and WAXS data have been collected to assess the activity of the receptor upon the ligand binding in the solution.

2. MATERIALS AND METHODS

2. 1. Protein constructs

Genes were synthesised by Genewiz and cloned into the pACMV-tetO vector. Constructs are described in detail in the results section and sequences are provided in the appendix.

2. 2. Transient transfection of mammalian cells

On the day of transfection cells were set to be 70% confluent. For a 15 cm (150x25 mm (dxh)) plate, 50 µg of purified DNA was mixed with 5 mL of serum free DMEM (high glucose (4.5 g/L) with L-glutamine (BioConcept)) and 100 µl PEI (25 kDa, branched (Aldrich)). The mixture was vortexed and left at room temperature for 10 minutes in order to form the DNA:PEI complex. 10 mL of medium with 2% FBS (Gibco, Serraglob) was added and plated on cells. After 4-6 hours the DNA:PEI complex was replaced with fresh medium supplemented with 10% FBS. In case of HEK293 GnTi⁻ cells, cells were already induced at this point (5 mM sodium butyrate (Aldrich) and 2 µg/mL tetracycline (Gerbu)). Medium was changed daily and the cells were harvested after 72 hours. The cells were cultured in an incubator at 37°C with 5% CO₂.

2. 3. Cell harvesting

Before harvesting, cells were screened for protein expression using a FLoid® Cell Imaging Station (ThermoFischer Scientific) as all constructs used in this work contained GFP fusion. Cells were then either scraped with a scraper or resuspended in media if they were loosely attached. The cell suspension was centrifuged in a 50 mL Falcon tube for 15 minutes at 3220xg and 4°C in an Eppendorf 5810 R centrifuge. The sample was washed twice with PBS Dulbecco, w/o Ca²⁺ and Mg²⁺ (Biochrom) before flash freezing the pellet in liquid nitrogen. The pellet was stored at -80°C. In case cells were harvested from a 6-well plate, the samples were centrifuged in an Eppendorf tube at 21000xg for 15 minutes at 4°C in an Eppendorf 5415R centrifuge. Samples were washed twice with fresh PBS, flash frozen in liquid nitrogen and stored at -80°C.

2. 4. Crude protein extract analysis

Pellets were solubilised either in PBS with 1% DDM and 0.1% CHS or in standard solubilisation buffer (20 mM HEPES pH 7.45, 150 mM NaCl, 10% glycerol (v/v), 1% DDM with 0.1% CHS). Pellets were resuspended with a pipette and then incubated at 4°C for 1 hour on a roller mixer. The samples were ultracentrifuged at 86000xg, 4°C for 30 minutes using a Beckman Coulter Optima MAX-CP tabletop ultracentrifuge and TLA 100.3 rotor. Supernatant was then analysed with FSEC using an Ettan LC (GE Healthcare) system and TSKgel® G3000SWXL HPLC Column (Tosoh Bioscience LCC) with excitation at 485 nm and emission at 520 nm (GFP fluorescence) and in gel fluorescence using Amersham Imager 600 (GE Healthcare) using blue filter (460 nm).

2. 5. In gel thermostability assay of crude extracts

Samples (one 10 cm or one 15 cm plate) were solubilised in 900 µl of PBS with 1% DDM and 0.1% CHS or standard solubilisation buffer and were then incubated for 1 hour at 4°C on a roller mixer. The samples were ultracentrifuged at 86000xg for 20 minutes using a Beckman Coulter Optima MAX-CP tabletop ultracentrifuge and TLA 100.3 rotor. The supernatant was aliquoted in 60 µl aliquots in Eppendorf tubes that were transferred into the heat block previously filled with water and preheated to 25°C. Samples were transferred all at once and were then heated at the desired temperature for 5 minutes. After this, one sample was taken out and put on ice while the temperature was increased by 5°C. Samples were left incubated at that temperature for another 5 minutes after the temperature stabilised. The heating was done from 25°C to 85°C. When the heating was finished, the Eppendorfs were centrifuged at 21000xg for 40 min at 4°C in an Eppendorf 5415R centrifuge. Samples were analysed by SDS-PAGE on a TruPAGE™ precast 12% gel (Sigma) and in gel fluorescence was measured. GFP fluorescence of unfolded protein at each temperature was determined with an in-house program (GelFit) and the data was fitted using a sigmoidal curve using Origin. The melting temperature (T_m) was determined for each protein.

2. 6. Preparation of stable cell lines and clonal selection

Cells were incubated at 37°C in a humidified atmosphere containing 5% CO₂ throughout the protocol. One 10 cm (100x20 mm) plate of HEK 293 GnT1⁻ cells was set to be 60-70% confluent on the day of transfection. The transfection was done with PEI in the same way as the transient transfection. The next day dilutions were done in a 6-well plate in the following ratios: 1:20, 1:40, 1:80, 1:200 and

1:400. DMEM medium used initially was changed for the selection medium one day later (DMEM with 10% FBS, antibiotics (penicillin-streptomycin-fungizone (ThermoFischer Scientific)), and selection antibiotics (blasticidin S HCl (10 µg/mL, InvivoGen) and geneticin (1 mg/mL, Thermo Fischer Scientific)). Medium was changed every second day in the first week and then every 3-4 days until well isolated colonies were observed in around 14 days. Medium was aspirated and clones were picked from a plate without any remaining liquid. Small filters were pre-soaked in Trypsin-EDTA (BioConcept), put directly on the isolated clones and transferred into 6-well plate already containing 2 mL of selection medium. At least 12 clones for each construct were chosen. When cells attached to the plate, filters were removed. Medium was changed every few days until cells reached 90% confluency. Each clone was then expanded into two wells: one well was frozen, while the second one was induced with tetracycline and sodium butyrate and was left to express the protein for 48-60 hours before harvesting. Cells were screened before harvesting for protein expression using FLoid® Cell Imaging Station.

Pellets were solubilised in PBS as written in section 2.3. The supernatant was loaded onto a gel and the fluorescence of each clone was analysed with the in-house program. Supernatants were also analysed with the BCA assay (Pierce BSA Protein Assay Kit, Thermo Fischer Scientific) for the total protein content. By dividing the amount of the fluorescence signal with the amount of the total protein in the sample, the clone expressing the highest amount of adrenergic receptor was chosen. Two rounds of the clonal selection were done, when in the first round all clones were expressed in one well of a 6-well plate and in the second round the 3-5 best expressing clones from the first round were expressed in a 10 cm plate, harvested and reanalysed as before.

2. 7. Expression of protein in shaker flasks

At least five 15 cm plates (90% confluency) were grown before they were transferred into the shaker flask. Cells were detached with trypsin, resuspended in DMEM medium with 10% FBS and centrifuged for 5 minutes at 800xg. The pellet was resuspended in 100 mL of medium for suspension cultures (PEM without L-glutamine (Gibco) with 10% FBS, antibiotics (penicillin-streptomycin-fungizone) and glutaMAX™ (Gibco)). Later, FBS was reduced to 5%. Cells were grown in 2 L shaker flasks (1 L of cell culture volume) in an incubator at 37°C with 5% CO₂. After getting the cells in suspension, cells were counted and diluted to 0.8-0.9x10⁶ cells/mL. Cells doubled approximately every 24 hours and were never diluted below 0.6-0.7x10⁶ cells/mL. Cells were induced with tetracycline and sodium butyrate when they reached 3-3.5x10⁶ cells/mL and were left to express for 50 hours. Cells were harvested for 30 minutes at 3000xg and 4°C using a Sorvall RC 3C Plus centrifuge and H-6000A rotor. The pellet was transferred to the 50 mL falcon tube and washed three

times with ice cold PBS. Each time, cells were resuspended with a 25 mL pipette and then centrifuged for 15 minutes at 3220xg and 4°C in an Eppendorf 5810 R centrifuge. Washed pellets were frozen at -80°C.

2. 8. CPM assay of purified proteins

In order to find a ligand that would additionally thermostabilise the protein, CPM (N-[4-(7-diethylamino-4-methyl-3-coumarinyl)phenyl]maleimide) assay was performed. The ligands were divided into three groups: agonists, antagonists and non-selective ligands depending on their predicted effect on the receptor (as defined by TOCRIS or Sigma from which all the ligands were bought where several additional references can be found). Each ligand was tested in three different concentrations: 12 µM, 120 µM and 610 µM.

Before the experiments with ligands were performed, the optimal amount of the protein and CPM dye had to be determined. Four amounts of the protein were tested (2, 4, 8 and 10 µg) as well as 3 amounts of the CPM dye (0.25, 0.5 and 1.0 µg). The total reaction volume was 82 µl, the protein was diluted in the buffer from the stock of concentrated protein, while 6.7 µl of the dye was added from freshly prepared 1:40 (dye: buffer) dilution of dye stock (3 mg/mL in anhydrous DMSO).

For the ligand tests, all experiments were firstly prepared in a 96 well plate. The dilutions of protein were prepared first when 2 (for α2C-T4L AR) or 4 (for β3-T4L AR) µg of the protein was diluted in the buffer (20 mM HPES pH 7.45, 150 mM NaCl, 10% glycerol and 0.02% DDM with 0.002% CHS). After the dilution of the protein was prepared, ligands were added. CPM dye (0.5 µg) was added at the end and mixed well with previously prepared mixture of protein and ligand using a multichannel pipette. Samples were left on ice for maximum of 5 minutes after the dye was added. 25 µl of the mixture was aliquoted into the PCR tubes (Qiagen) for testing, which allowed testing each sample in a triplicate.

Measurements were performed using a Rotorgene Q qPCR instrument (Qiagen, Germany). The temperature was ramped from 25°C to 85°C with 4°C increase per minute. The gain was set to the first sample in the run which was always the reference consisting of protein without ligand. CPM dye binding was monitored using 365 nm excitation and 460 nm emission. The data was analysed with the instrument software, using the program “melt” which calculates the first derivative and reports the reflection point. Data was smoothened using “heavy” digital filter settings. This filter smoothenes data using a sliding window of experimental data points. The signal was inverted to give a maximum representing the T_m on the positive site. The melting temperatures were calculated as an average of

each triplicate (triplicates on average did not differ for more than 0.5°C). Each ligand was tested in at least three separate experiments in order to determine standard deviation of the samples.

2. 9. 1D4 resin preparation and regeneration

2. 9. 1. 1D4 resin preparation

1D4 antibody was coupled to the sepharose resin in order to produce the affinity resin for the protein purification of proteins with the 1D4 peptide tag.

11.2 g of CNBr-activated sepharoseTM 4B resin (GE Healthcare) was resuspended in 500 mL of 1 mM HCl. After 1h incubation on a roller mixer at room temperature, it was transferred into BioRad Econo-column (volume: 150 mL) and washed with 200 mL of 1 mM HCl followed by 500 mL of 0.1 M NaHCO₃ and 0.5 M NaCl, pH 8.5. The resin was transferred into a 250 mL bottle, 154 mg of 1D4 antibody was added (14 mg of antibody/ g of resin before swelling) and diluted to 250 mL with 0.1 M NaHCO₃ and 0.5 M NaCl, pH 8.5. This was left on roller in cold room O/N. The next day, the resin was again transferred into the BioRad column and washed with 500 mL of 0.2 M glycine, pH 8.0, followed by 500 mL 0.1 M NaHCO₃ and 0.5 M NaCl, pH 8.5, then 200 mL 0.1 M NaOAc, 0.5 M NaCl, pH 4.0 and again with 500 mL of NaHCO₃ and 0.5 M NaCl, pH 8.5. At the end, the resin was washed with 200 mL 20 mM HEPES (pH 7.45), 150 mM NaCl and 0.02% (w/v) NaN₃ and stored in the same buffer as 50% slurry at 4°C.

2. 9. 2. 1D4 resin regeneration

The 1x used resin was transferred into the BioRad Econo-column, removing all the liquid. This was then washed with 5 column volumes (CV) of 3.5 M MgCl₂, followed by 20 CV of 20 mM HEPES (pH 7.45) and 150 mM NaCl. Finally the resin was resuspended as 50% slurry in 20 mM HEPES (pH 7.45), 150 mM NaCl, 0.02% (w/v) NaN₃. The regenerated resin retained approximately 100% of the original capacity.

2. 10. Preparation of cell membranes

To 1 g of cell pellet, 6 mL of buffer (20 mM HEPES pH 7.45, 1 mM EDTA and protease inhibitors (cOmplete, EDTA-free (Roche))) was added. The pellet was dounced 20-times with a tight douncer and then centrifuged for 2 hours at 185000xg at 4°C using a Beckman Coulter Optima XE-100 or

Optima XL1-100K ultracentrifuge and Ti45 rotor. The pellet was resuspended with an electric douncer (IKA Turax) at the lowest speed in 4 mL/g of starting material in identical buffer and centrifuged at 185000xg for 1.5 hours. The pellet was finally resuspended in 4 mL/g membranes with an electric douncer in 20 mM HEPES pH 7.45 with added protease inhibitors, flash frozen in liquid nitrogen and stored at -80°C.

2. 11. Protein purification

2. 11. 1. Initial protein purification

The purification protocol was changed several times during the course of PhD in order to improve the purity of the protein and increase the crystallisation probability.

Originally, cells were solubilised in the solubilisation buffer (20 mM HEPES pH 7.45, 150 mM NaCl, 1 mM EDTA, 10% glycerol (v/v), protease inhibitors, 1% detergent (w/v) and 0.1% CHS (w/v), 2 mg/mL iodoacetamide (Fluka)). Detergent was, depending on the crystallisation goal, either DDM, DM or LMNG. The concentration of NaCl was later increased to 300 mM to prevent non-specific binding to the column. For each g of cell pellet, 10 mL of the solubilisation buffer was used. Later, when membranes were used, 1 g of membranes was solubilised in 8 mL of the solubilisation buffer. Cells were resuspended well with a 25-mL pipette and then incubated for 1 hour at 4°C on a roller mixer. Solubilised material was ultracentrifuged for 1 hour at 185000xg using a Beckman Coulter Optima XE-100 or Optima XL-100K ultracentrifuge and Ti45 rotor. GFP fluorescence of the supernatant was measured and the amount of the protein in the sample was calculated. One mL of 1D4 resin was added to one mg of protein and left to incubate at 4°C for 3 hours on a roller mixer. The resin was loaded into BioRad column and the supernatant was eluted.

The resin with bound protein was washed with 20 CV of washing buffer (20 mM HEPES pH 7.5, 500 mM NaCl, 10% glycerol (v/v), detergent). This was later reduced to 10 CV in order to reduce the amount of lipids that were washed away. At this step the amount of detergent was already reduced to the amount used for the crystallisation: 0.02% (w/v) DDM, 0.3% (w/v) DM, 0.01% LMNG (w/v) or 0.35% (w/v) Hega-10 and 10-times less CHS (w/v). In case of Hega-10, protein was initially solubilised in DM and buffer was changed to Hega-10 during the washing step.

In case that the protein was used for biophysical methods and GFP did not need to be removed, 1 CV of elution buffer (20 mM HEPES pH 7.5, 150 mM NaCl, 10% glycerol (v/v), 0.02% DDM, 0.002% CHS and 80 µM 1D4 peptide) was added. This was left on a roller mixer for 30 minutes and then

eluted. This was repeated several times, the last column volume was left on the roller O/N before eluting. All fractions were analysed on the gel and concentrated to the amount needed for the biophysical characterisation. Before deciding whether to use a sample with or without GFP, both versions were tested in an assay. There was no difference between both samples. For example: in CPM assay GFP did not have an effect on the overall temperature of the protein, additionally, the melting temperature of the protein and GFP were separated well enough to distinguish both parts of the construct.

When the sample was used in crystallisation, 1.5 CV of cleavage buffer (20 mM HEPES pH 7.45, 300 mM NaCl, 10% glycerol, 10 μ M ligand, protease (0.12*n (protein), detergent (same as detergent used for the washing buffer), 2.8 mM of reduced glutathione and 0.45 mM of oxidized glutathione) was added to the resin and left to incubate on the roller at 4°C O/N. The buffer was eluted the next day and Protino® Ni-TED resin (Machery-Nagel) was added to remove the protease. Initially it was incubated for 1 hour at 4°C on a roller mixer. Since there was a substantial amount of the target protein that has bound unspecifically to the resin, the protocol was modified and the protein was directly eluted from 1D4 resin to Ni resin drop by drop to reduce the amount of the protein-resin contact. Both resins were washed twice with 1 CV of fresh buffer (20 mM HEPES pH 7.45, 300 mM NaCl, 10% glycerol, 10 μ M ligand, detergent). Samples were concentrated using 100 kDa concentrators (Merck Milipore) to approximately 15 mg/mL and a total volume of approximately 400 μ l, centrifuged at 21000xg using an Eppendorf 5415R centrifuge for 10 min and further purified by gel filtration (GF) using a self-packed Superdex 200, Tricorn 10/300 column. This was run with the buffer (20 mM HEPES pH 7.45, 300 mM NaCl, 10% glycerol, 10 μ M ligand, detergent) with a flow of 0.4 mL/min and a fraction size of 0.4-0.5 mL. Fractions showing appropriate UV signal were pooled and concentrated in a 0.5 mL concentrator, 100 kDa cut off (Vivaspin 500, Sartorius) to the concentration suitable for the crystallisation (5-15 mg/mL for vapour diffusion, 30-50 mg/mL for LCP crystallisation as determined by measuring absorbance at 280 nm using NanoDrop™ 1000 spectrophotometer (Thermo Scientific)).

In the first instance, 2 mg/mL iodoacetamide (Fluka) was added together with the solubilisation buffer. Additionally, 10 μ M ligand was added from cleavage on when the concentration of the protein in the solution was around 10 μ M. This purification protocol was used initially for the purification of the α 2C-T4L and β 3-T4L AR.

After getting the first potential crystal hits, the purification of the mutated β 3-T4L AR was further modified. 2 mg/mL of iodoacetamide and 1 μ M cyanopindolol hemifumarate (Tocris) was added to the protein and was left mixing for 1 hour at 4°C on a roller mixer before the solubilisation was done. The protocol was then performed as before but with 1 μ M cyanopindolol in all buffers. Before the GF,

EndoH (3 units/ 10 µg of protein) was added to the sample and left at RT for 2 hours in order to deglycosylate the sample. The sample was cooled down, concentrated and loaded on GF column. GF buffer was changed: glycerol was omitted and NaCl reduced to 150 mM.

2. 11. 2. Further improvements to the purification protocol

In order to reduce the amount of the buffer before the GF, an additional protocol was tried. After binding of the protein to the resin, the resin was packed into a XK-16/20 column (GE Healthcare) that was connected to Ettan LC (GE Healthcare). The column was washed with the same washing buffer as before with the flow 0.4 mL/min until the Trp signal dropped and stabilised (app. 2-3 CV). The protein was eluted with buffer with 1D4 peptide (20 mM HEPES pH 7.5, 300 mM NaCl, 10% glycerol (v/v), 0.02% DDM, 0.002% CHS and 150 µM 1D4 peptide). The flow-rate was set to 0.2 mL/min until the first increase in fluorescence was observed, then the flow was stopped and the column was incubated for 1 hour. Subsequent to protein elution, 3C protease was added in the same (protease: protein) ratio as before. The mixture was incubated O/N at 4°C on a roller mixer. The next day, 3 units/ mg of protein of EndoH was added and the sample was left at RT for 2 hours, then it was cooled on ice before being concentrated and centrifuged at 430000xg for 10 min using Beckman Coulter Optima MAX-CP tabletop ultracentrifuge and TLA 120.1 rotor. The sample was concentrated to ca. 15 mg/mL and 450 µl before loading on the GF column to reduce the concentration step. The initially used self-packed Superdex 200 Tricorn 10/300 was changed for Superdex 200 increase 10/300 GL (GE Healthcare) as it showed better resolution. The sample was collected in fractions of 0.3 mL and concentrated to 30 mg/mL for the crystallisation.

2. 12. Adjusting parameters for the purification

2. 12. 1. Optimisation of solubilisation conditions

The right amount of the solubilisation buffer had to be determined. To do so, prepared membranes, stored in 20 mM HEPES, were either directly solubilised in 1% DDM with 0.1% CHS and NaCl, EDTA and glycerol were added to final concentration 300 mM, 1 mM and 10% respectively (133 mg of membranes/ mL of solubilisation buffer). The rest were diluted in steps of 2 from 100 down to 12.5 mg of membranes/ mL of solubilisation buffer. The samples were left on a roller mixer for 1 hour at 4°C. The samples were centrifuged for 20 min at 86000xg and then loaded to Ettan LC, TSKgel® G3000SWXL HPLC Column with GFP detector (excitation at 485 nm and emission at 520 nm).

2. 12. 2. Determination of the right amount of washing and elution buffer of the resin

In order to determine the right amount of the washing buffer, washing buffer was added in 2.5 CV aliquots. Flow through was collected and loaded on the gel to determine when all unspecifically bound proteins were eluted. For the elution buffer, a similar protocol was used. In this case, 1 CV of buffer was added to the resin, incubated for 20 minutes and eluted. This was repeated as long as some signal on the gel was observed.

2. 12. 3. Determination of the right amount of the 3C protease for protein cleavage

In order to achieve the maximum cleavage of the protein, the optimal amount of the protease had to be determined. Two amounts of the protease were added to the same amount of the protein, the first one was added in the ratio $n(\text{protein}): n(\text{protease}) = 1: 0.12$ (mol/mol), while in the second case the protease was added in the ratio $n(\text{protein}): n(\text{protease}) = 1: 0.24$. Both samples were incubated O/N at 4°C on roller mixer and the samples were analysed the next day on an Ettan LC, TSKgel® G3000SWXL HPLC Column with Trp fluorescence (excitation at 280 nm and emission at 350 nm).

2. 12. 4. Deglycosylation tests

1, 3 or 5 units of EndoH enzyme (New England BioLabs® inc.) were added to 10 µg of protein in 10 µl total volume (20 mM HEPES pH 7.45, 300 mM NaCl, 10% glycerol, 0.02% DDM and 0.002% CHS) and were left to incubate for 1, 2 or 3 hours at RT. Loading buffer was added and the samples were analysed on 4-12% Bis-Tris Protein Gels at 140 V using MES running buffer.

2. 12. 5. Dephosphorylation tests

2 µg of the protein was incubated with 3 units of EndoH and 5 units of FastAP Thermosensitive Alkaline Phosphatase (Thermo Fischer Scientific) in 10 µl total volume (20 mM HEPES pH 7.45, 300 mM NaCl, 10% glycerol, 10 mM MgCl₂, 0.02% DDM and 0.002% CHS) for 2 hours at 37°C or 3 hours at RT. Additionally 2 µg of the protein was incubated with 5 units of FastAP in 10 µl total volume (20 mM HEPES pH 7.45, 300 mM NaCl, 10% glycerol, 10 mM MgCl₂, 0.02% DDM and 0.002% CHS, 1x FastAP buffer) and incubated for 2 hours at 37°C or 3 hours at RT. Loading buffer was added and the samples were analysed on the 4-12% Bis-Tris Protein Gels.

2. 12. 6. Determination of the stability of a purified protein in detergent using FSEC

A dilution of the sample was prepared and divided in 3 equal aliquots. One aliquot was left on ice and was run as a control (4°C sample), while one sample was heated at 50°C in a heat block for 30 minutes. Both samples were centrifuged in an ultracentrifuge for 20 min at 86000xg using a Beckman

Coulter Optima MAX-CP tabletop ultracentrifuge with TLA 100.3 rotor and then loaded on an Ettan LC, TSKgel® G3000SWXL HPLC Column at 4°C where Trp fluorescence was measured. The third sample was left at RT O/N, ultracentrifuged and loaded on FSEC as well. The buffer for the FSEC consisted of 20 mM HEPES, 300 mM NaCl, 10% glycerol, 0.02% DDM and 0.002% CHS. The pH was set to 7.20 to avoid running the samples at the pH limits of the column (the pH limit is 7.4)

2. 13. Crystallisation

2. 13. 1. Vapour diffusion set up

A protein sample was centrifuged in a tabletop centrifuge for 15 minutes at 21000xg. Protein was mixed in the ratio 1:1 with the crystallisation screen using Mosquito® LCP nanolitre protein crystallisation robot (TTP Labtech). The drops were set using the sitting drop method either with the ratio of 150 nL+ 150 nL or 200 nL+ 200 nL, depending on the available amount of the protein. The plates (MRC 2 Well Crystallisation Plates (SwissCI) UVP) were imaged using the Rock Imager (Formulatrix) automatic imager as well as manually under the microscope. Visible, UV and cross-polarisation imaging was performed.

2. 13. 2. Lipidic cubic phase set up

Purified protein was concentrated to 30-50 mg/mL. After a short spin (15 minutes at 21000xg), the protein was reconstituted into monoolein/CHS in the ratio 2 (protein): 3 (90% monoolein with 10% CHS) (w/w). Both components were mixed well using two 100 µl Hamilton syringes until the mixture turned completely transparent indicating the formation of cubic phase [112]. The syringe was mounted on the Mosquito® robot and plates (glass Laminex LCP base and plastic film cover or glass Laminex LCP base and cover) were set up with 40, 50 or 100 nL of LCP and 800 nL of precipitant dispensed over the LCP bolus. Plates were imaged using the Rock Imager automatic imager (visible imaging, UV imaging and cross polarisation imaging) as well as manually under the microscope (visible and cross- polarisation imaging).

2. 14. SAXS and WAXS experiments

1 g of cell pellet was solubilised in 10 mL of solubilisation buffer (20 mM HEPES pH 7.45, 300 mM NaCl, 1 mM EDTA, 10% glycerol (v/v), protease inhibitors, 1% DDM (w/v) and 0.1% CHS (w/v)) for 1 hour at 4°C on a roller. The sample was then centrifuged for 1 hour at 185000xg using Beckman

Coulter Optima XE-100 or Optima XL-100K ultracentrifuge and Ti45 rotor. The fluorescence was measured and 1 mL of 1D4 resin was added per 1 mg of protein. The protein was left to bind for 3 hours at 4°C on a roller mixer. The resin was spinned down at 800xg for 5 min and then transferred in a BioRad column before 10 CV of washing buffer (20 mM HEPES pH 7.45, 500 mM NaCl, 10% glycerol (v/v), 0.02% DDM (w/v) and 0.002% CHS (w/v)) was passed through the resin. 1.5 CV of cleavage buffer (20 mM HEPES pH 7.45, 300 mM NaCl, 10% glycerol, protease (0.12* μ n (protein), 0.02% DDM with 0.002% CHS, 2.8 mM reduced glutathione and 0.45 mM oxidized glutathione) was then added and left at 4°C O/N on a roller mixer. The next day cleavage buffer was eluted and the resin was incubated twice with 1 CV of elution buffer (20 mM HEPES pH 7.45, 300 mM NaCl, 10% glycerol, 0.02% DDM with 0.002% CHS) for 30 min. The sample was passed through the Ni resin in a dropwise manner in order to eliminate the protease. The protein was concentrated with a 100 kDa cut off concentrator to 450 μ l, spinned for 10 min at 21000xg and loaded on Superdex 200, Tricorn 10/300 column, self-packed. The sample was concentrated to 20 mg/mL, aliquoted in 100 μ l aliquots, flash frozen in liquid nitrogen and stored at -80°C.

Just before the measurements, the sample was transferred into 1 mL syringe (SGE Analytical Science). Buffer (20 mM HEPES pH 7.45, 300 mM NaCl, 10% glycerol, 0.02% DDM with 0.002% CHS) was loaded into a separate syringe as well. The third syringe was filled with 10 mM ligand (agonist CGP 12177 or antagonist cyanopindolol) diluted in the same buffer. Firstly the buffer was pumped using nEMESYS pumps (Cetoni GmbH) through the capillary at a rate of 0.04 μ l/s to collect the blank (buffer) sample. Afterwards the protein was flushed through the tubes and then collected to collect the apo form of the protein. Then the ligand was flushed through the tubes until reaching the mixer where the protein and the ligand were mixed. At that point the protein and the ligand were flown at the same time at a rate of 0.04 μ L/s and the data was collected. After collecting the data with antagonist (cyanopindolol), the tubes connected with the ligand were flushed with buffer before connecting the syringe with agonist (CGP12177). Then the agonist was flown through the tubes until reaching the mixer. The protein and agonist were then flown at the same rate (0.04 μ L/s), mixed in a mixer and the data was collected. Figure 2.1. represents the set up. The third syringe was added, so that there was no need to change the buffer syringe for the syringe with the ligand.

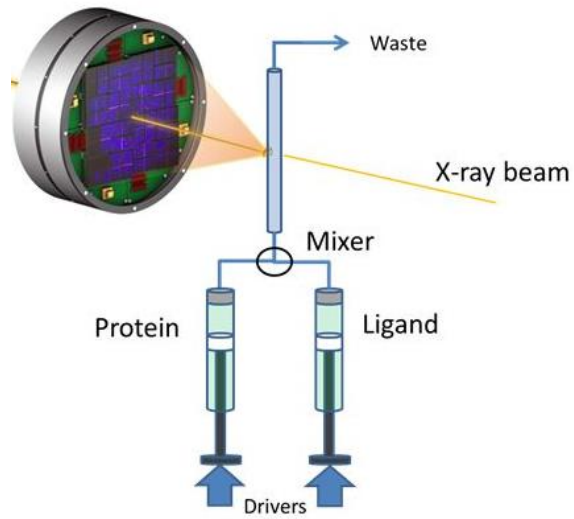


Figure 2.1.: the set up for the SAXS and WAXS measurements. The protein and ligands were loaded into the syringes that were pumped at the same rate, mixed in a mixer and the measured in the capillary.

3. RESULTS

3. 1. Constructs design

Original constructs were designed by F. Brueckner and R. Krammerer. Full construct sequences are attached in the appendix. All constructs included Kozak sequence to enhance the translation of the protein and a unique NheI sequence before the first methionine and NotI sequence at the end of the construct. This allowed simple cloning through NheI/NotI cleavage sites. All constructs included T4-lysozyme (T4L) encoded by NIFEMLRIDEGLRLKIYKDTEGYTIGIGHLLTKSPSLNAAKSELD KAIGRNTNGVITKDEAEKLFNQDVDAAVRGILRNAKLKPVYDSLDAVRRRAALINMVFQMGE TGVAGFTNSLRMLQQRWDEAAVNLAKSRYNQTPNRAKRVITTFRTGTWDAY instead of ICL3. Before the addition of T4L, ICL3 was cut, leaving between 2 and 9 AA on each side and adding a small portion of ICL3 from human β 2 AR before (AKRQL) and after (KFCLKEK) the T4L. All constructs included the X^{3,41}W mutation which was identified in human β 2 AR [116] where it increased the thermostability as well as the expression of the protein. Mutations can be transferred between closely related GPCR's [117]. The superscripts denote Ballesteros-Weinstein numbering [118] where the first number depicts the helix number followed by the amino acid position where the number 50 is assigned to the most conserved amino acid in the helix. The numbers are decreasing to the N-terminal and increasing towards the C-terminal end of the helix. Additionally β 3 AR included the mutation E^{1,31}A that is predicted to increase the expression of the protein (communication with C. Tate). Unless C-terminus is very short (for example 27 AA long C-terminal in α 1A AR), C-terminal was cut after 15-25 AA. At the C-terminal end, 3C protease cleavage site was added, followed by GFP, TEV protease cleavage site and 1D4 peptide (TETSQVAPA) sequence used for the affinity purification. The N-terminus was left intact (figure 3. 1.). All genes were cloned into pACMV-tetO vector for the expression.

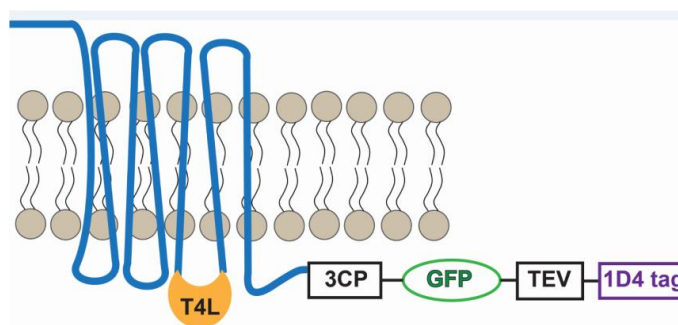


Figure 3.1.: A general scheme of the crystallisation constructs. ICL3 was cut and replaced with T4L, C-terminal was cut and followed by 3C protease cleavage site, GFP tag, TEV cleavage site and 1D4 tag for affinity purification.

3. 1. 1. Design of $\alpha 2C$ and $\beta 3$ AR constructs with transferred mutations

In order to increase the chances for crystallisation, more constructs were introduced. Since an extensive thermostabilisation has been done on turkey $\beta 1AR$, which has led to successful crystallisation, the mutations that were introduced in this construct were taken as a basis for the new construct design [119]. Some thermostability assays have been done on $\alpha 1A$ and $\alpha 1B$ ARs that have also been considered, especially for the mutation of $\alpha 2C$ AR [120]. Additionally all newly designed constructs were computationally checked so that they did not introduce additional clashes in 3D structure. The mutations were adjusted according to all the acquired knowledge at the time of design. $\beta 3$ and $\alpha 2C$ AR belong to the same family as turkey $\beta 1$ AR with a reasonable sequence similarity: 62% between human $\beta 3$ and turkey $\beta 1$ AR and 42% between human $\alpha 2C$ and turkey $\beta 1$ AR. The sequence similarity between human $\alpha 2C$ and human $\alpha 1A$ ARs is 49%, while the similarity between human $\alpha 2C$ and human $\alpha 1B$ ARs is 48% as determined by using EMBOSS Water (EMBL-EBI). Transferring mutations might therefore be beneficial in increasing the melting temperature and “locking” the protein in a single conformation.

The first construct of $\alpha 2C$ AR included the following mutations: $I^{3.40}V$, $V^{3.41}W$, $Y^{5.58}A$, $L^{7.48}M$ and $Y^{7.53}L$ (m2 $\alpha 2C$ -T4L AR). The second construct included the following mutations: $S^{2.45}Y$, $A^{2.49}V$, $L^{3.29}T$, $I^{3.41}W$, $S^{3.53}A$ and $F^{7.39}L$ (m $\alpha 2C$ -T4L AR). Mutations are represented on figure 3.2.

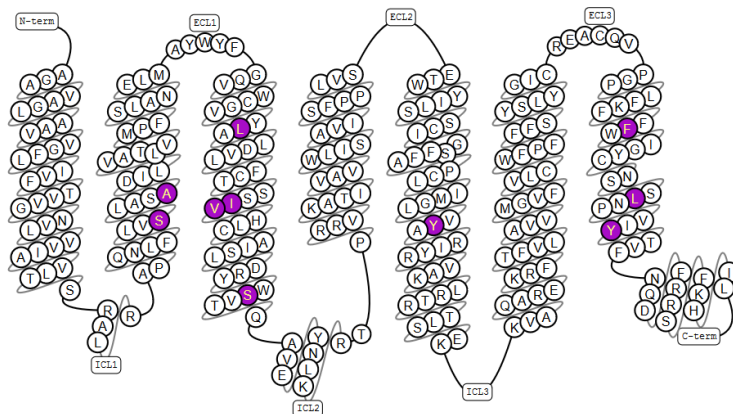


Figure 3.2.: mutations included in $\alpha 2C$ adrenergic receptor. The mutated amino acids are represented in violet. Figure prepared using GPCRdb [121, 122].

Two mutations ($E^{1.31}A$ and $E^{3.41}W$) were included in all $\beta 3$ AR constructs. The first construct of $\beta 3$ AR additionally included the following mutations: $M^{2.53}V$, $I^{3.40}V$, $Y^{5.58}A$, $F^{7.48}M$ and $Y^{7.53}L$ (m2 $\beta 3$ -T4L AR), while to the second one the following mutations: $M^{2.53}V$, $I^{3.40}L$, $Y^{5.58}L$, $F^{6.44}H$, $F^{7.48}M$ and

Y^{7.53}L were added (mβ3-T4L AR). The second construct is referred in the rest of the thesis as the “mutated mβ3-T4L AR”. Mutations are graphically represented on figure 3.3.

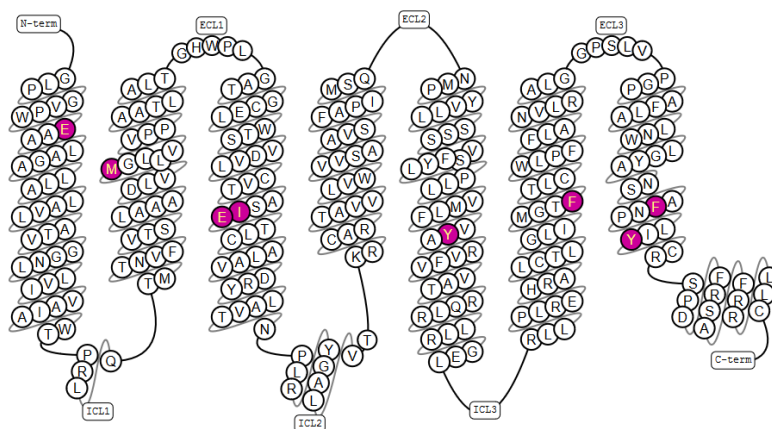


Figure 3.3.: mutations included in β3 adrenergic receptor. The mutated amino acids are represented in dark pink. Figure prepared using GPCRdb [121, 122].

All 4 constructs were cloned into the pACMV-tetO vector for the expression in HEK293 GnTi- cells.

3. 2. Constructs test

3. 2. 1. Expression tests

All constructs were firstly assessed for their suitability for crystallisation. The criteria included the amount of the adrenergic receptor expression, monodispersity of the sample and the localization of the protein in the cell. For this, the proteins were expressed in 6 well plates. The amount of the expression and the localization of the proteins were checked with the in-plate screening for the GFP fluorescence using FLOID® Cell Imaging station (figure 3. 4.). After harvesting, the level of expression and the oligomerization state of the proteins were checked with in gel fluorescence (figure 3. 5.) and FSEC (figure 3. 6.).

From the in-plate screening, it was obvious that some constructs (β3-T4L, β1-T4L) expressed well, while others (α1D-T4L(2)) expressed to lower extent. Besides the extent of expression, the imaging provided information about the localization of the protein as well as the state of the cells. While some cells changed the morphology to spherical (α1D-T4L (2)), others still preserved the normal morphology of the HEK293T cells and the GFP fluorescence could clearly be seen in the membranes of the cells (β1-T4L).

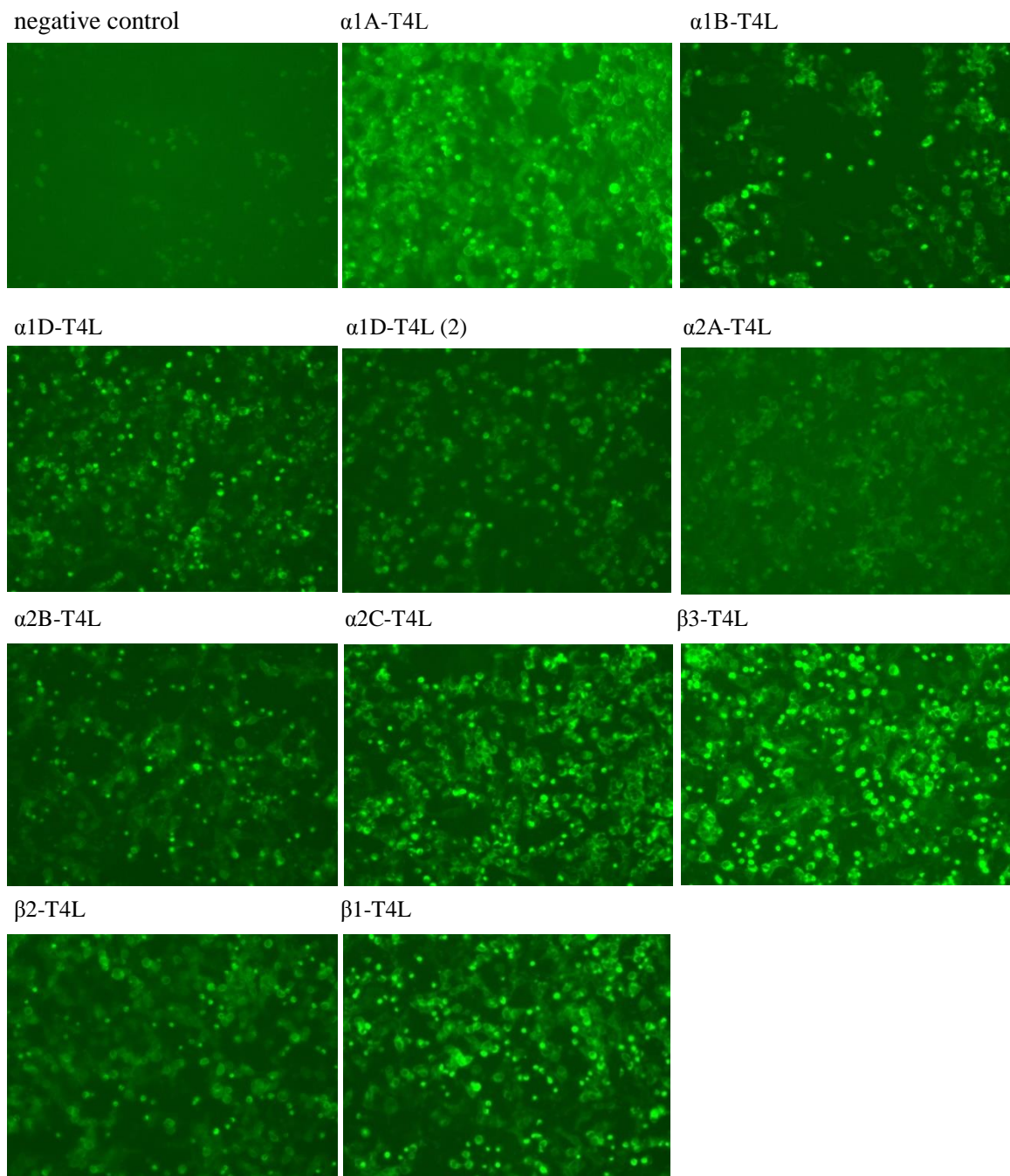


Figure 3. 4: in plate GFP fluorescence of all constructs expressed in 6 well plates. The samples were checked just before harvesting (72 hours after transfection). The light exposure was set to 40% in order to allow comparison between the constructs. Together with other tests, this was an important method to prove how well and where the protein is expressed.

In gel fluorescence was the essential test for determining the amount of the expression of proteins (figure 3. 5.). The extent of protein expression was judged through the GFP fluorescence observed on the gel. If the protein was not expressed, there was no or very weak signal as in the case of $\alpha 1D$ adrenergic receptors. When GFP fluorescence was clearly observed, the extent of the protein

expression was judged as reasonable, while proteins expressing very well showed very strong GFP fluorescence as in the case of $\beta 3$ adrenergic receptor. While some proteins were expressing really well (for example $\alpha 2B$ -T4L, $\beta 3$ -T4L, $\beta 1$ -T4L ARs), others expressed to a reasonable extent ($\alpha 2C$ -T4L, $\beta 2$ -T4L, $\alpha 1A$ -T4L ARs) and some showed almost no expression ($\alpha 1D$ -T4L ARs). It was obvious that in all cases, there was also a small amount of free GFP expressed (bands at 25 kDa). Figure 3. 5. also shows that some samples ran as a single band ($\alpha 2B$ -T4L, $\beta 1$ -T4L) but the majority displayed broad bands due to different glycosylation. Negative control, where cells were transfected with PEI and distilled H₂O, showed no expressed GFP tagged protein.

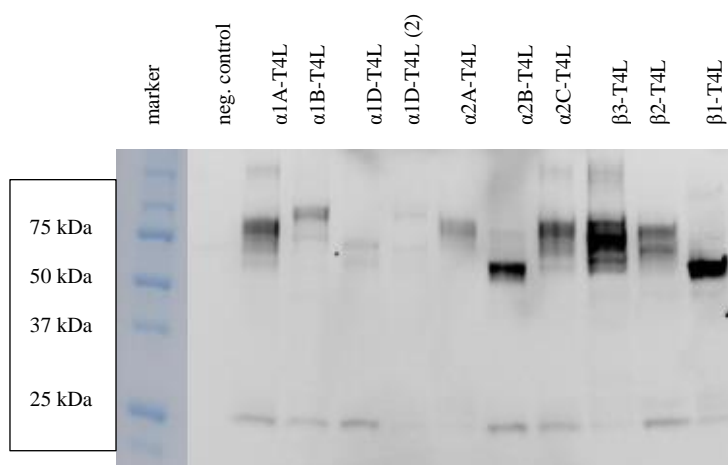


Figure 3. 5: in gel fluorescence of transiently transfected adrenergic receptors in HEK293T cells. The samples were run on 12% Tris-Glycine gel at 120 V for 1 hour 40 min. The gel was analysed using Amersham Imager 600 (GE Healthcare) using blue filter (460 nm). The intensity of the bands gave a rough estimate of expression level of proteins.

The position of the peak and the shape of the curve in FSEC (figure 3. 6.) gave additional information about the extent of the expression, the monodispersity and the size of the protein. FSEC tests confirmed that $\alpha 1B$ -T4L, $\alpha 1D$ -T4L and $\alpha 1D$ -T4L(2) ARs showed very low expression as the signal was basically the same as the signal of the negative control. The rest of the constructs showed different levels of expression, with $\beta 3$ -T4L and $\beta 1$ -T4L ARs showing the highest expression, followed by $\alpha 1A$ -T4L, $\alpha 2B$ -T4L and $\alpha 2C$ -T4L ARs. While the majority of the samples eluted at approximately 2.5 mL, $\alpha 2B$ -T4L and $\beta 1$ -T4L ARs eluted at 2.7 mL which gives an implication that these samples have lower molecular weight. Even though that the samples did not always give perfect monomeric peaks and occasionally showed multiple peaks, the assay provided sufficient information about the aggregation state and monodispersity of the analysed samples.

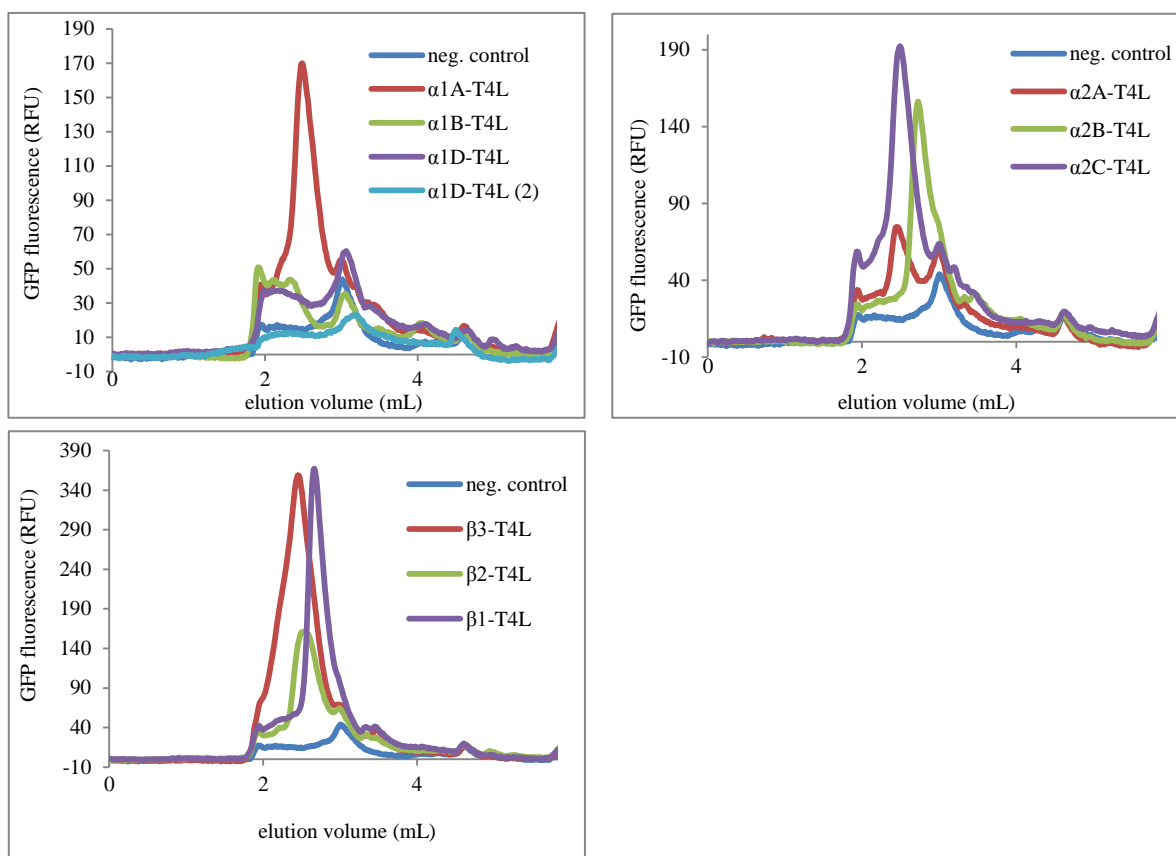
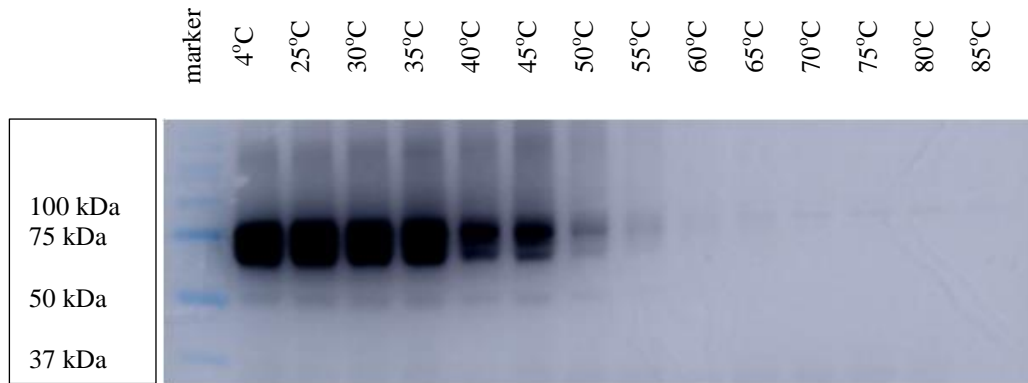


Figure 3. 6.: FSEC analysis of crude extracts. The proteins were solubilized in 20 mM HEPES pH 7.45, 150 mM NaCl, 10% glycerol (v/v), 1% DDM with 0.1% CHS, the supernatant was run on an Ettan LC using TSKgel® G3000SWXL HPLC Column and running buffer: 20 mM HEPES pH 7.20, 150 mM NaCl, 10% glycerol (v/v), 0.02% DDM with 0.002% CHS. Since the same amount of the protein was analysed, the extent of the expression can be assessed by the height of the signal, while the elution volume is connected with the size of the molecule.

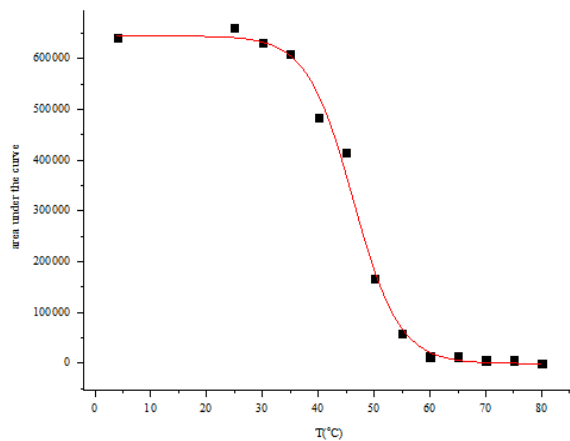
3. 2. 2. In gel thermostability assays with crude protein samples

To determine the stability of the constructs, in gel thermostability assays were performed (figure 3.7.). After heating the proteins, the aggregates were removed from the sample by centrifugation. The supernatant was loaded on the gel to determine the amount of the protein in the sample. The melting temperature was determined for all the constructs, however $\alpha 1D-T4L$, $\alpha 1D-T4L (2)$ and $\alpha 2A-T4L$ were expressing at such low levels that only one temperature ramping experiment was performed. For the rest, the experiments were performed in duplicate. The deviation was between 0-2°C, except for $\alpha 1A-T4L$ where higher discrepancies were observed. The highest T_m was determined for $\alpha 1B-T4L$ AR, but the construct was not expressing well enough to perform a duplicate.

a)



b)



c)

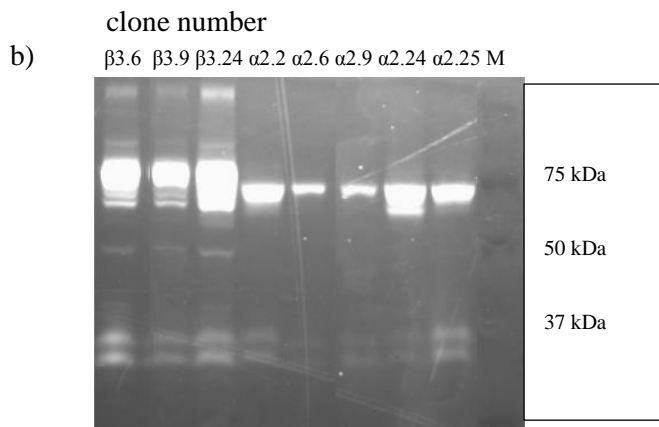
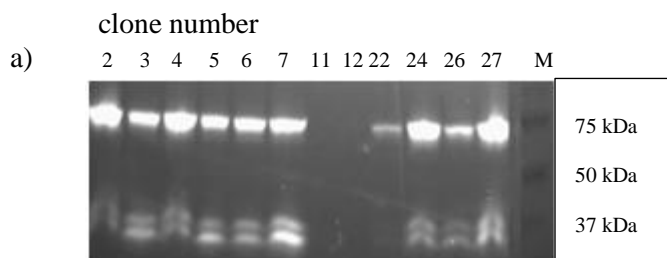
| construct | apparent T_m (°C) |
|---------------------|---------------------|
| α 1A-T4L | 50.4 \pm 5.7 |
| α 1B-T4L | 57.2 |
| α 1D-T4L | 51.1 |
| α 1D-T4L (2) | 43.0 |
| α 2A-T4L | 46.1 |
| α 2B-T4L | 39.1 \pm 2.4 |
| α 2C-T4L | 44.5 \pm 0.4 |
| β 3-T4L | 53.2 \pm 0.2 |
| β 2-T4L | 51.0 \pm 1.1 |
| β 1-T4L | 43.3 \pm 1.4 |

Figure 3. 7.: in gel thermostability assay. Samples were loaded on 12% glycine gel and run at 120 V for 1 hour and 40 min. GFP fluorescence was imaged (a). The amount of the GFP fluorescence was determined with the in-house program and was plotted against the T at which the samples were incubated (b). The melting temperatures (mid-point of transition) determined with this method for the constructs are presented in c).

3. 3. Stable cell line production and selection, protein production

Stable cell lines of HEK 293 GnTi- cells were produced for all selected constructs in order to be able to produce proteins in large extent. In the first round of clonal selection the number of clones were reduced from 15-20 to the 3-5 best expressing clones. Since only one vial of each clone was frozen after the first round and some clones were lost through this process, the number of clones chosen after the first round needed to be high enough to account for these losses. Figure 3. 8. a) shows that in the first round clones were expressing to different extent. Some clones did not express any protein at all (clones number 11 and 12) due to the incorporation of the gene in a wrong place in the genome. Others expressed more protein (for example clones number 24 or 27). In the second round, the clones

were expressed in 10 cm plates, so the amount of the protein for analysis was higher. In both cases, the amount of protein was determined by analysing the GFP signal observed on the gel. BCA assay was performed to determine the total amount of the protein. Figure 3. 8. c) shows the summary of the GFP analysis of individual clones and BCA analysis for the total protein for the second round of clonal selection of α 2C-T4L and β 3-T4L ARs. From the ratio of (GFP fluorescence)/(total protein amount) the best expressing clones were chosen for the large scale protein production: clone number 6 for β 3-T4L AR and clone number 24 for α 2C-T4L AR. Figure 5 c) also shows that a lot of clones in the second round showed similar GFP fluorescence/total protein ratio which means that one round was sufficient to get the best expressing clone for the large scale protein expression.



c)

| Clone | GFP fluorescence [mg/mL] | Total protein concentration [mg/mL] | Ratio: GFP fluorescence/ total protein |
|-----------------|--------------------------|-------------------------------------|--|
| β 3.6. | 11843.7 | 6.173 | 1918.6 |
| β 3.9. | 5707.4 | 6.131 | 930.9 |
| β 3.24. | 17025.7 | 10.198 | 1669.5 |
| α 2C.2. | 5079.6 | 20.620 | 246.3 |
| α 2C.6. | 972.6 | 2.431 | 400.1 |
| α 2C.9. | 1170.1 | 4.112 | 284.6 |
| α 2C.24. | 3517.4 | 9.229 | 381.1 |
| α 2C.25. | 3966.5 | 15.706 | 252.5 |

Figure 3. 8.: clonal selection for α 2C-T4L and β 3-T4L ARs. Figure a) shows the results from the first round of the clonal selection for α 2C-T4L, where it can be clearly seen that some clones were not expressing, while others were expressing the protein to different extents. Figure b) shows the second round of clonal selection for both constructs. Figure c) shows the summary of the second round of clonal selection.

The expression of clones and localisation of the protein was also assessed with in plate screening. Figure 3.9. shows expression of two different clones. While 3.9. a) shows a good expression of the protein where most of the protein is expressed in cell membranes, figure 3.9. b) has less expressed protein and, while the protein is expressed in the membranes, it is also expressed inside the cells. Figure 3.10. represents the difference in expression of β 3-T4L and m β 3-T4L ARs when expressed in suspension cell cultures. It can be seen that the mutated receptor expressed to lower extent than the non-mutated one, which means that the mutations influenced the expression of the receptor.

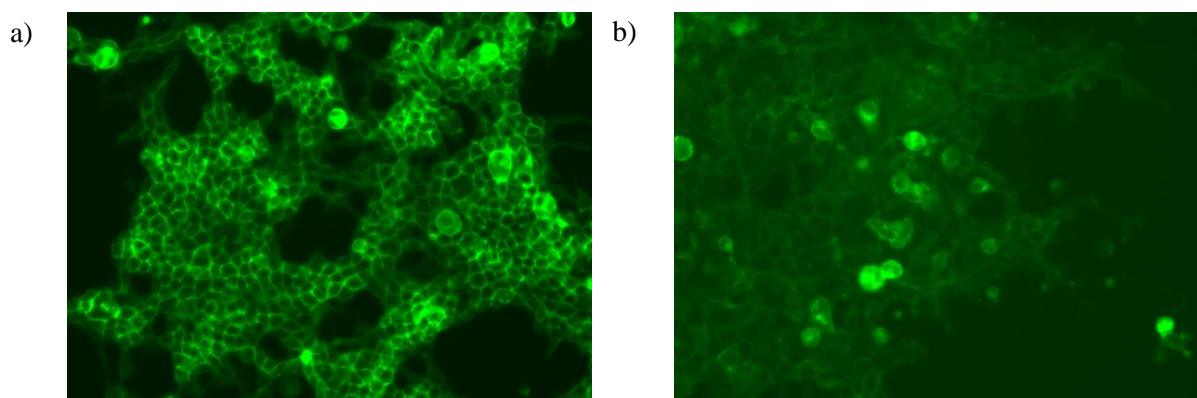


Figure 3.9.: GFP imaging of two different clones expressing the same protein. In plate screening can clearly show the differences between different clones in protein expression and localization.

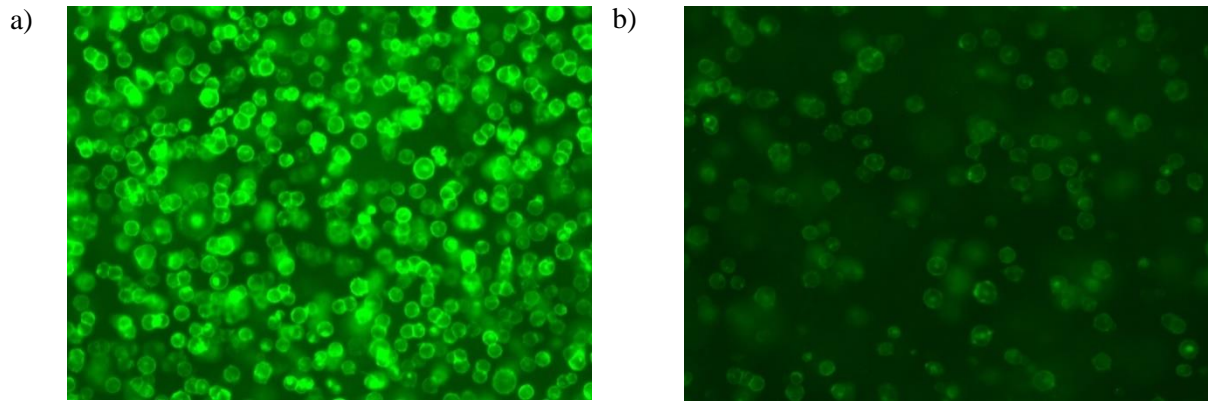


Figure 3.10.: GFP imaging of the protein expressed in the shaker flask. a) represents the $\beta 3$ -T4L 50 hours post-induction and b) represents the $m\beta 3$ -T4L 50 hours post induction.

GFP imaging of cells was also used for the suspension cultures which was extremely useful as a quick check how well the protein is expressing after the induction in order to determine the right time to harvest the protein (figures 3.11.).

Figure 3.11. represents how the expression of the protein increased over time following the induction of the cells. While there was basically no protein expression at 4 hours after the induction, protein started to be expressed at 20 hours post-induction when the protein can be clearly seen in the membrane of the cells. The amount of the protein then increased at 50 hours after the induction when the protein was harvested.

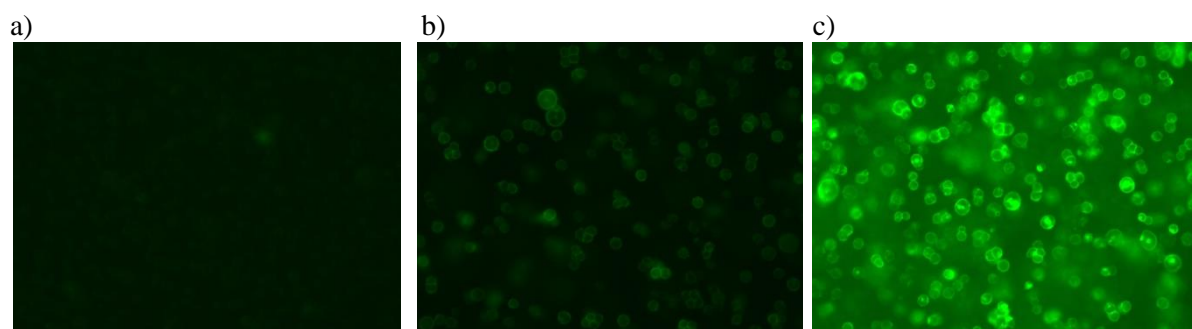


Figure 3.11.: GFP imaging of the same shaker flask showing the increase in the GFP fluorescence (hence in the protein production) in the time following the induction of cells. The same sample was checked 4 (a), 20 (b) and 50 (c) hours post-induction.

3. 4. Testing the temperature stabilisation by ligands

The apparent melting temperature (T_m) was determined in an assay where the protein was heated at regular intervals (4°C/min). Exposed cysteines from the core of the protein bind to the CPM (N-[4-(7-diethylamino-4-methyl-3-coumarinyl) phenyl]maleimide) dye which in turn results in the increase of fluorescence (figure 3.12. a)). The first derivative (figure 3.12. b)) allowed us to determine the T_m .

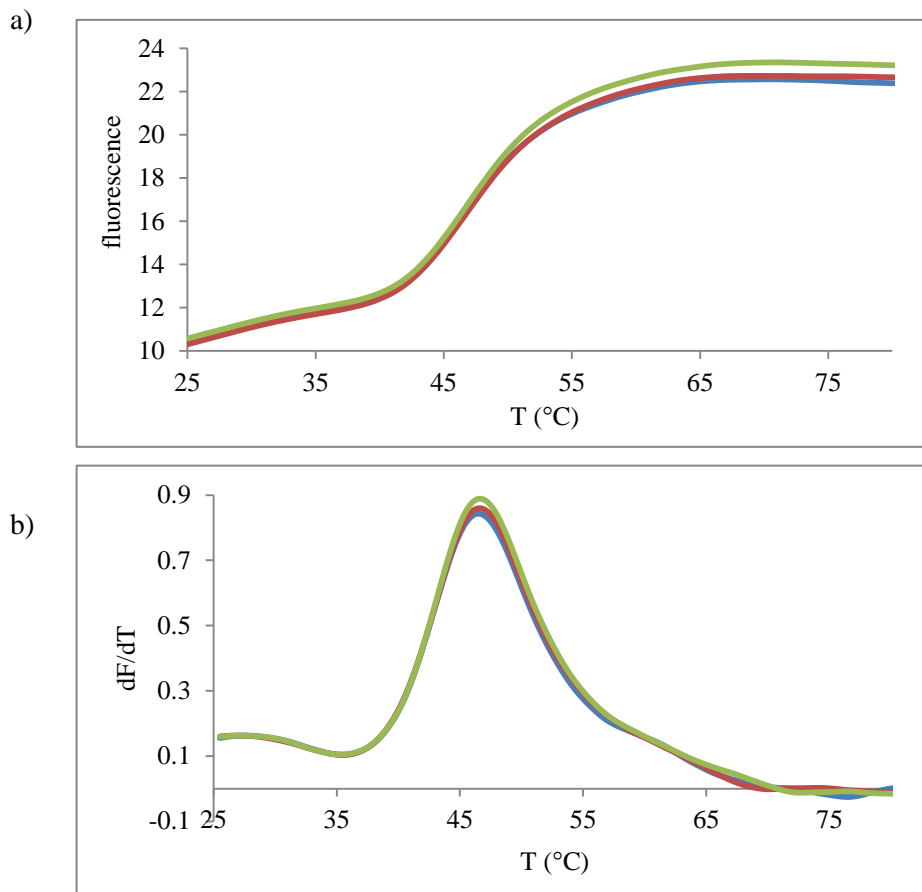


Figure 3.12.: CPM assay results. a) The CPM assay experiment profile: the increase in the fluorescence during the heating of the protein. A triplicate of the same sample was measured. b) The first derivative of a) that was used to determine the T_m .

3. 4. 1. Optimisation of the CPM assay

When the T_m of proteins with and without GFP were tested, the addition of GFP did not have an effect on the melting temperatures as the transitions are well separated (T_m of GFP is 85°C). Addition of GFP also did not have an effect on the absolute melting temperature of the protein. The proteins were purified several times and the melting temperatures between different preparations have not shown a significant difference. The right concentration had to be determined first. For this, four different

amounts of the protein (2, 4, 8 and 10 μg) were tested in order to choose the lowest concentration of the protein that gives a reasonable signal and shows reliable transition between the folded and unfolded protein. 2 μg was chosen for $\alpha 2\text{C-T4L AR}$ and 4 μg /reaction was chosen for $\beta 3\text{-T4L AR}$ (figure 3.13.).

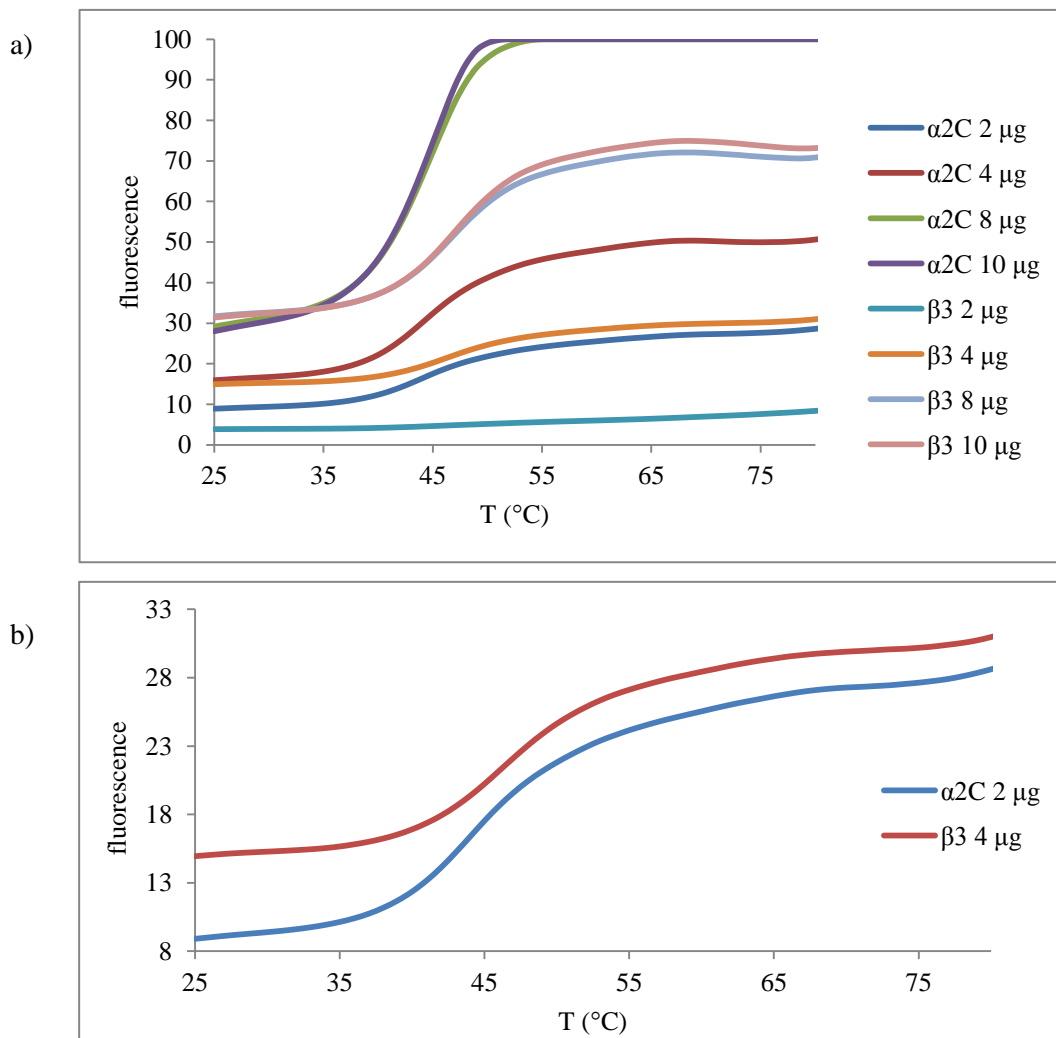


Figure 3. 13. CPM assay for $\alpha 2\text{C-T4L}$ and $\beta 3\text{-T4L ARs}$. Four different amounts of the protein were tested. Each concentration was done in triplicate and the average is shown on the figure a). The most optimal amounts of the proteins are shown in b). Triplicates did not differ for more than 0.5°C which is also the temperature accuracy of the method.

When different concentrations of the dye were tested, the smallest amount (0.25 μg) always showed a higher melting temperature than the rest (figure 3.14.). This was true for both receptors and all the amounts of the protein used. This was probably due to the lack of the dye to react with exposed cysteines. Since the rest of the curves showed similar transitions, 0.5 μg of CPM dye per reaction was chosen for both proteins

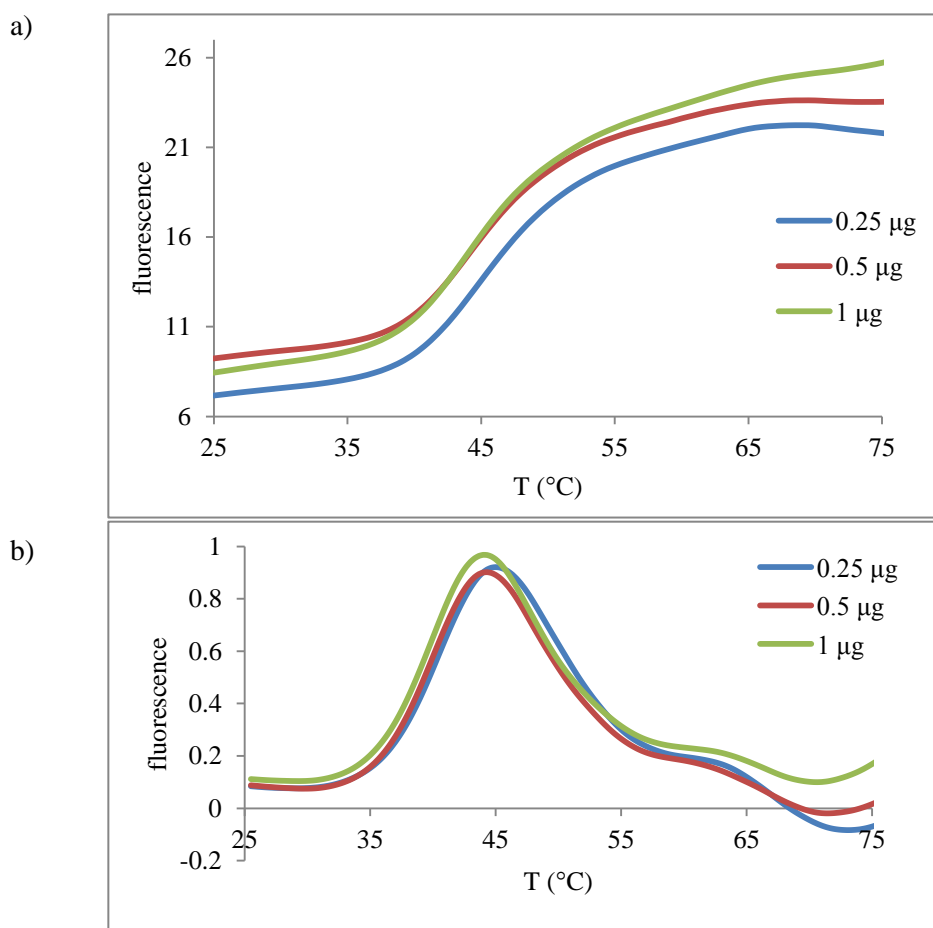


Figure 3. 14.: the determination of the right amount of the dye for the assay. Different amounts of the dye (0.25, 0.5 and 1 µg) were tested with the same amount of the protein. The original data (a) and the first derivative (b) are represented. 0.5 µg was chosen as the right amount of the dye. In both cases, the curves are the averages of triplicates that were measured.

3. 4. 2. Ligand-induced stabilisation of α 2C-T4L AR

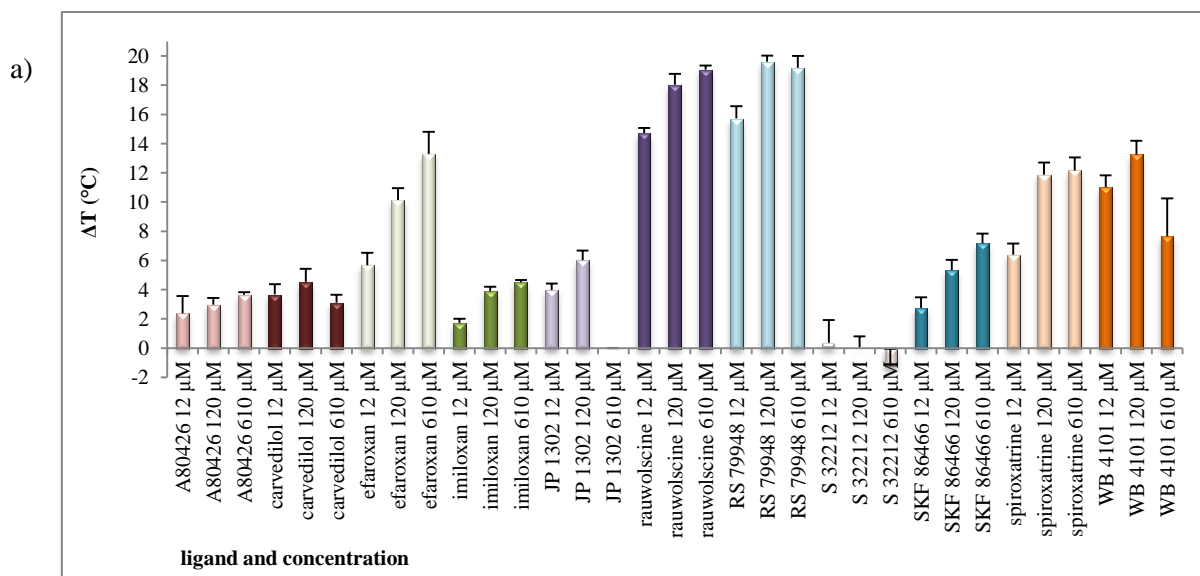
11 antagonists (figure 3. 15. a)) and 3 agonists (figure 3. 15. b)) have been tested for this receptor. As a control, also 16 ligands that were defined as β ARs ligands were tested (figure 3. 15. c)).

With the exception of S32212 hydrochloride, all antagonists and agonists showed an increase in apparent T_m compared to the apo form of the receptor (45.2 ± 1.0)°C. With one ligand, JP 1302 dihydrochloride, T_m was not determined at the highest concentration of the ligand due to the strong orange colour that interfered with the assay. While the majority of the ligands thermostabilised the receptor to a small extent, there were two ligands, rauwolscine hydrochloride and RS 79948 hydrochloride, which stabilised the receptor for more than 14°C even at the lowest concentration of the ligand used and for 18°C when 610 µM ligand was added. These two ligands were chosen to be

used for crystallisation trials. Additionally, three more ligands were identified that stabilised the receptor for 10°C when higher concentrations were used: efaroxan hydrochloride, spiroxatrine and WB 4101 hydrochloride. All ligands also showed an increase in the thermostability with increasing amount of the ligand added. The only exception was WB 4101 hydrochloride that showed a smaller stabilisation at the highest concentration compared to lower concentrations of the ligand.

All three agonists showed an increase in T_m . The stabilisation was at least 4°C at the lowest ligand concentration and they all increased the T_m for at least 10°C at the highest concentration with ST 91 showing an increase of 18°C in T_m when 610 µM ligand was used.

When ligands that are not classified as ligand having an effect on $\alpha 2C$ -T4L receptor were tested, the majority did not show any effect. Three ligands, cyanopindolol hemifumarate, formoterol hemifumarate and isoproterenol hydrochloride, increased the T_m for less than 4°C. While cyanopindolol showed bigger effect with $\beta 3$ -T4L AR, the other two had similar effect on both receptors. A ligand that increased the melting temperature of $\alpha 2C$ -T4L AR for more than 14°C at the highest two concentrations was roxindole hydrochloride. This ligand is classified as dopamine/serotonin receptor agonist, but obviously it also has an effect on $\alpha 2$ ARs.



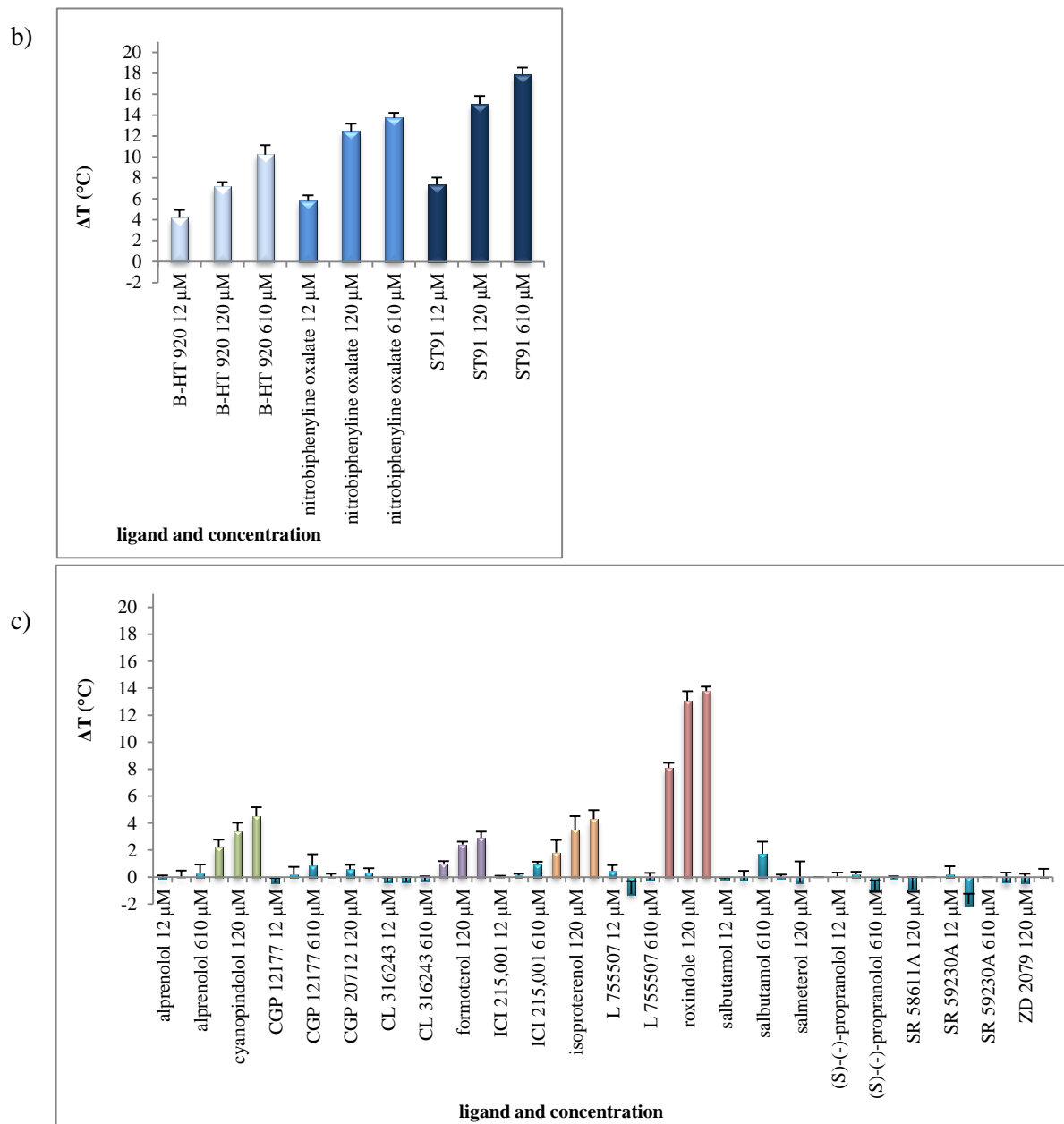


Figure 3.15.: ligand tests with $\alpha 2C$ -T4L AR. Ligands were divided according to their effect on the receptor on antagonists (a)), agonists (b)) and ligands not supposed to have an effect (c)).

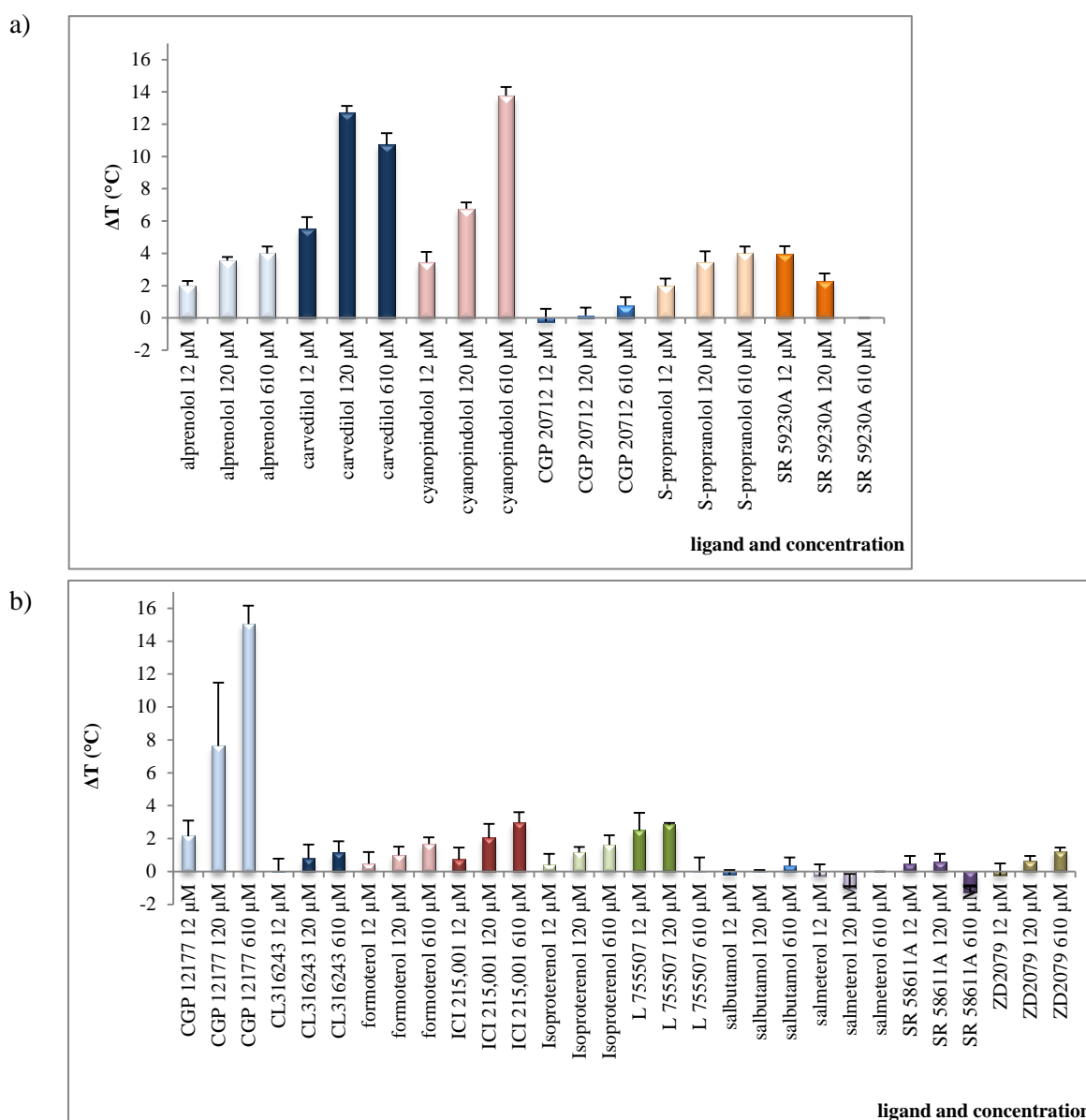
3. 4. 3. Ligand-induced stabilisation of $\beta 3$ -T4L AR

For $\beta 3$ -T4L AR, six antagonists (figure 3.16. a)) and ten agonists (figure 3.16. b)) were tested. In contrast to the ligand test with $\alpha 2C$ -T4L AR, a lot of the ligands only showed a small additional thermostabilisation (up to 4°C) of the apo (46.7±1.0)°C form of the receptor.

However, a few ligands did increase the T_m significantly when added. These were: carvedilol and cyanopindolol hemifumarate among the antagonists that increased the T_m for more than 10°C at the

highest concentration and CGP 12177 hydrochloride among the agonists that increased the T_m for 14°C when 610 μM ligand was used. However, CGP 12177 hydrochloride was also a ligand that showed inconsistent results when 120 μM concentration was used. From this, a high standard deviation arised, which was not normally present for the rest of the ligands.

When the agonists and antagonists of $\alpha_2\text{C}$ AR were cross tested, none of the ligands showed any effect (figure 3.16. c)). As it was hypothesised, the temperature only oscillated for 1-2°C around the temperature of the apo form of the receptor.



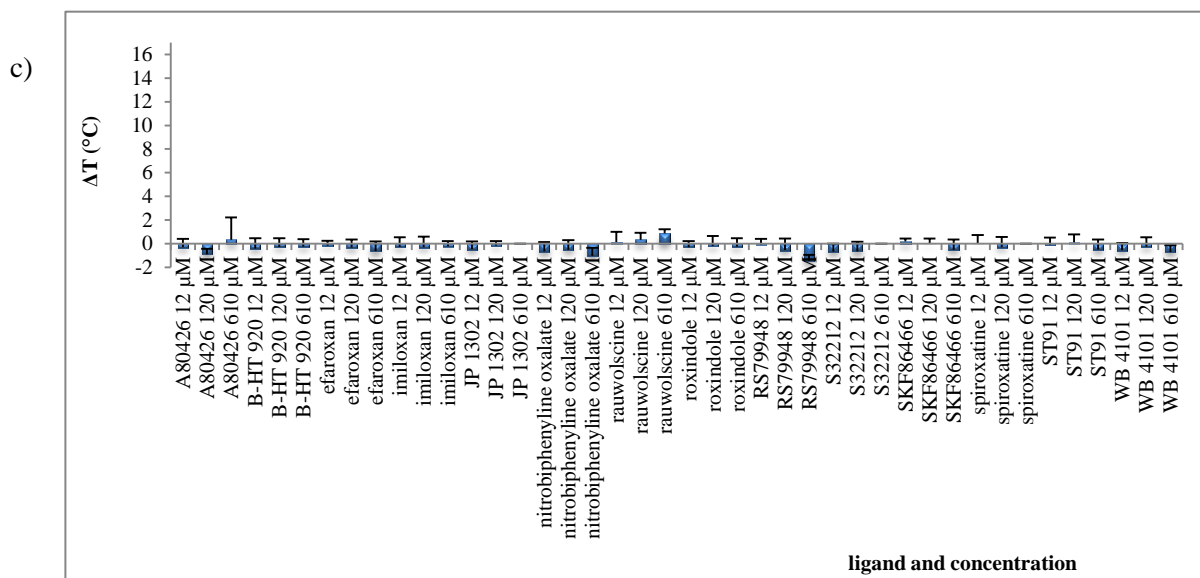


Figure 3.16.: ligand tests with β 3-T4L AR. Ligands were divided according to their effect on the receptor on antagonists (a)), agonists (b)) and ligands not supposed to have any effect (c)).

3. 4. 4. Comparison of stability between the non-mutated and mutated human β 3-T4L AR

The T_m of the mutated receptor was $(48.1 \pm 0.5)^\circ\text{C}$ comparable to the non-mutated receptor: $(46.7 \pm 1.0)^\circ\text{C}$. However, there was a big difference in the effect of ligands on both receptors (figure 3.17.). While some ligands still did not show a big effect, others led to a huge increase in the melting temperature. Cyanopindolol hemifumarate had the biggest increase when 120 μM ligand was used, then the stabilisation of the receptor was approximately 15°C which was similar to the thermostabilisation with 610 μM ligand in the β 3-T4L AR. There was also a substantial increase in the thermostabilisation of carvedilol when the smallest amount of ligand was used. The stabilisation at this concentration was 14°C , again around 10°C more than in the non-mutated receptor. When the highest concentration of carvedilol was used, the stabilisation was over 30°C , however, the whole transition curve of the concentration of this ligand was inconclusive, so it would need to be additionally proven that this stabilisation is due to the influence of the ligand and not the quality of the data.

When agonists were tested, four ligands (salbutamol hemisulfate, salmeterol, SR 58611A hydrochloride and ZD 2079) have still not shown any significant stabilisation. CGP 12177 hydrochloride had a similar transition in both constructs, but have shown a higher T_m and less discrepancy in the mutated receptor. L 755507 had shown the biggest increase in the T_m , the T_m measured was ca. 16°C in the case of all three concentrations, which was almost 10°C more than in the non-mutated receptor. CL 316243 disodium salt, formoterol hemifumarate and isoproterenol

hydrochloride have shown similar behaviour at lower concentration of ligands in both receptors, but increased the T_m for ca. 6°C in the mβ3-T4L AR when the highest concentration of ligand was used.

In tests with alprenolol hydrochloride and ICI215,001 hydrochloride double transitions were observed. While in the case of ICI215,001 hydrochloride the first transition showed similar T_m in both receptors, the second transition had for 10°C higher T_m in the mβ3-T4L AR. Alprenolol hydrochloride also showed over 10°C higher T_m in the case of second transition with more than 30°C thermal stabilisation at the highest ligand concentration. Since this melting temperature is at the limit of the method, this would still need to be confirmed, but the same behaviour was observed in all independent repeats.

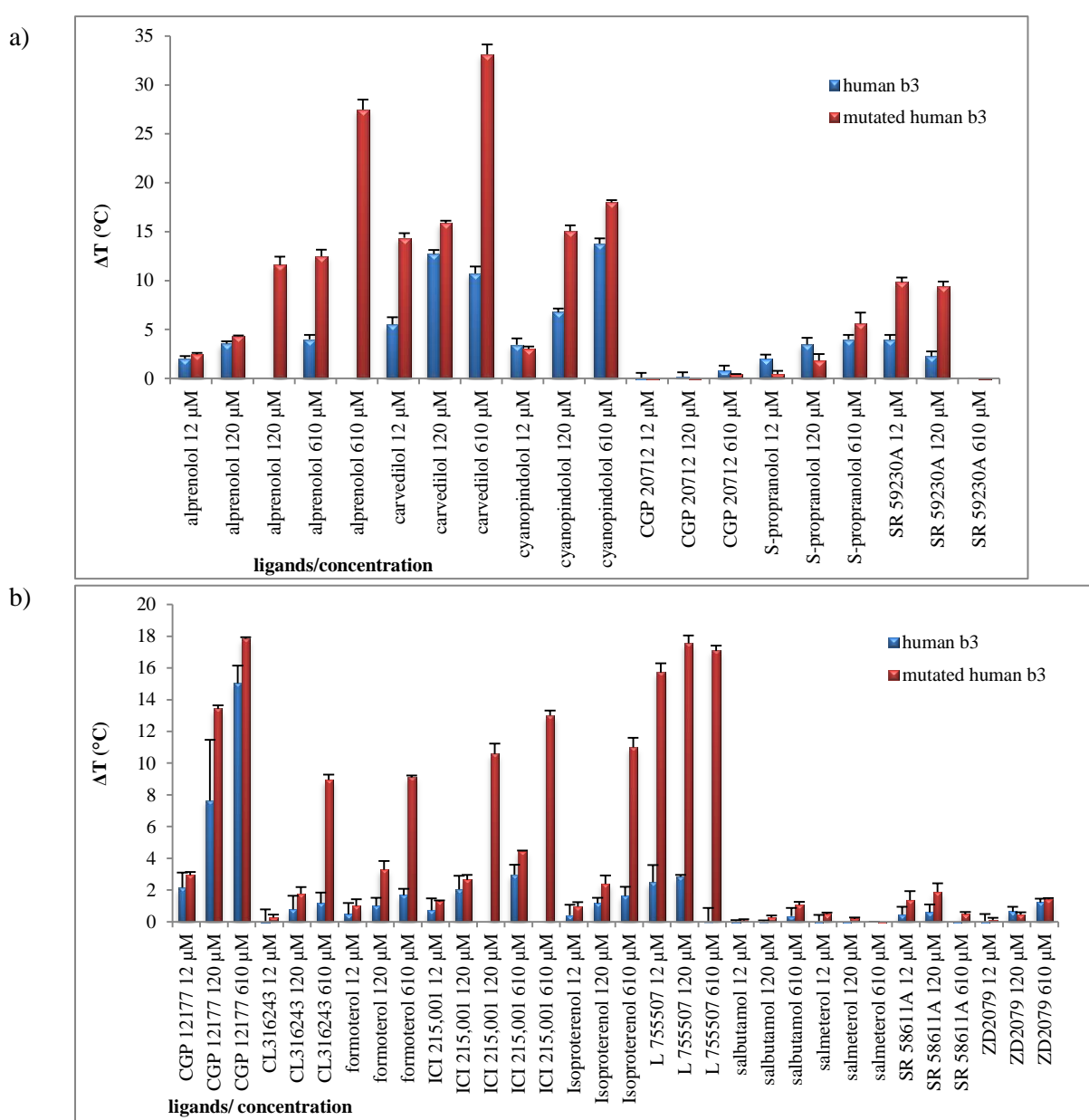


Figure 3.17.: comparison of the thermostabilisation by ligands of mβ3-T4L (red) and β3-T4L (blue) AR's. Comparison of antagonists is presented in a) and comparison of agonists in b).

3. 5. Protein purification

3. 5. 1. Adjusting the parameters for the purification

To determine the appropriate detergent:protein ratio during solubilisation, different concentrations of membranes (weight of membrane in mg/ml of solubilisation buffer) were solubilised in the solubilisation buffer and run on FSEC (figure 3.18.). All samples showed similar curves: a maximum between 2.45 and 2.50 mL with the same height (450 RFU) and a preceding small peak at 1.89 mL. This peak, eluting at the void volume of the column, belonged to the aggregates and got smaller with increased amount of solubilisation buffer which might imply that higher amount of the solubilisation buffer decreased the aggregation. However, the difference was very small and it corresponded with differences in the main peak. When membranes were solubilised at 133 mg/ml, FSEC showed a small signal after the main peak which can be assigned to smaller molecules (free GFP). From these results I decided that solubilisation of 100 mg of membranes/ mL will be used in the purification protocols for the crystallisation.

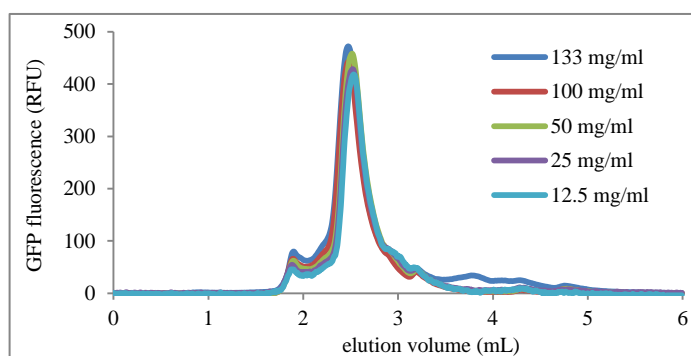


Figure 3.18.: testing the buffer dilutions in order to determine the right amount of the solubilisation buffer. The running buffer was 20 mM HEPES pH 7.20, 300 mM NaCl, 10% glycerol, 0.02% DDM and 0.002% CHS. All the curves were normalized to the amount of the protein present in the sample. 100 mg of membranes/ mL was chosen as the optimal solubilisation volume.

Since the purification was done under gravity flow, proper amount of washing buffer had to be determined. In order to determine the right amount, a sample was taken during the washing at regular interval (every 2.5 CV). The majority of unspecifically bound proteins eluted in the first 3 fractions (W1-W3, figure 3.19.). Fractions 4-5 did not show any additional elution of the protein, therefore 10 CV was chosen for the washing in order to completely wash all the unspecifically bound proteins from the resin.

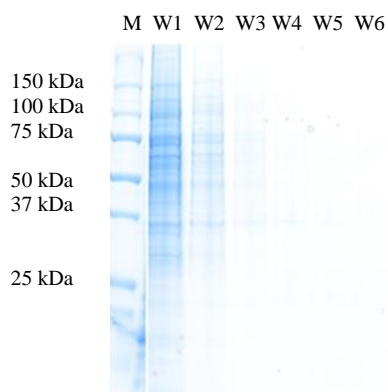


Figure 3.19.: determining the right amount of the washing buffer. Samples were collected every 2.5 CV of washing. 10 CV of washing buffer was chosen for the purification.

The right amount of the protease for the cleavage of the protein from GFP and 1D4 purification tag had to be determined as well in order to achieve a high yield of purified protein. A standard amount of the protein: protease was taken as 1:0.12 (mol/mol). As a test, double amount of the protease was tested as well (figure 3.20.). Samples were tested on FSEC after O/N cleavage. Even though that, in this specific case, the curves were not optimal (a broad main peak and big shoulder before the main peak), both curves showed similar behaviour with exactly the same height. We cannot assign this sample behaviour to the possible degradation as a result of excess protease concentration. Since the height of both samples was the same, already smaller amount of the protease was sufficient for the cleavage of the majority of the protein. This was confirmed by measuring protein concentration by UV absorption. Around 90% of the protein bound to the resin was eluted from the resin after cleavage.

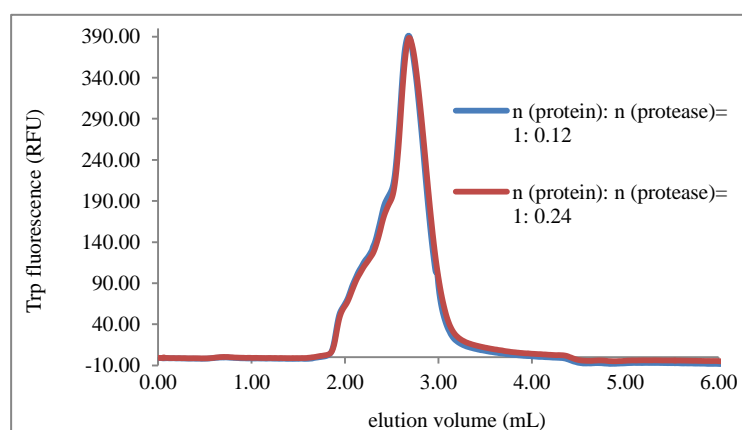


Figure 3.20.: determining the right amount of the protease for protein cleavage. Two concentrations were tested. Since the same height has been obtained, it can be concluded that smaller amount of the protease completely cleaved the protein

The optimal amount of the elution buffer had to be determined. The protein was cleaved O/N in 1.5 CV (ACI) and then eluted several times with 1 CV elution buffer (E1-6) in order to evaluate until when the protein was eluting. The goal was to elute as much protein as possible, however, excessive elution would lead to a huge amount of sample volume that would need to be concentrated. This is not preferential when dealing with membrane proteins since detergent is concentrated together with the protein as well. Excessive detergent concentration would lead to protein unfolding and aggregation. After the third elution (E3), there was almost no more protein eluting (Figure 3.21.). By adjusting the time of elution, the volume was limited to 2 elutions after the O/N cleavage. Even though that some protein was still left on the resin, this was an acceptable compromise between the amount of protein eluted and the amount of the buffer that had to be concentrated.

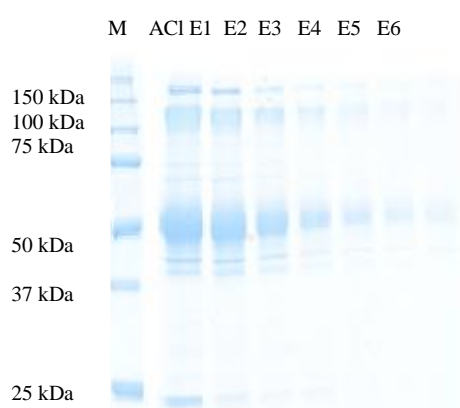


Figure 3.21.: Elution of protein from the resin with increasing volumes of the elution buffer.

After the third elution, only a small fraction of the protein was still eluting and with five elutions it was possible to elute all the protein from the resin. However, this amount of the buffer would lead to too much buffer that would need to be concentrated before the gel filtration.

In order to reduce the amount of detergent in the sample, two different amounts of detergent were tested (figure 3.22.). DDM was used for the test as this detergent was used as the detergent of choice in the majority of purifications. The amounts of the detergent and CHS tested were: 0.02% with 0.002% CHS and 0.01% DDM with 0.001% CHS. Gel profiles of both samples are shown on figure 3.22. From the GF profiles it can be seen that 0.01% DDM with 0.001% CHS was not sufficient and a lot of protein aggregated (figure 3.22. b)) compared to the GF profile on figure 3.22. a), where the aggregate peak was much smaller. Therefore 0.02% DDM with 0.002% CHS was kept as the lowest amount of detergent for the purification.

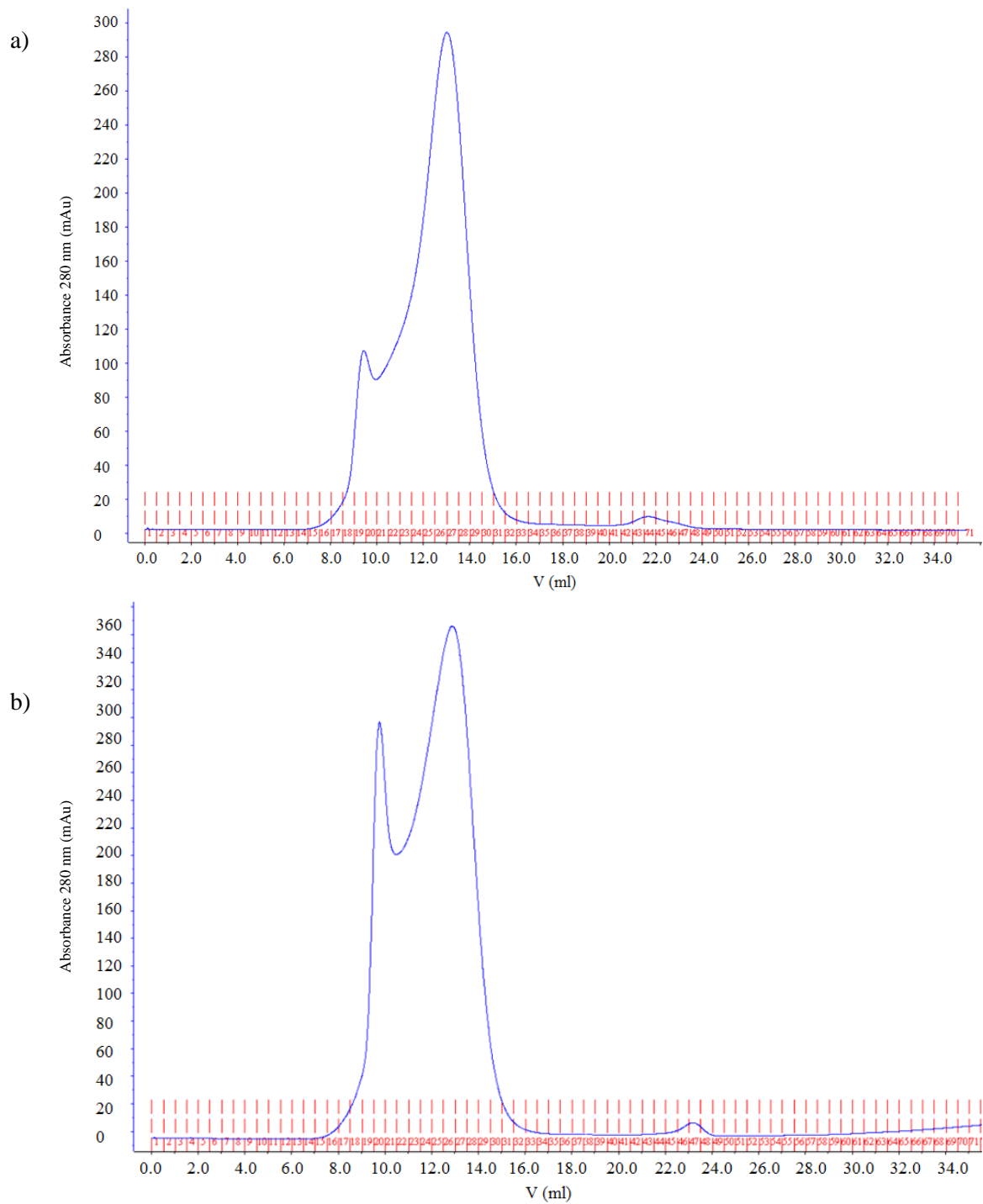


Figure 3.22.: comparison of GF run with two different amounts of detergent: **0.02% DDM with 0.002% CHS (a)** and **0.01% DDM with 0.001% CHS (b)**. Both GFs were performed on the same sample since samples also differed between different expressions. It can be seen that the smaller amount of detergent was not sufficient since the aggregation peak was almost the same as the sample peak.

3. 6. Purification of β 3-T4L AR

A purification example is shown on figure 3.23. The same profile was obtained in all detergents, but it did slightly differ between expressions. Protein eluted as a major peak at 50 kDa with another band at ca. 40 kDa. Before GF a band around 100 kDa could be observed that belongs to higher oligomers or aggregates, an artefact on SDS-PAGE that is common upon GPCRs. This band was mostly removed from the sample during GF. Ni resin removed the protease (band at 25 kDa), but it also bound some protein. Some protein was leaking through the 0.5 mL concentrator that was used to concentrate the sample before crystallisation, however these were acceptable losses. The crystal trials were set up with different detergents as well as with and without GF.

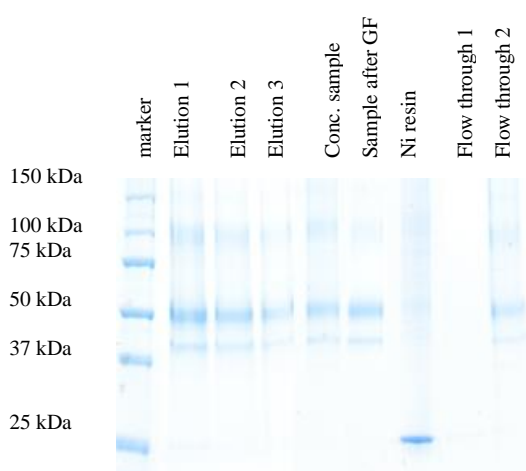


Figure 3.23.: purification of β 3-T4L AR. Sample eluted as a single band at 50 kDa with a faint band at 40 kDa. GF removed the majority of higher order oligomers/aggregates.

3. 6. 1. Detergent tests for crystallisation trials of β 3-T4L AR

Four different detergents were tested, two most commonly used for the LCP crystallisation: DDM and LMNG as well as DM and Hega-10 that were as well used for vapour diffusion experiments.

The protein was stable in all detergents tested (figure 3.24.) and eluted as a single, monodisperse peak when measured with FSEC. It can be seen from figure 3.24. that different detergents slightly shifted a peak. While the protein purified in DM and DDM eluted at 2.60 mL, the protein purified in Hega-10 eluted at 2.43 mL, but when LMNG was used, the protein eluted at 2.80 mL.

Interestingly, the signal of the protein purified in DM showed narrower and slightly more monodisperse signal than DDM. Protein purified in LMNG eluted as a monodisperse peak as well, but

it was slightly wider than the peak of DM and DDM. When the protein was purified in Hega-10 a small shoulder before the main peak was present. Since all detergents showed a good behavior of the protein, crystallisation trials were performed with all of them.

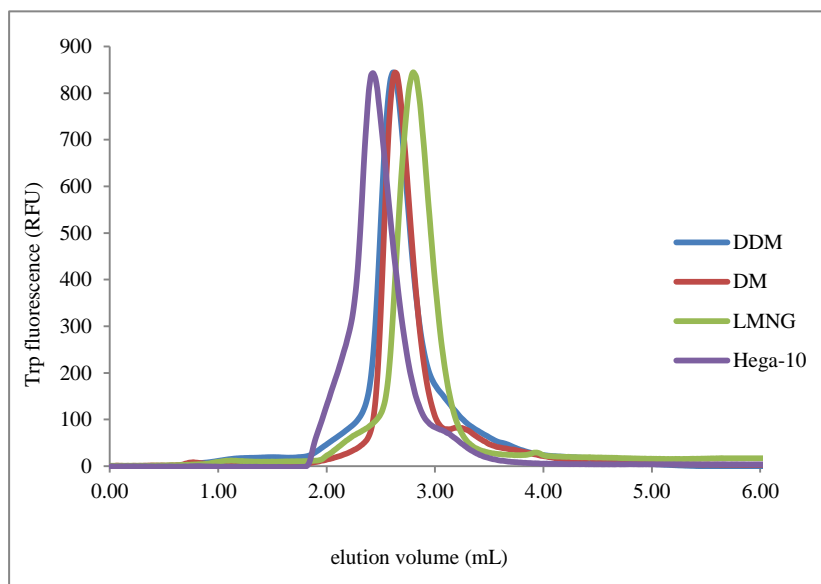


Figure 3.24: FSEC test of different detergents for β 3-T4L AR purified at 4°C. From FSEC traces, all detergents seemed suitable for the crystallisation of β 3-T4L AR. The traces were normalised to the same size for easier comparison.

3. 6. 2. Stability of β 3-T4L AR in different detergents

Samples were tested for the stability in different detergents. DDM and LMNG (figure 3.25.) were used for LCP crystallisation. When the protein in DDM was left at RT O/N, some of the protein aggregated, but 74% of the protein still eluted at 2.6 mL. When the protein was heated to 50°C, 50% of the protein aggregated, however, for crystallisation the RT stability is crucial. When the sample in LMNG was tested, the sample left at RT O/N showed no aggregation. When the sample was heated to 50°C, some aggregation was observed, however, the peak of monomeric protein still showed the same height. From this, it can be concluded that LMNG definitely increases the thermostability of the receptor in detergent. A small shift between the green and red curves in figure 3.25. b) is most probably the result of the experimental error and not caused by the changes in the aggregation state of the protein. Both detergents have shown a similar FSEC trace, which means that the protein was stable in both detergents when purified at 4°C (figure 3.25.) and the sample, was never left at RT during the purification.

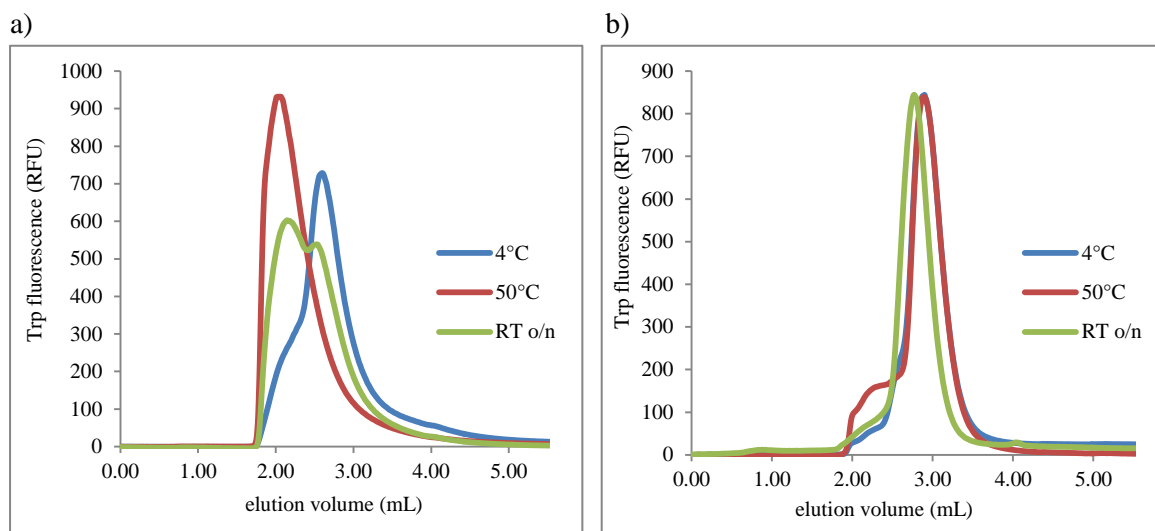


Figure 3.25.: stability of β 3-T4L AR in DDM (a) and LMNG (b) detergents. The protein was stable in both detergents, but LMNG improved stability of the protein compared to DDM.

For VD experiments β 3-T4L AR was purified in DM/Hega-10 mixture. Since, in this case, the protein was left in detergent over a longer time period, the stability is crucial. The stability of the protein in Hega-10 is shown in figure 3.26. Approximately 50% of the protein survived at RT O/N while the majority of the protein aggregated when the protein was heated to 50°C. This was expected since Hega-10 is much smaller detergent than DDM and might not be able to keep the protein as stable. However, the protein still remained relatively stable at RT, therefore VD experiments were set up at RT as well as at 4°C.

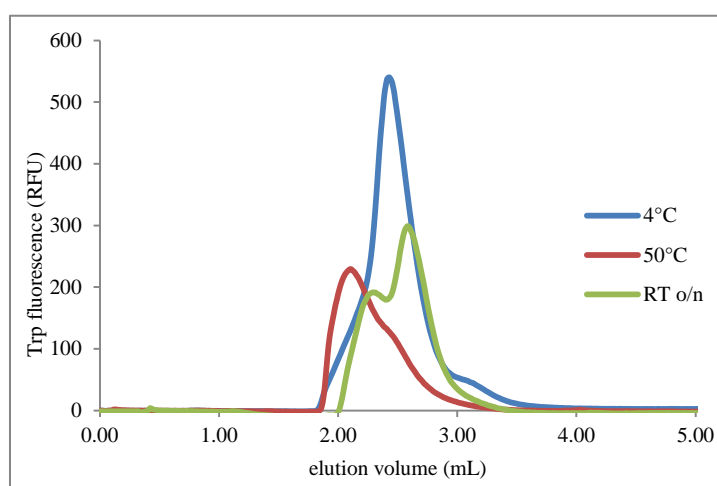


Figure 3.26.: stability tests with Hega-10 detergent. The protein was less stable in this detergent compared to DDM or LMNG. However, still 50% of the protein did not aggregate O/N, therefore VD experiments were set up at RT and 4°C.

3. 7. Purification of mβ3-T4L AR

This construct was initially purified in the same way as all the constructs before. While the instant blue stained gel (figure 3.27.) showed a relatively pure sample, it still had a double band: one at around 50 kDa corresponding to the protein and another at around 40 kDa. There was also an obvious band at 100 kDa that corresponds to dimers. It is obvious that the sample after the GF (last lane) was purer than the one before the GF. It can be seen from the GF (figure 3.28.) that there was a substantial amount of aggregates in the sample loaded on the GF. The sample was also run on the FSEC (figure 3.27.). Even after the GF there was still a small shoulder present before the main peak at 2.7 mL.

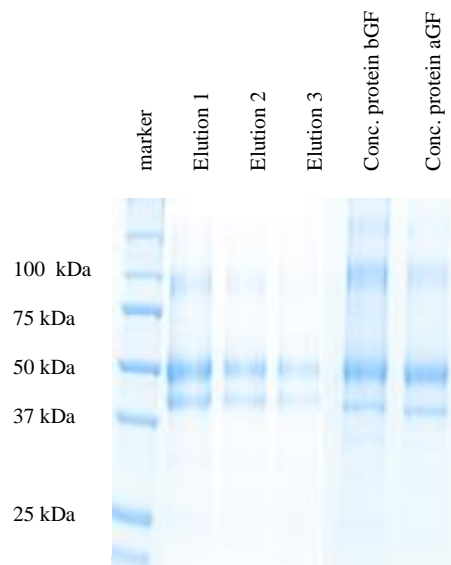


Figure 3.27.: instant blue staining of the purification of mβ3-T4L AR. The first three lanes represent the elution from the column, the last 2 are concentrated samples before and after GF. As seen from the gel, GF did improve the purity of the sample and removed higher oligomers from the sample.

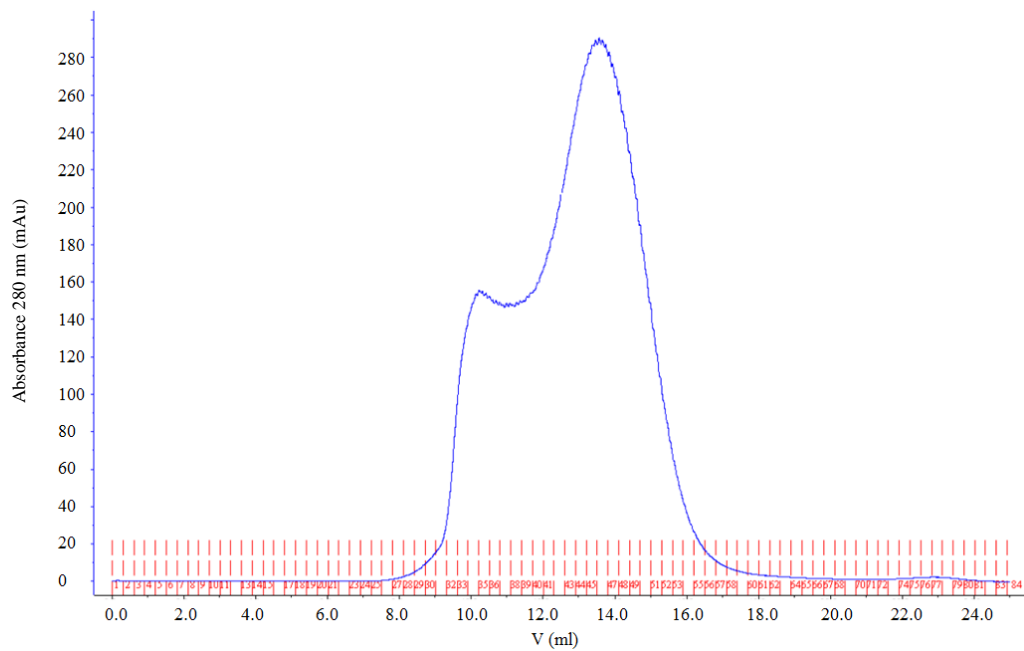


Figure 3.28.: GF profile of the sample. Two major peaks can be observed: aggregates at the void volume (10 mL) of the column and the main protein peak around 14 mL.

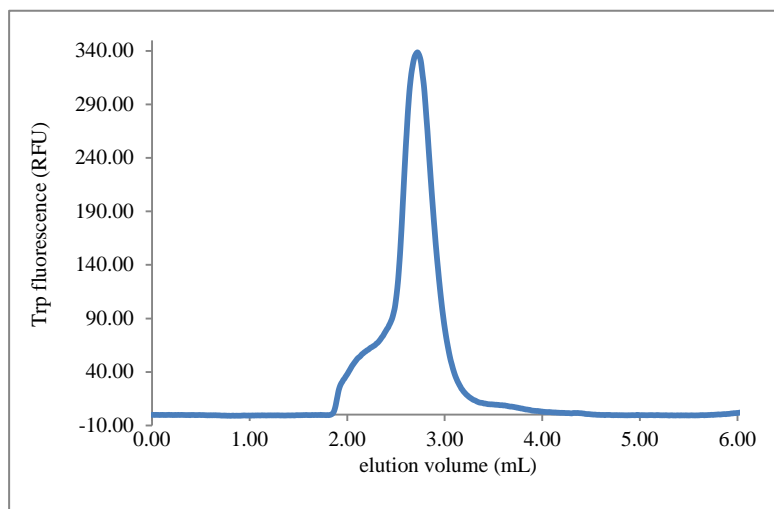


Figure 3.29.: FSEC profile. The main protein peak is quite symmetric, but it still has a small preceding shoulder that might influence the crystallisation process.

3. 7. 1. Optimisation of the purification protocol

After the first potential hits, no bigger crystals were able to be grown and therefore the purification protocol was changed in order to make the construct preparations more monodisperse. The construct was firstly checked for potential glycosylation (figure 3.30.) and phosphorylation (figure 3.31.). The protein before deglycosylation displayed a broad band at around 50 kDa followed by a second band at around 40 kDa. It can be observed that after the treatment with EndoH the main band moved slightly to the smaller size and the band started to separate into two bands. When one unit of the enzyme was used, at least 3 hours of the incubation at RT were needed while with 3 units deglycosylation can be observed already after 2 hours. When 5 units were used, 1 hour was sufficient. This result has shown that the purified protein from HEK GnTi- cells was glycosylated and this glycosylation could be removed by treatment with EndoH.

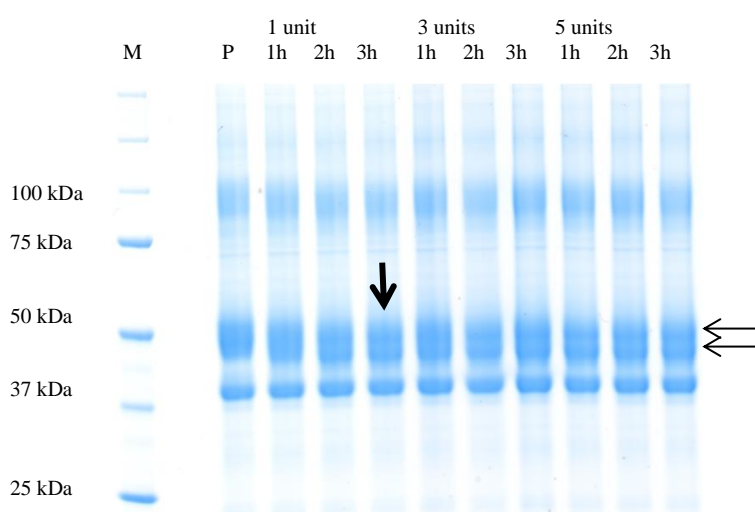


Figure 3.30.: deglycosylation of mβ3-T4L AR. 3 different concentrations of EndoH were tested as well as 3 different times for the incubation. With 1 unit at least 3 hours incubation was necessary, while already 2 hours were sufficient when more enzyme was used. Since the differences are very small, arrows show the slight movement of the band towards smaller molecular weights and the separation of one band into two bands.

The main protein band was still very broad. There is an example in the literature, when the use of alkaline phosphatase on turkey β1 AR led to more uniform electrophoretic mobility [123] suggesting that the sample was phosphorylated. Therefore the sample was incubated with calf intestinal phosphatase (CIP) to find out if this might be the case with β3 AR as well (figure 3.31.). The protein was incubated with EndoH and CIP at RT and 37°C and with CIP in CIP buffer (lanes 5 and 6) at the same temperatures. While EndoH had an effect on the protein and the main protein band did move to lower molecular weight size, the phosphatase did not have any effect on more uniform electrophoretic

mobility. The additional two bands observed corresponded to the phosphatase (lower band, a dimer of 69 kDa) and BSA (molecular weight of 66.5 kDa) that is added to the phosphatase buffer. Either the sample did not contain phosphorylation sites, or the phosphorylation site(s) were not accessible due to steric repulsion with the T4L fusion in ICL3.

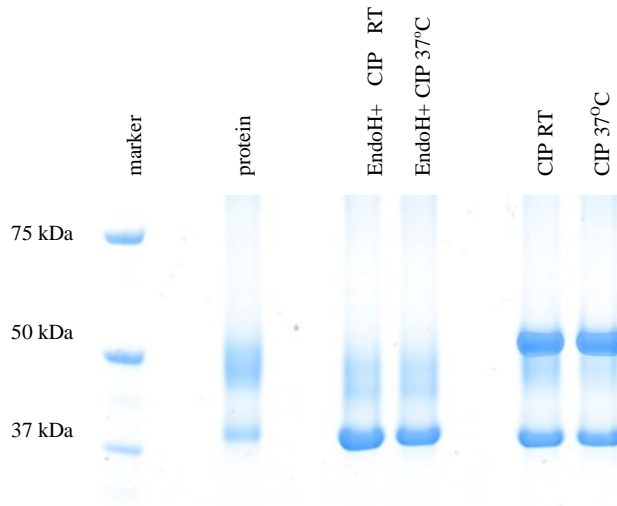


Figure 3.31.: dephosphorylation of the sample. Phosphorylation could lead to the non-uniform mobility of the samples on the gel. The sample did not get more uniform after the treatment with CIP.

Delipidation of membrane proteins during purification often leads to reduced stability of the protein. Therefore, the purification protocol was optimised to minimise washing cycles so that more of the original lipids were retained. The amount of the washing was reduced to 2-3 CV by packing the resin to the XK-16 column that was connected to the Ettan LC. This allowed a constant slow flow through the resin in a controlled way (figure 3.32.).

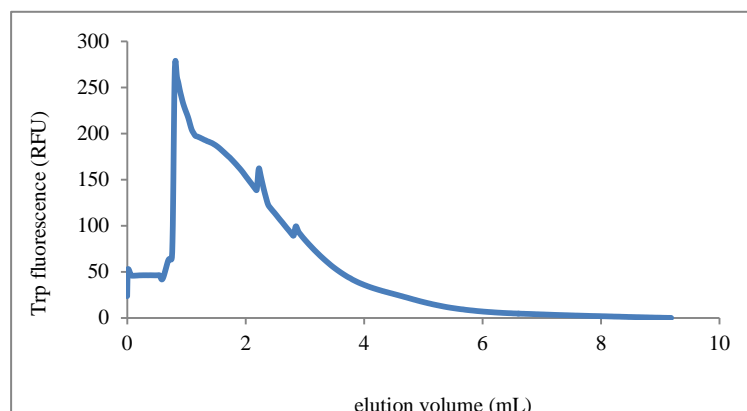


Figure 3.32.: washing of unspecifically bound protein from the resin. Under the controlled way and slow flow, the unspecifically bound proteins were washed in 2-3 CV.

Additionally, the amount of sample before concentration for GF was reduced. For this, the sample was eluted from the column using 150 μ M 1D4 peptide. Protein elution was monitored by Trp fluorescence. It eluted in a single peak between 6 and 10 mL as seen on figure 3.33.

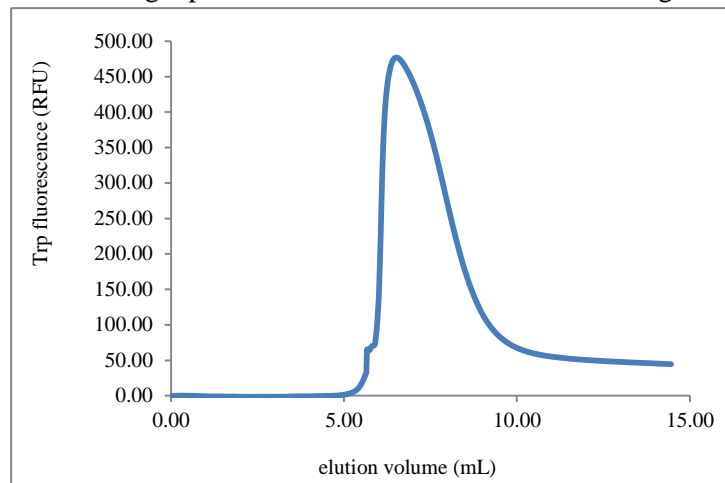
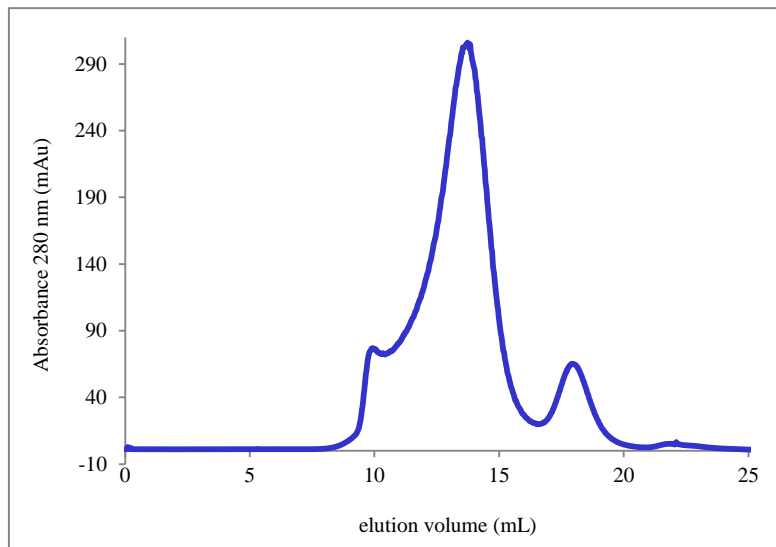


Figure 3.33.: the elution of the protein with 1D4 peptide. The protein eluted in a single sharp peak in less than 1 CV. The small shoulder at ca. 5 mL corresponds to the stop in the flow in order to allow the protein to elute from the resin.

The protein and GFP could be separated on the GF column (figure 3.34. a) and b)) since the protein elutes at around 14 mL, while the GFP elutes at 18 mL. Figure 3.34. b) represents fractions collected from the GF. There was practically no GFP observed around the fraction 47 where the protein eluted. However, only GFP was present (together with the 3C protease) from fraction 54 onwards. This proved that GF is enough to separate GFP and the protease from the protein. Since the gradient gel was used, a double band can be observed in the main protein peak.

a)



b)

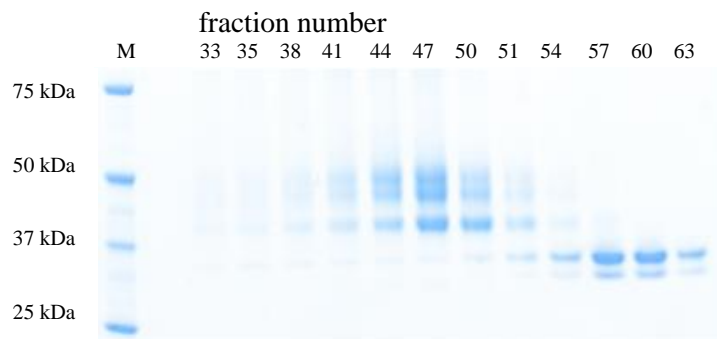


Figure 3.34.: gel filtration profile (a) and fractions run on a 4-12% gel (b). These two examples clearly showed that the protein could be separated from contaminants (GFP and 3C protease) using GF.

A sample before and after the EndoH treatment was run on 12% Tris-glycine gel (figure 3.35.) as well as both flow throughs that passed the concentrators. It can be seen that after the deglycosylation, the main peak at 50 kDa moved a little lower suggesting that glycosylation was removed from the sample. The lower band remained at the same position. Certain amount of GFP passed the concentrator, while the majority was concentrated together with the protein and was only separated on the GF. Not much protein leaked through either of both of the concentrators (before and after GF).

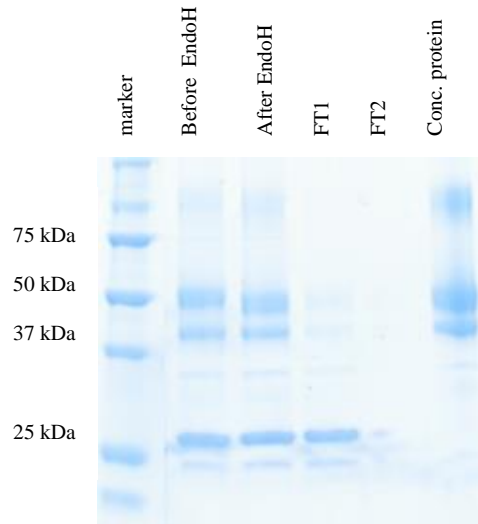


Figure 3.35.: instant blue staining of the purification. Lanes 2 and 3 represent the same sample before and after the EndoH treatment. FT1 and FT2 represent the flow through though the concentrators before (1) and after (2) GF. Conc. protein is the protein finally concentrated for the crystallisation.

Concentrated sample after the GF was run on FSEC (figure 3.36.). Protein ran as a single, sharp, monomeric peak eluting at 2.78 mL. This sample ran very uniformly and the crystallisation trials were repeated.

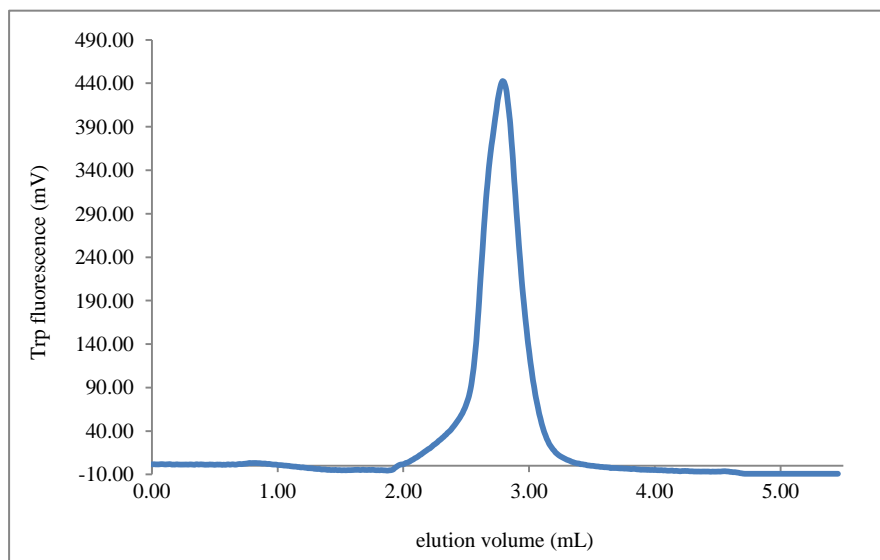


Figure 3.36.: FSEC profile of the mβ3-T4L AR. The protein eluted uniformly, there was also no big shoulder present before the main peak as it was the case in previous purifications.

With all the modifications, the sample was very pure and crystallisations were set up. Since LMNG has been shown to stabilise β 3-T4L AR even more than DDM, a purification and crystallisation with this detergent was set up as well. The column was also changed to Superdex 200 increase 10/300 GL to check if the purification can be improved further (figure 3.37.). The protein eluted in a monomeric peak at 12.2 mL. The void volume of the column was around 8 mL where the aggregates eluted. A peak just before the main monomeric peak therefore belongs to dimer/higher oligomer of the protein and cannot be assigned to protein aggregates. A commercial column also separated the GFP from the protein better than the self-packed column (peak at 15 mL).

The sample was concentrated and loaded on FSEC. A sharp, monodisperse peak can be observed. When the sample is compared with the one purified in DDM, it can be seen that the protein purified in LMNG eluted in slightly sharper peak than the protein purified in DDM (figure 3.38.).

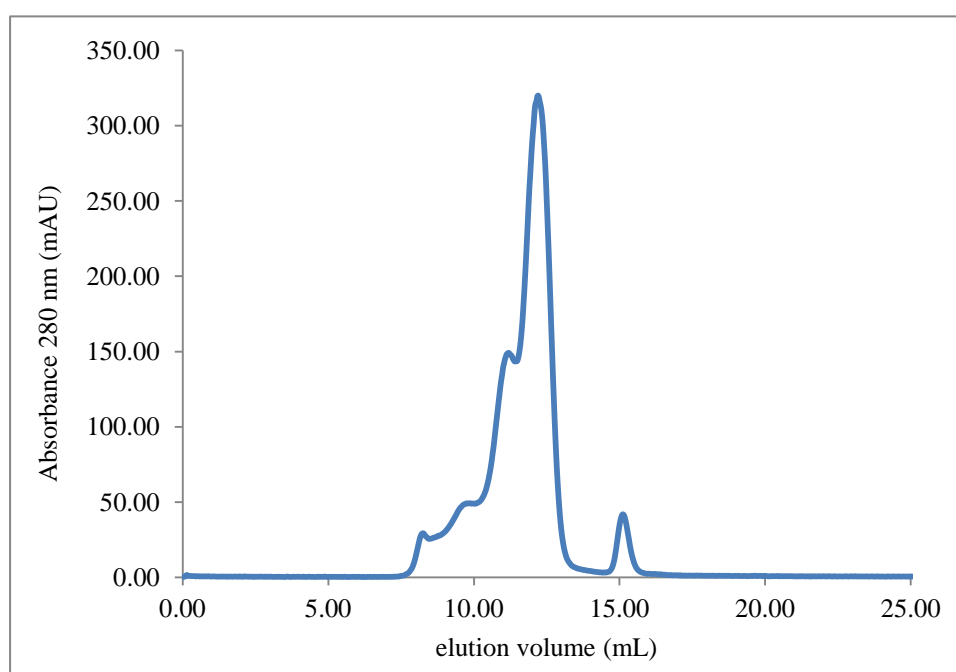


Figure 3.37.: gel filtration profile of mβ3-T4L AR purified in LMNG and ran on Superdex 200 increase 10/300 GL column. Protein eluted as a monomeric peak with some aggregates and a peak that belonged to dimer/higher oligomer. GFP was separated well, eluting at around 15 mL.

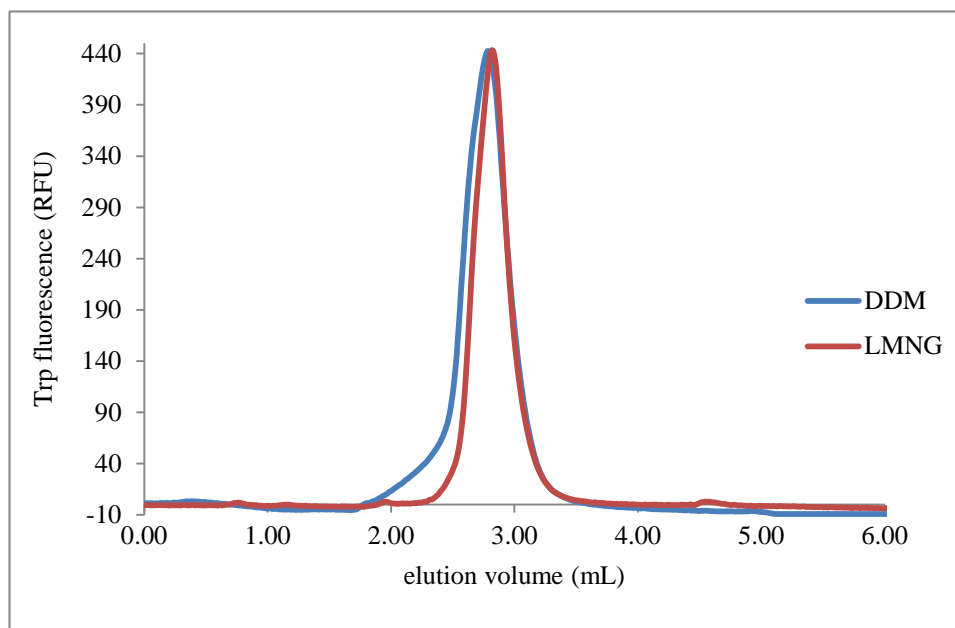


Figure 3. 38.: FSEC comparison of m β 3-T4L AR purified in DDM and LMNG. In both cases protein eluted as a monomeric peak, but the peak was sharper in the case of LMNG.

3. 8. Purification of α 2C-T4L AR

Compared to β 3-T4L AR, α 2C-T4L AR was expressing to a lower extent. Additionally, the purity of the protein was lower compared to other constructs (figure 3.39.). A typical expression yield was around 1 mg of expressed receptor/L of culture, which was a reason why less purification trials as well as fewer experiments were done with this construct. The protein was mainly purified in DDM for LCP crystallisations. Additionally, purification in DM and Hega-10 was done to perform VD experiments. GF profile also showed a big aggregation peak where the size of this peak was basically the same as the size of the main peak (figure 3.40.) suggesting that a lot of the protein aggregated during the purification process. FSEC profile of the purified samples (figure 3.41.) showed a uniform peak for the protein at 2.6 mL, however it always had a preceding shoulder at around 2 mL showing that there was still a fraction of aggregates present in the sample.

The protein was not expressed as well as β 3-T4L AR and did not have the same purity, but the stability of the protein was similar as proved by the CPM and FSEC assays.

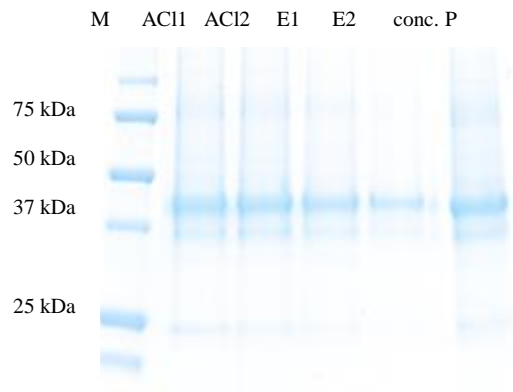


Figure 3.39.: instant blue staining of the purification gel. In the samples AC11 and AC12 which are the samples after the cleavage and after the Ni²⁺-TED resin purification, it can be seen that the 3C protease was removed from the sample. Two elution steps were enough for the complete elution of the protein. Concentrated sample eluted as a double band at 45 kDa, however the whole sample was very smeary and had also present a band at 75 kDa.

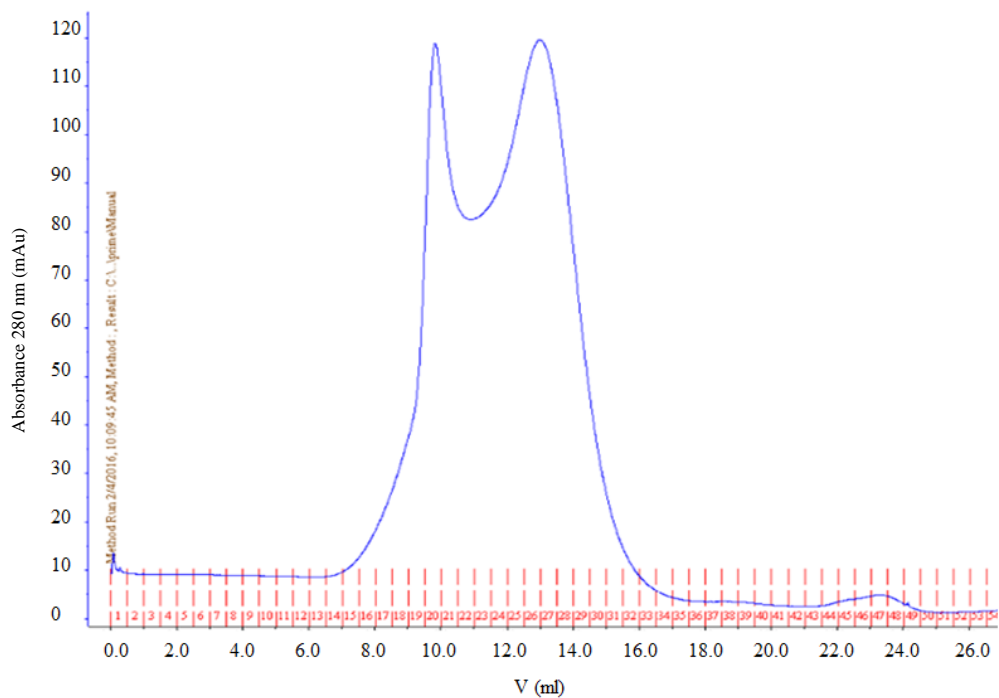


Figure 3. 40.: GF profile of α 2C-T4L AR in DDM with 10 μ M rauwolscine. The main protein peak at 13 mL and aggregate peak at 9.5 mL have almost the same height showing that the sample contained a lot of aggregates.

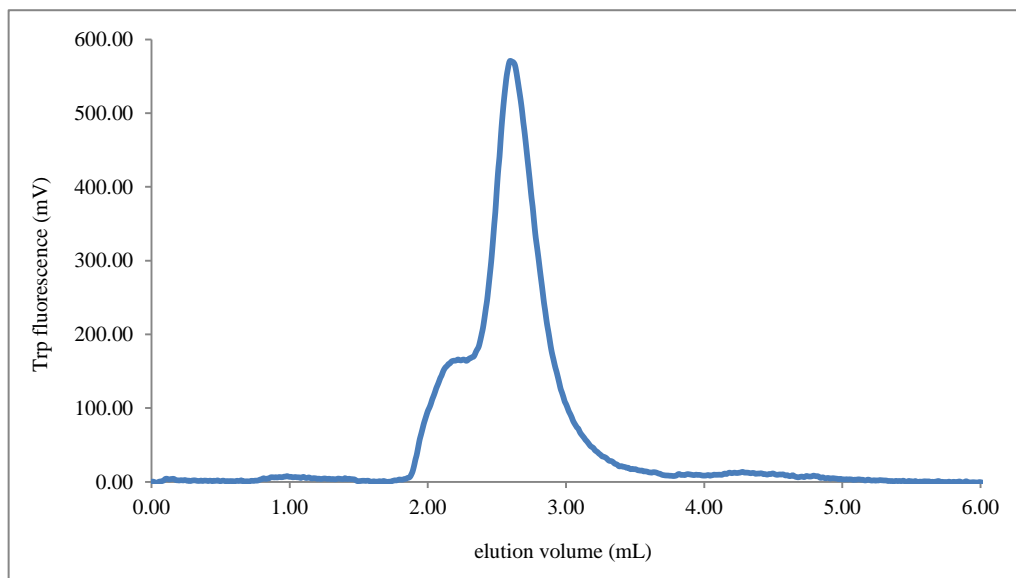


Figure 3.41.: FSEC profile of the purified $\alpha 2C$ -T4L AR in DDM. Besides the main peak at 2.6 mL that was uniform and monodisperse, there was also a substantial peak of aggregates at ca. 2.1 mL. Either not all aggregates were removed from the sample during the purification or they reformed during the concentration process. In either case, these might influence the crystallisation process.

3. 9. Crystallisation tests

VD and LCP crystallisation were set up. The overview of the crystallisation trials is shown on figure 3.42.

| | |
|---|---|
| <p>Vapour diffusion Detergents: DM, Hega-10 Protein concentration: 4-10 mg/mL T= 4 and 20°C Drop size: 150 nL+ 150 nL and 200 nL+ 200 nL</p> | |
| <p>$\alpha 2C$-T4L AR Ligand: RS79948</p> | <p>$\beta 3$-T4L AR Ligands: carvedilol and cyanopindolol ICI215,001 and G-protein peptide</p> |

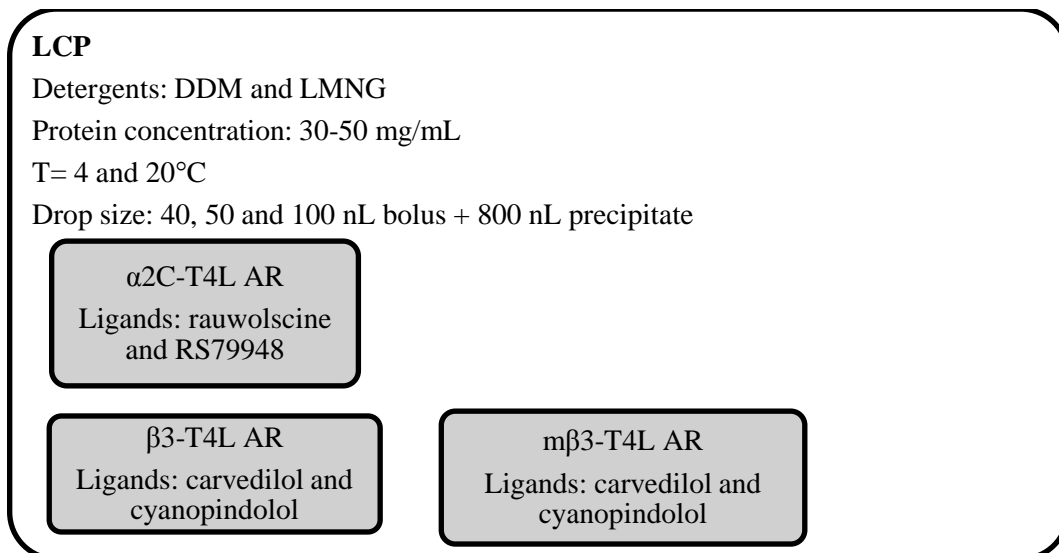


Figure 3. 42.: overview of the crystallisation trials.

Both constructs have shown some objects when VD experiments were set up. VD crystallisation of constructs in DM led to hexagonal crystals that appeared within a few days after the set up. These showed a signal under the cross polarizers as well as UV fluorescence signal. The crystallisation in Hega-10 detergent led to sea urchins (figure 3.43.) that showed an UV fluorescence signal as well. These objects were harvested, but no obvious protein diffraction was obtained. Seeding was tried, but this did not yield single crystals that could be used for diffraction testing.

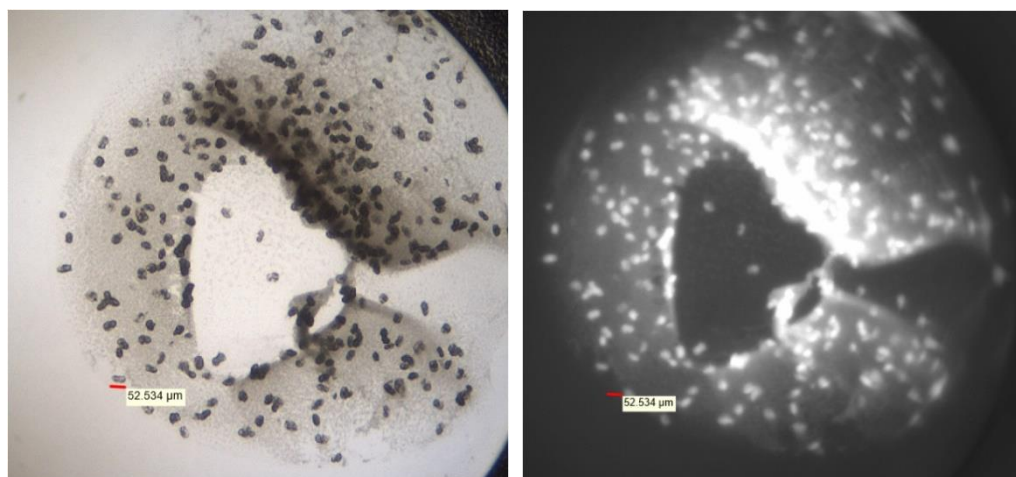


Figure 3. 43.: sea urchins of β 3-T4L grown in 0.225 M (NH₄)₂SO₄, 0.05 Na acetate pH 4.0, 12% (w/v) PEG 4000. These grew in 3-5 days. Visible light (left) and UV signals (right) are shown.

When LCP crystallisations were set up, there were no crystals observed with α 2C-T4L. Some crystals were observed with β 3-T4L in conditions containing 30% PEG 400, 100 mM Na MES pH 6.5 and salt (figures 3. 44. and 3. 45.). However, crystals started to grow after a long time (56 days or longer) and it was possible that these were only artefacts due to the drying of the plates with time. Increasing the protein concentration did not help in getting crystals faster.

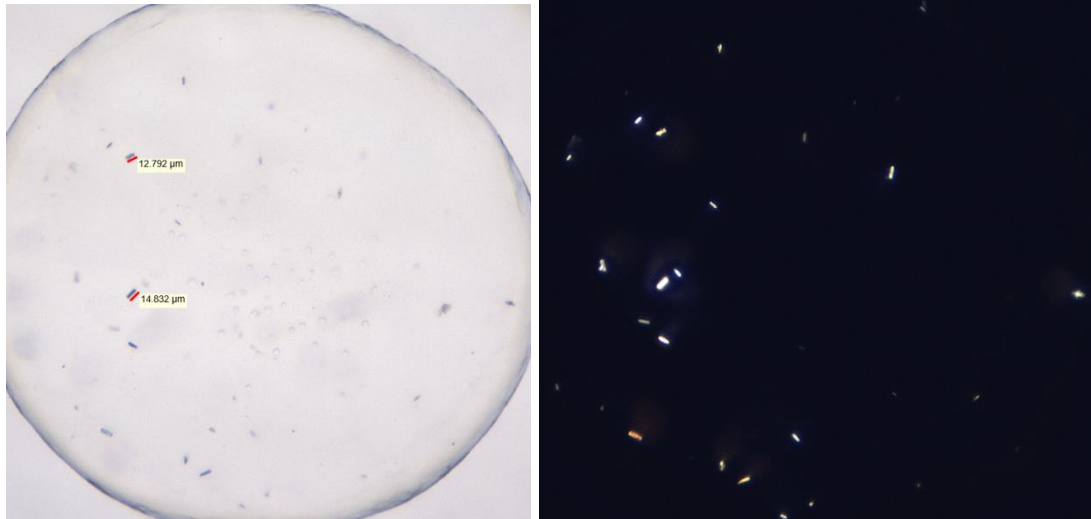


Figure 3. 44.: crystals of β 3-T4L AR in 30% PEG 400, 100 mM Na MES pH 6.5, 100 mM succinic acid. Crystals grew after 56 days. Cross polarisation picture is shown on the right as crystals were set in glass/glass plates that did not allow UV imaging.

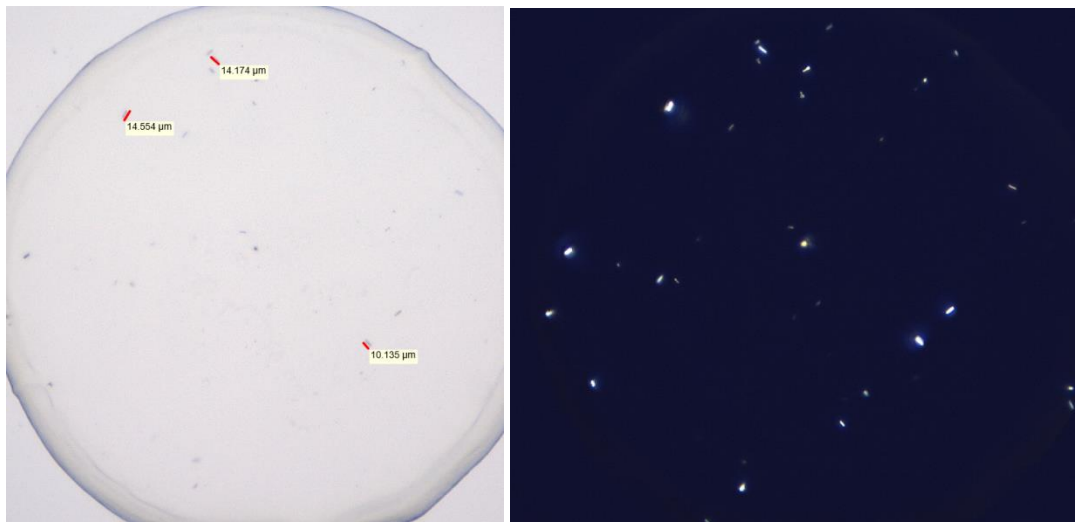


Figure 3. 45.: crystals of β 3-T4L AR in 30% PEG 400, 100 mM Na MES pH 6.5, 100 mM potassium acetate. Crystals grew after 56 days. Cross polarisation picture is shown on the right since the crystals were set in glass/glass plates that did not allow the UV imaging.

When the mutated β 3-T4L AR was set up, crystals were observed in the conditions containing 0.1M potassium fluoride, 0.1M MES pH 6.5, 30% PEG 400. Crystals appeared after 21 days and then grew to 10-20 μ m in the following 3 weeks. Optimisation screen was set up around these conditions. Crystals grew in all conditions containing different amounts of KF and 100 mM Na MES and at least 28% PEG 400. Crystals grew faster in higher % PEG. They appeared in 8 days (figure 3.46. a)) and then grew to 5-10 μ m within 21 days (figure 3. 46. b-c)).

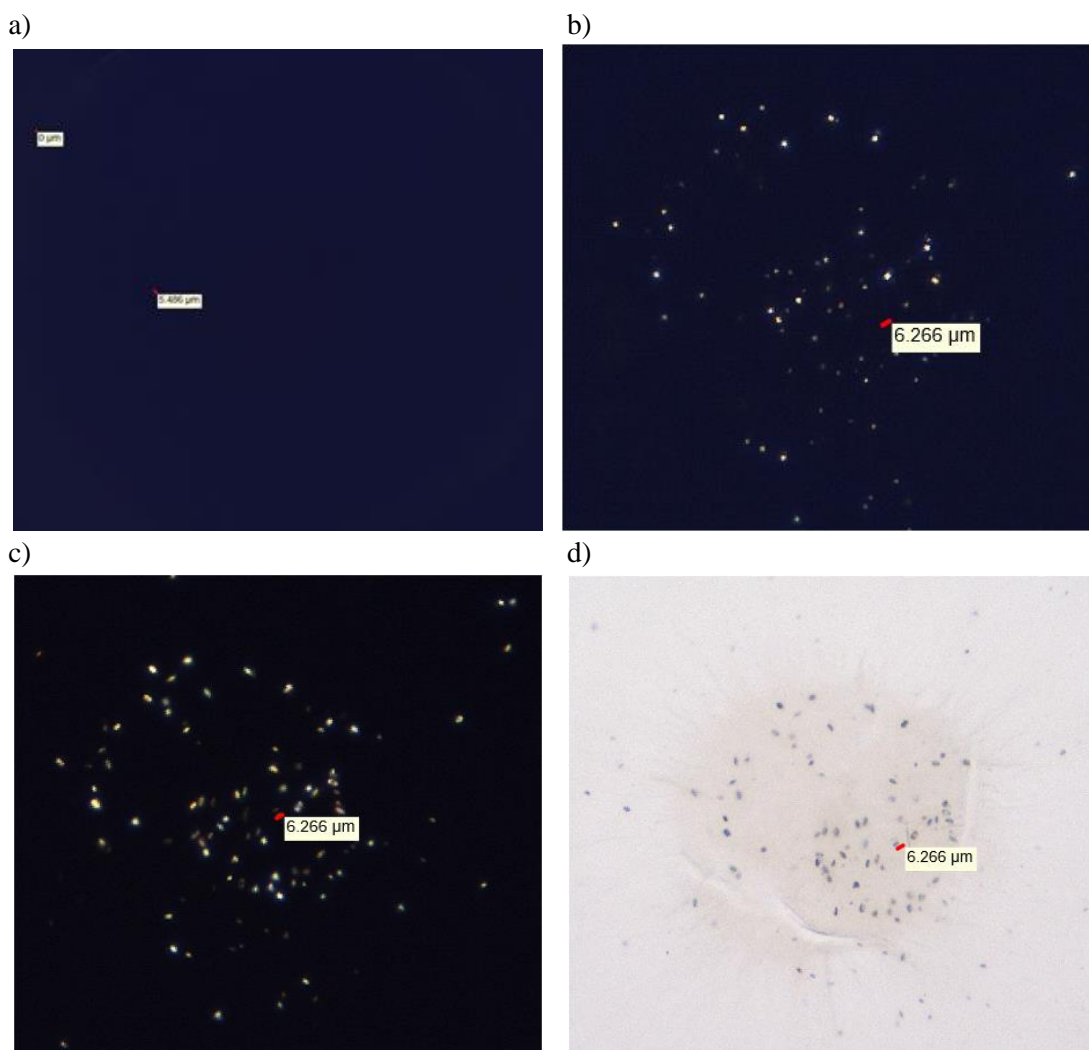


Figure 3. 46.: crystals of m β 3-T4L AR grown in 0.1M potassium fluoride, 0.1M MES pH 6.5, 38% PEG 400. The crystals appeared within 8 days (b) and then grew to 10 μ m within 21 days (c). Pictures on a-c are cross polarisation pictures, d) represents the light picture of the same condition as in c).

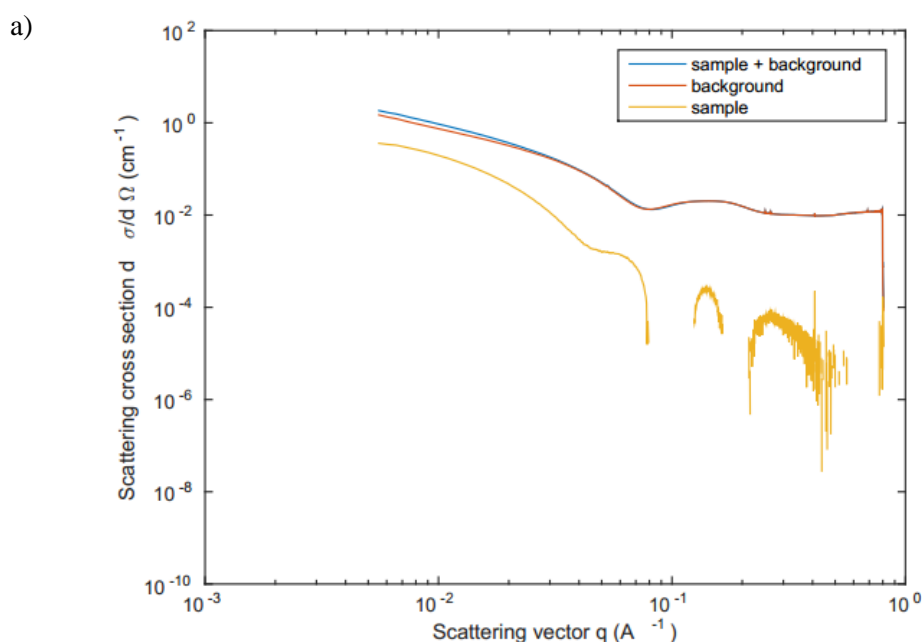
Second Order Nonlinear Imaging of Chiral Crystals (SONICC) has also shown positive correlation, however it was difficult to connect it with the UV signal obtained with the detector at our facility. Crystals have been harvested, but were impossible to detect in the loop during diffraction testing.

Raster scans were done, but no protein diffraction was obtained. In certain samples, some salt diffraction was detected, but we cannot be sure whether this was due to those crystals harvested or due to salts that could have formed during harvesting. Optimisation trials were carried out with additives, but no bigger crystals were obtained.

3. 10. SAXS and WAXS experiments

In order to analyse the conformational flexibility of the protein in solution, SAXS and WAXS experiments were done. The protein binds both ligands: antagonist cyanopindolol hemifumarate and agonist CGP 12177 hydrochloride. The data upon ligand binding is presented on figure 3.47. In the state when no ligand was bound, the protein existed in one conformation or an ensemble of conformations. Upon the binding of the agonist the protein moved to the active-like state as shown by the change of the curve in 3.47. a). Similarly, upon the antagonist binding to the receptor, the conformation of the receptor moved toward the inactive-state as observed by the change of the curve in 3.47. b).

These are only a preliminary data, but this showed that the protein is still active and is able to achieve two different conformations depending on the ligand used.



b)

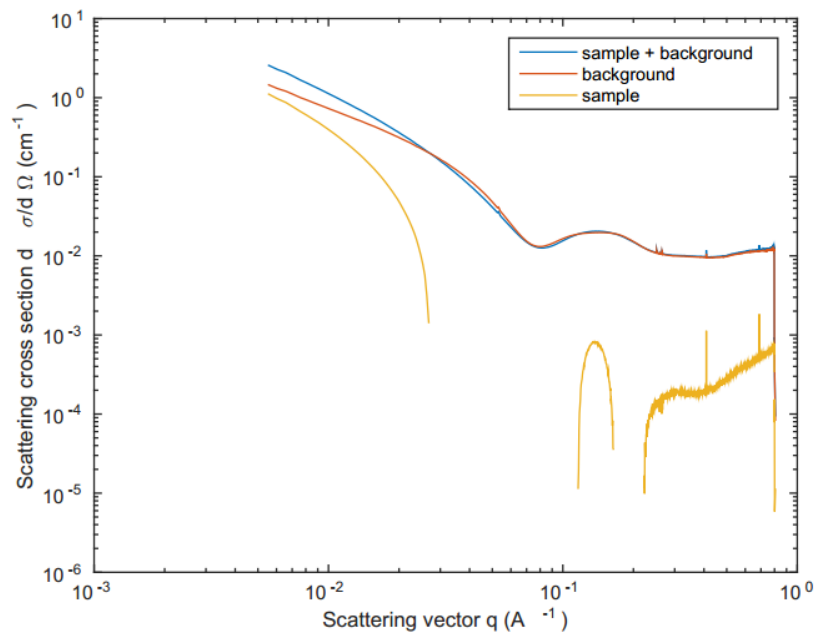


Figure 3.47.: SAXS/WAXS data for protein with agonist (a) and protein with antagonist (b). In both cases apo form of protein is shown in red curve (named background on the scheme) and the protein with the ligand is represented in blue. The yellow curve represents the difference between both curves.

4. DISCUSSION

4. 1. Choice of the construct

Three methods have been used in order to choose the most promising construct for crystallisation. In plate screening of live cells for GFP fluorescence, FSEC and fluorescence screening of the samples loaded on the gel (in gel fluorescence) have been used for expression tests and tests of monodispersity of the samples. Additionally thermostability of the receptor in crude extracts was determined by heating of the protein in regular intervals and analysing the amount of fluorescence on the gel.

4. 1. 1. In plate screening of cells

The screening of live cells allowed a fast screen of the cells for protein expression, localisation and cell survival. Since the test is done with live cells, it gives the information already soon after the transfection/induction. It is also the only assay that gives the information about the localization. α 1D-T4L and β 2-T4L ARs cells showed fluorescence signal, however it was observed uniformly all over the cell which suggested that the protein was not processed into the membranes of the cell. Cells also changed the morphology to a spherical shape which is not usually the morphology of healthy HEK293 cells. The majority of the samples (α 1A-T4L, α 1B-T4L, α 1D-T4L, α 1D-T4L (2), α 2B-T4L and β 1-T4L ARs) showed that protein was mainly expressed inside the cells, however they also showed a mixed morphology, where some cells still retained morphology of healthy cells. α 2C-T4L and β 3-T4L ARs showed the protein expressed inside the cells as well as in the cell membranes. While β 3-T4L AR showed the morphology of healthy cells, α 2C-T4L AR showed mixed morphology where some cells turned spherical while the others still remained healthy. Taking into the account the cell survival and the extent of protein expression and localisation, β 3-T4L and α 2C-T4L ARs were picked as the most promising proteins for the expression. It is also important to stress that the transient transfection of cells with PEI has a huge effect on the cells which might lead to cells dying or changing shape, so one needs to be careful with judging when the changes are due to protein expression or the stress that cells are put under due to transfection.

4. 1. 2. In gel fluorescence assays

When samples were solubilised and in gel fluorescence of crude extracts was checked, α 1D-T4L ARs again showed very weak or almost no signal. α 2B-T4L, α 2C-T4L, β 3-T4L and β 1-T4L, on the other hand, have shown a very strong signal, corresponding to high amounts of expressed proteins. What could also be observed from the gel is that the majority of samples ran as a smear which implied that these were heterogeneous populations of protein, which can be assigned to different glycosylations on

the N-terminal part of these receptors. This was confirmed with $\alpha 2B$ -T4L and $\beta 1$ -T4L ARs that ran as a single band. These two receptors are the only samples that do not have an asparagine that can be glycosylated.

4. 1. 3. FSEC tests of receptor constructs in solubilised crude samples

FSEC of crude solubilised samples have shown consistent results to the other two methods. $\alpha 1B$ -T4L and $\alpha 1D$ -T4L ARs have shown no signal (the signal has been the same as the signal of negative control). The highest signal was obtained for $\beta 3$ -T4L and $\beta 1$ -T4L ARs (360 RFU) followed by $\alpha 2C$ -T4L AR (190 RFU). FSEC has also given a confirmation about the size of constructs that has been consistent with the in gel fluorescence. While the majority of samples showed a peak between 2.40 and 2.50 mL, $\alpha 2C$ -T4L and $\beta 1$ -T4L ARs had a peak between 2.65 and 2.75 mL suggesting that these two samples are smaller, which again could be due to the absence of glycosylation. Even though all constructs have very similar molecular weight, they most likely contain different post-translational modification which was suggested by both methods. Different glycosylations of a single protein have been clearly seen on the in gel fluorescence, but have not been observed on the FSEC since the mass difference is too small to be distinguished. Only a single peak has been observed in all cases. This shows how important it is to use different methods in order to get the most information about the initial constructs.

Even though there were some differences between the methods, all methods were consistent that $\alpha 2C$ -T4L and $\beta 3$ -T4L ARs were expressing the best and FSEC traces of crude extracts were relatively monodisperse. Besides that, the protein was mostly expressed in the membranes, which is a good sign that the protein might be functional. Since GPCRs are membrane proteins responsible for transmitting signals from the outside to the inside of the cell, protein expressed in the cell membrane indicated that the receptor has been processed properly and inserted in the cell membrane where it can serve its function. However, the only way to really prove that would be by activating the receptor with agonist and monitor the intracellular response.

4. 1. 4. In gel thermostability assays

The protein stability was checked by heating the protein at regular intervals and monitoring the amount of the fluorescence signal left in the sample after the aggregates were removed by centrifugation. The method is prone to several errors, however, it can still give a good estimation on how stable the protein is. Errors include inconsistency in pipetting and variations during heating, aliquoting the protein and especially loading the protein on the gel. Since a crude extract is analysed, there is no need for purification which allows the test to be done on transiently transfected cells and early in the crystallisation pipeline. The stability of the protein is measured through the fluorescence

change of the GFP protein attached to the protein of interest, so the test can be done already with a sample expressed in 10 cm plate. On the other hand, the crude extract system is different to the purified system, with plenty of other proteins present, which might influence the stability of protein of interest. The melting temperatures of all samples were determined, but some expressed so poorly ($\alpha 1B$ -T4L, $\alpha 1D$ -T4L and $\alpha 2A$ -T4L ARs) that only one test has been done. $\alpha 1A$ -T4L AR showed a high discrepancy between the samples, while the majority of the others showed highly reproducible results. The least stable receptor was $\alpha 1D$ -T4L (2) with 43°C, while the most stable receptor was $\alpha 1B$ -T4L AR with 57.2°C, but the sample did not express well. From samples expressing well, the most stable construct was $\beta 3$ -T4L AR with (53.2±0.2)°C. The thermostability tests confirmed $\alpha 2C$ -T4L and $\beta 3$ -T4L constructs as good candidates for the crystallisation.

4. 2. Clonal selection and protein expression

Clonal selection is an essential part of the protocol since clones not expressing the protein and those that express the protein might divide at different rates. It is possible that those that do not express the protein divide faster since the cellular machinery is not overloaded by the overexpression of the recombinant protein. The first round of clonal selection showed how heterogeneous the batch population is. At least one round of clonal selection is therefore essential to select good expressors. The second round did not show big differences between single clones, so one round was already sufficient to select well expressing clone sub-batches. In stable transfection, the protein is integrated into the DNA of the cell and cells are affected by this to lower extent than in the case of transient transfections where the transfection chemical (for example PEI) is used to get the DNA into the cell. As seen on figure 3.9. in stable transfection cells keep the morphology of healthy cells and the protein is expressed in the cell membrane which is expected for membrane protein. Checking the cells directly under the microscope, or other device that allows live imaging, allows detection of the protein and, contrary to other methods (for example in gel GFP measurements), allows the localisation of the protein as well. This method is also very useful for checking the expression of the protein in the course of time as shown on figure 3.11. It is obvious that there is no protein expressed at 4 hours post-transfection and the amount of the protein, measured through the GFP fluorescence, increased over time until it reached maximum at 50 hours after transfection when the cells were harvested. Leaving cells in the culture for longer did not lead to higher expression of proteins.

4. 3. Temperature stabilisation of crystallisation constructs by ligands

4. 3. 1. Optimisation of the method

CPM assay allows a quick, efficient and reproducible determination of T_m , using a small amount of purified protein. By exchanging the buffers, detergents or adding different additives/ligands, it allows determination of the stabilisation of the receptor by additives. It is also extremely time efficient: 24 samples can be tested in triplicates within 15 minutes of running time. In our case we used this method in order to test 30 ligands for the temperature stabilisation of the receptor. In this way, we were able to determine the ligands that can be used in the crystallisation.

Figure 3.12. represents a typical result of an experiment. Figure a) shows a direct output of the method where there is initial very small fluorescence signal. When the heating starts the fluorescence stays almost the same until the protein completely unfolds. The mid-point of the transition is defined as the melting temperature T_m . During unfolding previously buried cysteines become exposed and the CPM dye can bind which results in an exponential increase in fluorescence that then stabilises at maximum fluorescence. Figure 3.12. b) shows the first derivative of the same experiment where the T_m is represented by the peak on the graph.

When testing $\alpha 2C$ -T4L AR for the appropriate amount of the protein, curves for higher amounts of the protein (8 and 10 μg) reached saturation which was probably due to the lack of available CPM dye in the reaction (figure 3. 13.). This led to a higher discrepancy between the triplicates and slightly higher T_m . The other two amounts showed a nice transition curve and similar T_m (44.1°C for 2 μg of protein and 44.3°C for 4 μg of the protein). When the experiments were done in duplicate, results were similar as in the first experiment. Therefore 2 μg of $\alpha 2C$ -T4L AR/test was used.

When testing $\beta 3$ -T4L AR for the appropriate amount of the protein, none of the amounts reached saturation, but the smallest amount showed a very low signal (figure 3.14.). Since the rest of the signals showed similar transition curves, 4 μg of the protein was chosen for the rest of the tests (T_m for this amount of the protein was 46.4°C). The experiment was performed in duplicate where the transition curves were similar and the melting temperature was 47.5°C.

$\alpha 2C$ AR has 11 cysteine residues, six of them are in transmembrane helices, and one disulphide bond between the extracellular residues 124-202. $\beta 3$ AR has 13 cysteines, four of them in transmembrane helices, and two disulphide bonds between the extracellular residues 110-196 and 189-195. This explains why higher amounts of the protein needed to be used for the experiment in the case of $\beta 3$ AR.

4. 3. 2. Stabilisation of α 2C-T4L and β 3-T4L AR by ligands

30 different ligands have been tested in order to test the effect of ligands on the thermostability of the protein and to find the ligands that could be used during purification. With the exception of one ligand, all agonists and antagonists have increased the T_m of α 2C-T4L AR. Additionally, a few ligands that are not classified as α 2C AR agonists or antagonists showed an increase in T_m . While three of them only showed a small effect (up to 4°C), roxindole hydrochloride increased the T_m for almost 14°C. This ligand is classified as dopamine receptor and serotonin transporter ligand, but obviously also has an effect on α 2C-T4L AR.

When ligands were tested with β 3-T4L AR, only a few ligands have increased the T_m for more than 4°C. None of the ligands that are not specific for this receptor has shown an effect. Crystal structures have shown that upon the ligand binding the receptor either adapts an inactive or active conformation. Even though that binding of the ligand does not necessary result in the change of the T_m , some ligands have shown a significant increase in T_m and have therefore also been used in crystallisation trials. These were: rauwolscine hydrochloride and RS 79948 hydrochloride as antagonists for α 2C-T4L AR and carvedilol and cyanopindolol hemifumarate as antagonists for β 3-T4L AR. A few agonists have also been found that could be used in case the active form of the receptor would like to be crystallised. Stabilisation of the receptor by ligands can be used as a screening tool to distinguish specific ligands from non-specific ones. Several ligands are still not classified as agonists/antagonists and the affinity of the ligands to the receptors is still largely unknown. Having this information might be important information for successful crystallisation. Additionally, this screening also allows determination of ligands that can additionally stabilise the receptor for the purification.

4. 3. 3. Comparison between the non-mutated and mutated human β 3-T4L AR

The comparison between the β 3-T4L AR and m β 3-T4L AR has shown that transferred mutations obviously changed the receptor affinity toward the ligands. In all cases the thermostability of m β 3-T4L AR has been equal or higher than the one of β 3-T4L AR. However, in both classes only approximately 50% of the ligands stated as agonists or antagonists increased the T_m in m β 3-T4L. Since the mutations were transferred from turkey β 1 AR, I also checked if the receptor responded stronger to ligands specific for this receptor, but this was not the case.

Additionally, the test with alprenolol hydrochloride and ICI215,001 hydrochloride showed double transitions. One reason for a double transition could have been that binding of the ligand could have induced dimerisation where the dimers showed a different melting temperature to the monomers. An additional explanation could be that receptors have allosteric ligand binding site besides the traditional orthosteric site. After the binding of the ligand to the orthosteric binding site, the excess ligand binds

to the allosteric binding side, increasing the T_m of the receptor. The last explanation could be that excess ligand binds unspecifically to the receptor, therefore changing the T_m . However, a similar behaviour should have been observed in the non-mutated receptor as well in case this hypothesis would be true.

While the introduced mutations did not have major influence on the melting temperature of the apo form of both constructs (the difference was only 1.4°C between both proteins), it did have a major effect on the effect of ligands on both constructs. The transferred mutations obviously did influence the ligand binding to the receptor.

4. 4. Protein purification

4. 4. 1. Optimisation of the purification protocol

For the optimal purification protocol several factors had to be assessed: the amount of the solubilisation buffer to completely solubilize the protein, the amount of washing buffer needed for the removal of unspecifically bound proteins, the amount of the protease used for the cleavage, the number of elution steps and the amount of the detergent in the last SEC step.

The right amount of detergent is crucial since a lack of detergent will lead to inefficient solubilisation of protein from the membrane and formation of heterogeneous mixture of protein:lipid:detergent micelle, while too much detergent can lead to protein inactivation/unfolding due to excess removal of essential lipids. Any partially solubilised protein could lead to protein aggregation resulting in lower yields of pure protein. If proteins are not properly solubilised, this can also lead to fractions of proteins with different amount of lipids resulting in sample heterogeneity which would interfere with purification and crystallisation. An excess of detergent can interfere with the crystallisation as at high concentrations and low temperature, most detergents stay in crystalline form [37]. While samples are normally solubilised in 1% detergent, it is important to keep the detergent concentration just above CMC (2-3x CMC) during the rest of the purification process. Since the majority of the proteins have been purified from insect cells and the membrane and lipid composition of insect cells differs from the mammalian one, the right amount of the solubilisation buffer had to be determined. From initial experiments it was determined that using the same amount of the solubilisation buffer as in insect cells purification led to major aggregation of the protein. HEK cells might have less total lipids than insect cells. From the tests when different amount of the solubilisation buffer was used (figure 3.18.), it was determined that 1 mL of the buffer per 100 mg of cell membranes is sufficient. Using more buffer gave the same FSEC profile, but has led to larger volume which reduced the binding efficiency to the affinity resin.

Determining the right amount of the washing buffer was also essential. Unspecifically bound proteins needed to be washed in this process, but extensive washing might lead to the loss of essential lipids which could destabilise the protein. Since gravity flow was used, the amount of the washing buffer was determined by taking a sample after washing at regular intervals (figure 3.19.). From this the optimal amount of the washing buffer was determined to be 10 CV. Later, the resin was packed into the XK-16 column and Trp fluorescence during washing was monitored (figure 3.32.). In this case Trp fluorescence fell to 0 already after 2-3 CV. This might be because washing was done in a controlled way with a slow and constant flow (0.4 mL/min). However, when the resin was loaded onto the gel, there were still some unspecifically bound proteins present. This did not interfere with the purity of the protein at the end of the purification protocol and 3 CV of washing buffer under the controlled way was sufficient amount of washing buffer to remove the unspecifically bound proteins that might co-elute during the elution of adrenergic receptor with 1D4 peptide.

The GFP had to be cleaved from the protein using 3C protease. The ratio of protein:protease generally used was 1:0.12 (mol/mol). Since the cleavage was done on the resin, which might be less efficient than in the solution, a ratio of 1:0.24 was also tested. 3C protease is very specific, cutting only after Gln in the sequence Leu-Glu-Val-Leu-Phe-Gln-Gly-Pro, therefore it is unlikely that the protease would cleave our protein unspecifically in case too much protease is used. The size of the protease is 22 kDa and includes a 10 His tag, so it can easily be removed by Ni resin as it was done at the beginning or during SEC since the weight difference between the proteins is big enough. FSEC measurements have shown that the same amount of the protein was cleaved from the resin using both amounts of the protease, therefore 1:0.12 ratio of protein:protease was used for the purification.

In order to reduce the amount of the concentration step before the SEC, the resin was packed into a XK-16 column. The protein was eluted with 1D4 peptide (figure 3.33.) which allowed elution of the protein in 0.5-1 CV instead of previously 3-3.5 CV used previously. This reduced the amount of concentration steps by a factor of five. Because detergents are, to some extent, concentrated together with the protein [124], it is important to minimise the concentration factor. Apart from problems in the crystallisation when the detergents can crystallise in VD or when the cubic phase is not formed in LCP, a high concentration of detergent might also have an influence on protein quality. Eluting the protein from the resin with 1D4 peptide allowed cleavage of GFP off the protein in solution. A fraction of GFP passed through the 100 kDa concentration membrane, while the rest was separated from the protein during SEC (the size of GFP is ca. 28 kDa) as seen on figure 3.34. Ni resin was omitted, the protease (22 kDa) was as well separated in SEC step. Changing the self-packed column to Superdex 200 increase GL 10/300 led to an additional improvement in the GF profile (figure 3.35.)

The amount of DDM in the final SEC step was also tested. Two amounts have been tested: normally used 0.02% DDM with 0.002% CHS and 0.01% DDM with 0.001% CHS. Using the smallest possible amount of detergent was especially crucial, since the use of 1D4 resin led to a big concentration step (up to 100-times) which most probably increased the amounts of free micelles. Despite this influencing the LCP set up and crystallisation, it might also have an influence on the stability of the protein in the solution. It was obvious from the SEC profile that 0.01% DDM with 0.001% CHS was not sufficient to keep the protein in a stable, solubilised form and a lot of protein aggregated (figure 3.19.). However, one has to be very cautious with these conclusions since it is protein dependant and it was also observed that not all expressions batches showed the same behaviour. Since it was possible to reduce the amount of the buffer to concentrate by eluting the protein with 1D4 peptide and 0.02% DDM is already low enough, I decided to continue using this amount of detergent.

4. 4. 2. Purification of β 3-T4L and m β 3-T4L AR

When the protein was run on 12% glycine gel, the protein showed 3 bands: a band belonging to the monomeric protein at 50 kDa, a faint band running at around 40 kDa and a band at 100 kDa most probably belonging to higher oligomers/aggregates. Samples of lower two bands were sent for Edman degradation in order to determine if these bands are potential proteolytic products. Even with extensive trials, we were not able to determine the amino acid sequence of the N-terminal part of both bands and to determine whether these two bands are a result of proteolytic cleavage as Edman degradation did not return any amino acid sequence. However, other proteins showed similar behaviour and they have still formed crystals, which means that this might not be the only reason why crystallisation has not been successful.

Four different detergents have been used for the purification and subsequent crystallisation of the protein: LMNG, DDM, DM and Hega-10. The protein was purified in these detergents and run on FSEC using Trp fluorescence. The curves on figure 3.24. have been normalised to the same amount of protein for easier comparison. Except Hega-10, they all show a single, monomeric peak. While DDM and DM eluted at 2.60 mL, LMNG eluted at 2.80 mL. The width of the curves was similar in all three cases. Hega-10, on the other hand, eluted at 2.43 mL and has shown a small shoulder before the main peak. However, the profile still looked satisfying and all four detergents have been used for crystallisation. An important test was also the stability of the protein in these detergents. Two tests were done in order to check the stability of protein: in the first one the protein was heated for 30 min at 50°C and in the second test the protein was left at room temperature O/N. There is a speculation in the field that if 50% of the protein survive the heating to 50°C for 30 min, the protein is stable enough for crystallisation. However, from the crystallisation point of view, it is more important how long the protein survives at RT and how it is affected during this time. While this is true for VD experiments, it is more difficult to assess what exactly is happening to the protein in LCP. LCP mimics a membrane

environment, which should be beneficial for the protein stability and integrity compared to the micelle environment. When DDM and LMNG were tested, it was obvious that the protein was more stable in LMNG than in DDM. Also leaving the protein at RT O/N did not affect the shape or height of the curve, but the curve did show a small shift to higher molecular weight on SEC. This is rather due to the experimental error than the protein itself. When the protein was heated to 50°C, there was a small peak around 2 mL, which corresponded to the void volume of the column representing the aggregates. The peak height of the monomeric protein still remained the same, suggesting that the majority of the protein survived this treatment. The protein was less stable in DDM detergent when 74% of the protein remained in its monomeric form when it was left at RT O/N and 50% survived the heating to 50°C for 30 min. This is still reasonable for the crystallisation, especially because the protein was set in LCP for that. Hega-10 was also tested for the thermostability, since the protein in this detergent was set in VD. The protein was less stable with only around 50% of the protein remaining in monomeric form after leaving the protein at RT O/N and almost completely aggregated (around 20% of the protein still eluted where the monomeric protein elutes) when heating the protein to 50°C for 30 min. Therefore, the crystallisation with this detergent was set up at 4°C as well as at 20°. Even though that the detergents showed similar peak when the protein was tested after the purification was finished, it was obvious they provide very different environment. This might be important to take into account and try the crystallisation with different detergents. DDM was kept as detergent of choice for initial crystallisation trials and other detergents were tested at a later time point. The choice of detergents is most likely protein specific and cannot be generalised.

Similar to the tests with β 3-T4L AR, m β 3-T4L AR has shown good behaviour in DDM and LMNG (figure 3.38.), but the peak in LMNG was slightly sharper which might be beneficial for crystallisation as the protein is more monodisperse. Both detergents have been used for the crystallisation trials.

4. 4. 3. Purification of α 2C-T4L AR

When α 2C-T4L was run on the gel two bands could be observed: one at 45 kDa and one at 37 kDa. Similar to the other proteins, a faint band at 75 kDa was observed as well, most probably belonging to higher oligomers. GF profile (figure 3.40.) showed two peaks of similar heights, which means that the amount of the aggregate is similar to the amount of the monomeric protein. Also FSEC at the end of the purification (figure 3.41.) still showed a substantial amount of aggregates. This could interfere with the crystallisation since the sample is not homogeneous enough. Crystallisation was set up with this protein, but since it did not express well and I did not manage to improve the purification to sufficient extent, this construct was not explored further.

4. 5. Crystallisation of α 2C-T4L, β 3-T4L and m β 3-T4L ARs

Three constructs have been tested for the crystallisation: α 2C-T4L, β 3-T4L and m β 3-T4L.

In VD experiments some crystals were observed in the case of α 2C-T4L and β 3-T4L AR. When the protein was crystallised in DM, crystals were in the shape of hexagons that have later turned spherical. In case of the protein purified in Hega-10 detergent, sea urchins have been observed. Both samples have shown a strong UV signal. Similar objects have formed when the buffer with high concentration of detergent was set up as a negative control, but no UV signal was observed. It is known that the detergents stay in crystalline form in high concentrations and low temperature [37], therefore I suspect that these crystals were detergent crystals and the protein precipitated on the surface of the formed crystals giving false positive signal. Additionally, when the hexagonal/spherical objects were harvested from the screen, the consistency was oily, adding to the conclusion that those crystals were indeed detergent crystals.

Several objects have been observed in LCP screens, but I was not able to optimise these crystals. Salt diffraction was observed upon diffraction testing, suggesting these are likely to be salt crystals.

4. 6. SAXS/WAXS experiments

While these experiments cannot provide structural detail at the atomic level, they are important as a complimentary technique to crystallography as they are done with a protein in a solution and at room temperature. The sample is therefore closer to the physiological conditions and the protein is not “locked” in a crystal lattice environment. The movements upon ligand binding can therefore be observed as well. While it cannot be distinguished whether the receptor occupies a single state or an ensemble of states in the absence of a ligand, upon binding of the ligand, the receptor adopted a different structural state as observed by the change in the curves on figure 3.47. The difference in the curves upon binding of the agonist and antagonist also suggested that the receptor adopted active and inactive conformation respectively. Interestingly, it seems that already binding of the agonist without the additional presence of the G protein is enough for the change in the conformational state. The protein most probably reached a partially activated state. The presence of T4L in ICL3 might also have an effect as it has been shown by the research on human β 2 AR [125]. This experiment proved that the purified β 3-T4L was in a functional state where it was able to bind the ligand and change the conformational state upon ligand binding.

5. CONCLUSIONS AND OUTLOOK

Since structures of turkey $\beta 1$ and human $\beta 2$ adrenergic receptors have been determined in the past few years, I wanted to expand the existing knowledge by determining structure of other members of this family. From the initial tests I have chosen $\beta 3$ and $\alpha 2C$ ARs since these two receptors have shown reasonable expression and stability to work with. The development of methods leading to successful crystallisation has been vast in recent years. I have shown that a combination of in gel fluorescence, FSEC and imaging of live cells allows a fast and efficient screening and selection of constructs for crystallisation experiments. I have also shown that the thermostability of the receptor can be assayed in crude solubilised samples where protein is heated at regular intervals and the amount of non-aggregated protein is analysed on the gel. The determined apparent melting temperatures were consistent with the melting temperatures that were determined later with purified proteins.

I have showed that stable cell lines of HEK 293 GnTi- can be produced in three weeks including clonal selection. This has been proven to be a good expression system that assures a consistent expression of the protein. I have shown that proteins express in the range of 1-4 mg of protein/ L of suspension culture. However, the extent of expression mainly depends on the specific protein and cannot be generalised.

I have shown that CPM assay can be used for quick and efficient testing for several additives in a reasonable time. I have used it to determine the effect of ligands on both receptors and developed it in a way that allows us to work in a high throughput. Antagonists that increased the T_m and can thus be used in crystallisation were determined: cyanopindolol for $\beta 3$ AR and rauwolscine for $\alpha 2C$ AR. Additionally ligands have also been tested with the receptor with transferred mutations from turkey $\beta 1$ AR and have shown that even though that the mutations did not increase the T_m of the apo form, the mutations did have an effect on the binding of ligands to the protein. Around half of all ligands increased the T_m of the m $\beta 3$ -T4L compared to $\beta 3$ -T4L.

I have also improved the purification protocol in order to obtain the best quality in terms of purity and homogeneity. The major improvement resulted by packing the resin into a column and eluting the protein with 1D4 peptide. This reduced the concentration step from previously 100-times to 20-times which was crucial since the empty detergent micelles can concentrate together with the protein therefore influencing the crystallisation. Switching from the self-packed GF column to the commercial one also led to better separation of species and resulted in more pure protein. Besides that I have shown the protein was stable in all tested detergents (DDM, DM, Hega-10 and LMNG). The protein eluted as a single monomeric peak in DM, DDM and LMNG. LMNG has stabilised the receptors the most, however there is still controversy about the ability of this detergent to solubilise

the protein and the tightness of binding to the receptor which might be less beneficial for the crystallisation

The conformational stability of β 3-T4LAR was analysed with SAXS/WAXS experiments. I have observed that upon ligand binding the receptor changed the conformation from one state or an ensemble of states to a new state after the binding of the ligand. Since I observed different movements after binding of agonist and antagonist, I propose that active and inactive states were achieved.

However, crystal structures of both receptors have not been solved so far. There are several options that could be investigated in order to find a construct that would crystallise. Firstly, removing the N-terminal might be beneficial in order to remove the glycosylation sites and make the sample more uniform. This could be done either by cutting the N-terminal completely or by inserting a cleavage site after the N-terminal part since complete removal of this part might impair expression of the protein. Alternatively, those asparagines could be mutated, but the constructs would again need to be checked for the expression afterwards. Our constructs included T4 lysozyme in the ICL3. Other fusion partners could be exploited as well either by replacing the ICL3 or by fusing it to the N-terminal. In case the fusion partner is fused to the N-terminal part of the protein, the ICL3 can be restored. In case of α 2C AR ICL3 would need to be, at least partially truncated since it might be too flexible for the crystallisation due to its size. Two fusion partners, BRIL and minimal T4L, have been proven promising for the crystallisation and might be used for the continuation of the project. Additionally, nanobodies could be raised against the protein, which is nowadays also more available and might be beneficial for the crystallisation.

Methods that have been developed in the GPCR community in recent years and that I have implemented in our lab are now available to test a large amount of constructs for expression and monodispersity of the sample in a short time. While GFP is very useful for these initial tests, it needs to be cleaved before the crystallisation leading to protein losses. By designing a construct without GFP, cleavage would not be needed anymore. The whole purification could be done in one day, additionally the possibility of contamination of the sample with leftover GFP/protease would be eliminated. LCP would still be a preferential method, however, since the protein is stable in small detergents, vapour diffusion could also be explored. The major issue with the VD experiments was the formation of detergent crystals that then provided the surface for the protein precipitation which gave rise to false positive signal under UV. Improvement in the purification protocol decreased the concentration step which led to lower amounts of the detergent being concentrated. This reduced the amount of detergent available to crystallise or interfere with the LCP. Recently developed microlytic plate, which utilises free interface diffusion on a small scale might be beneficial since it produces concentration gradients that increase the efficiency of sampling the crystallisation space.

Crystallisation is still mainly a “trial and error” process and testing as many options as possible is the only way that would increase the likelihood for successful crystallisation. However, methods developed in the past few years allow very efficient tests of small amounts of samples, which allow researchers to proceed faster and have higher chances to obtain the sample that will be able to crystallise.

APPENDIX

α 1A adrenergic receptor (471 aa, 52663.1 Da)

MVFLSGNASDSSNCTQPPAPVNISKAILLGVILGGLILFGVILGNILVILSVACHRHLHSVTHYYI
VNLA VADLLLTSTVLPFSAIFEVLGYWAFGRVFCNIWAAVDVLCCTASIWGLCIISIDRYIGVS
YPLRYPTIVTQRRGLMALLCVWALSLSVISIGPLFGWRQPAPEDETICQINEEPGYVLFSAALGSF
YLPLAILVMYCRVYVVAKRQLNIFEMLRIDEGLRLKIYKDTEGYTIGIGHLLTKSPSLN
AAKSELDKAIGRNTNGVITKDEAEKLFNQDVDAAVRGILRNAKLKPVYDSLDAVRRRAAL
INMVFQMGETGVAGFTNSLRMLQQKRWDEAAVNLA KSRWYNQTPNRAKRVITTFRTG
TWDAYKFCLKKEKKA AKTLGIVV GCFVLCWLPFFLVMPIGSFFPDFK PSETVFKIVFWLGYLN
SCINPIIYPCSSQEFKKA FQNVLRIQCLCRKQSSKHALG

- C-terminal truncation Δ 358-466
- M^{3.41}W stabilizing mutation

α 1B adrenergic receptor (488 aa, 54688.1 Da)

MNPDLDTGHNTSAPAHWGELKNANFTGPNQTSSNSTLPQLDITRAISVGLVLGAFILFAIVGN
ILVILSVACNRHLRTPNYFIVNLA MADLLLSFTVLPFSAALEVLGYWVLGRIFCDIWA AVDV
LCCTASIWSLCAISIDRYIGVRYSLQYPTLVTRRKAILALLSVWVLSTVISIGPLLGWKEPAPND
DKECGVTEEPFYALFSSLSGFYIPLAVILVMYCRVYIVAKRQLNIFEMLRIDEGLRLKIYKDT
EGYYTIGIGHLLTKSPSLNAAKSELDKAIGRNTNGVITKDEAEKLFNQDVDAAVRGILRN
AKLKPVYDSLDAVRRRAALINMVFQMGETGVAGFTNSLRMLQQKRWDEAAVNLA KSR
WYNQTPNRAKRVITTFRTGTWDAYKFCLKKEKKA AKTLGIVVGMFILCWL PFFIALPLGSLF
STLKPPDAVFKVFWLGYFNSCLNPIIYPCSSKEFKRAFVRILGCQCRGRGRRRRR

- C-term. truncation Δ 378-520
- L^{3.41}W(stabilizing mutation

α 1D adrenergic receptor (471 aa, 52243.5 Da)

MGEPGSAGAGGDVNGTAAVGGLVVS AQGVGVVFLAAFILMAVAGNLLVILSVACNRHLQ
TVTNYFIVNLA VADLLLSATVLPFSATMEVLGFWAFGRAFCDVWAAVDVLCCTASIWSLCTI
SVDRYVGVVRHSLKYP AIMTERKAAAILALLWVVALVVS VGPLLGWKEPVPDERFCGITEEA
GYAVFSSVCSFYLPMAVIVVMYCRVYVVAKRQLNIFEMLRIDEGLRLKIYKDTEGYTIG
IGHLLTKSPSLNAAKSELDKAIGRNTNGVITKDEAEKLFNQDVDAAVRGILRNAKLKPV
YDSLDAVRRRAALINMVFQMGETGVAGFTNSLRMLQQKRWDEAAVNLA KSRWYNQTP
NRAKRVITTFRTGTWDAYKFCLKKEKKA AKTLAIVVGVFVLCWF PFFVLPGLSLFPQLKPS
EGVFKVIFWLGYFN SCVNPLIYPCSSREFKRAFLRLLRCQRRRRRRRPLW

- N-terminal truncation (D2-69)
- C-terminal truncation Δ 432-572
- L^{3.41}W stabilizing mutation

α 1D adrenergic receptor (2) (700 aa, 77456.1 Da)

**MRAWIFFLLCLAGRALAAPLADTPSSPSIDQVEPYSSTAQVQFDEPEATGGVPILKYKAEWR
AVGEEVWHKSWYDAKEASMEGIVTIVGLKPETTYAVRLAALNGKGLGEISAASEFKTQPVR
EPSAPKLEGQMGEDGNSIKVNLIKQDDGGSPIRHYLVRYRALSSEWKPEIRLPSGSDHVMLKS
LDWNAEYEVYVVAENQQGKSKAAHFVFR TSAQPTAIPLEVLFGPEPGSAGAGGDVNGTAA
VGGLVVS AQGVGVFLA AFILMAVAGNLLVILSVACNRHLQTVTNYFIVNLAVADLLLSA
TVLPFSATMEVLGFWAFGRAFCDVAAVDVLCCTASWSLCTISVDRYVGVGRHSLKYP AIM
TERKAAAILALLWVVALVVS VGPLLGWKEPVPPDERFCGITEEAGYAVFSSVCSFYLPMAVI
VVMYCRVYVVAKRQLNIFEMLRIDEGLRLKIYKDTEGYTTIGIGHLLTKSPSLNAAKSEL
DKAIGRNTNGVITKDEAEKLFNQDVDAAVRGILRNAKLKPVYDSLDAVRR AALINMVF
QMGETGVAGFTNSLRMLQQKRWDEAAVNLA KSRWYNQTPNRAKRVITTFRTGTWDA
YKFCLKEKKA AKTLAIVGVFVLCWF PFFFVLP LGS LFPQLK PSEGVFKVIFWLGYFN SCVN
PLIYPCSSREFKRAFLRLLRCQRRRRRRRPLW**

- C-terminal truncation Δ 432-572
- L^{3.41}W stabilizing mutation
- fibronectin type III repeats 1 and 2 of neural cell adhesion molecule 1 (NCAM1) added before N-terminal

α 2A adrenergic receptor (474 aa, 53418.7 Da)

**MGSLQPDAGNASWNGTEAPGGGARATPYSLQVTLTLVCLAGLLMLLTVFGNVLVIIAVFTSR
ALKAPQNLFLVSLASADILVATLVIPFSLANEVMGYWYFGKAWCEIYLALDVLCTSSWHL
CAISLD RYWSITQAI EYNLKRTPRRIKAIITVWVISAVISFPPLISIEKKG GGGGPQPAEPRCEIN
DQKWYVISSCIGSFFAPCLIMILVYVRIYQIAKRQLNIFEMLRIDEGLRLKIYKDTEGYTTIG
IGHLLTKSPSLNAAKSELDKAIGRNTNGVITKDEAEKLFNQDVDAAVRGILRNAKLKPV
YDSLDAVRR AALINMVFQMGETGVAGFTNSLRMLQQKRWDEAAVNLA KSRWYNQTP
NRAKRVITTFRTGTWDA YKFCLKEKRFTFVLA VVIGVFVVCWF PFFFTYTLTAVGCSVPRT
LKF FFFWFGYCNSSLNPVIYTIFNHDFRRAF KILCRGDRKRIV**

- V^{3.41}W stabilizing mutation

α 2B adrenergic receptor (453 aa, 51853.9 Da)

**MDHQDPYSVQATAAIAAAITFLILFTIFGNALVILAVLTSRSLRAPQNLFLVSLAAADILVATLI
IPFSLANELLGYWYFRRTWCEVYLALDVLCTSSWHLCAISLD RYWAVSRLEYNSKRTPR
RIKCIILTVWLIAAVISLP LIYKGDQGPQPRGRPQCKLNQEAWYILASSIGSFFAPCLIMILVYL
RIYLIAKRQLNIFEMLRIDEGLRLKIYKDTEGYTTIGIGHLLTKSPSLNAAKSELDKAIGR
NTNGVITKDEAEKLFNQDVDAAVRGILRNAKLKPVYDSLDAVRR AALINMVFQMGETG
VAGFTNSLRMLQQKRWDEAAVNLA KSRWYNQTPNRAKRVITTFRTGTWDA YKFCLKE
KRFTFVLA VVIGVFVLCWF PFFFSYSLGAICPKHCKVPHGLFQFFFWIGYCNSSLNPVIYTIFN
QDFRRAFRRILCRPWTQTAW**

- V^{3.41}W stabilizing mutation

α 2C adrenergic receptor (492 aa, 54744.9 Da)

MASPALAAALAVAAAAGPNASGAGERGSGGVANASGASWGPPRGQYSAGAVAGLAAVVG
FLIVFTVVG NVLVVIAVLT SRALRAPQNLFLVSLASADILVATLVMPFSLANELMAYWYFGQ
VWCGVYLALDVL FCTSSIWHLCAISLD RYWSVTQAVEYNLKRTPRRVKATIVAVWLISAVIS
FPPLVSLYRQPDGAA YPQCGLNDETWYILSSCIGSFFAPCLIMGLVYARIYRVAKRQLNIFEM
LRIDEGLRLKIYKDTEGYTIGIGHLLTKSPSLNAAKSELDKAIGRNTNGVITKDEAEKLFN
QDVDAAVRGILRNAKLKPVYDSLDAVRRRAALINMVFQMGETGVAGFTNSLRMLQQ
KRWDEAAVNLA KSRWYNQTPNRAKRVITTFRTGTWDA YKFCLK EKRFVFLAVVMGV
FVLCWF PFFFSYSLYGICREACQVPGPLFKFFFWIGYCNSLNPVIYTVFNQDFRRSFKHILFRR
RRRGFRQ

- V^{3.41}W stabilizing mutation

β 3 adrenergic receptor (485 aa, 53178.4 Da)

MAPWPHENSSLAPW PDLPTLAPNTANTSGLPGVPWA AALAGALLALAVLATVGGNLLVIVA
IAWTPRLQTM TNVFTSLAAADLVMGLLVPPAATLALTGHWPLGATGCELWTSVDVLCV
TASIWITL CALAVDRYLAVTNPLRYGALVTKRCARTAVVLVWVVSAAVSFAPIMSQWWRVG
ADAEAQRCHSNPRCCAFASNMPYVLLSSSVSFYLP LLVMLFVYARV FVVAKRQLNIFEMLR
IDEGLRLKIYKDTEGYTIGIGHLLTKSPSLNAAKSELDKAIGRNTNGVITKDEAEKLFN
QDVDAAVRGILRNAKLKPVYDSLDAVRRRAALINMVFQMGETGVAGFTNSLRMLQQKR
WDEAAVNLA KSRWYNQTPNRAKRVITTFRTGTWDA YKFCLK EHRALCTLGLIMGTFTL
CWL PFFFLANVLRALGGPSLVPGPAFLALNWLG YANS AFNPLIYCRSPDFRS AFRLLC RCGR
LPPEP

- C-terminal truncation Δ 372-408
- E^{3.41}W stabilizing mutation
- Point mutation E^{1.31}A

β 2 adrenergic receptor (476 aa, 54132.4 Da)

MGQPGNGSAFL LAPNRSHAPDHDVTQQRDEVWVVG MGIVMSLIVLAI VFG NVLVITAI AKFE
RLQTVTNYFITSLACADLVMGLAVVPFGAAHILMKMWTFGNFWCEFWTSIDVLCVTASIWIT
LCVIAVDRYFAITSPFKYQSL LTKNKARVILMVWIVSGLTSFLPIQMHWYRATHQEAINCYA
EETCCDFFTNQAYAIASSIVSFYVPLVIMVFVYSRVFQEAKRQLNIFEMLRIDEGLRLKIYKD
TEGYTIGIGHLLTKSPSLNAAKSELDKAIGRNTNGVITKDEAEKLFN QDVDAAVRGILR
NAKLKPVYDSLDAVRRRAALINMVFQMGETGVAGFTNSLRMLQQKRWDEAAVNLA KSR
WYNQTPNRAKRVITTFRTGTWDA YKFCLK EHKAL KTLGIIMGTFTLCWL PFFIVNIVHVIQ
DNLIRKEVYILLNWIGYVNSGFNPLIYCRSPDFRIAFQELLCLRRSSLK

- C-terminal truncation Δ 349-413
- E^{3.41}W stabilizing mutation

β1 adrenergic receptor (458 aa, 52039.3 Da)

M**GAEI**LSQQWTAGMGLLMALIVLLIVAGNVLVIVAIKTPRLQTLTNLFIMSLASADLVMGL
LVVPPGATIVVWGRWEYGSFFCELWTSVDVLCVTAS**I**W**TLCVIALDRYLAITSPFRYQSL**TR
ARARGLVCTVWAISALVSFLPILMHWWRAESDEARRCYNDPKCCDFVTNRAYAIASSVVSF
YVPLCIMAFVYLRVFREA**KRQLNIFEMLRIDEGLRLKIYKDTEGYTIGIGHLLTKSPSLN**
AAKSELDKAIGRNTNGVITKDEAEKLFNQDVDAAVRGILRNAKLKPVYDSLDAVRAAL
INMVFQMGETGVAGFTNSLRMLQQKRWDEAAVNLAKSRYNQTPNRAKRVITTFRTG
TWDAYKFCLKEQKALKTLGIIMGVFTLCWLPFFLANVVKAFHRELVPDRLFVFFNWLGYA
NSAFNPIYCRSPDFRKA**FQRL**LCCARRAARRRHA

- C-terminal truncation Δ404-477
- E^{3.41}W stabilizing mutation
- N-terminal truncation as in turkey beta1AR-36 with the first 4 residues of the truncated construct replaced by the turkey beta1AR-36 sequence

m2 β3 adrenergic receptor (485 aa, 52975.0 Da)

MAPWPHENSSLAPWPDLPNTANTSGLPVGPW**A**AALAGALLALAVLATVGGNLLVIVAI
AWTPRLQTMNTNFVFTSLAAADLV**V**GLLVVPPAATLALTGHWPLGATGCELWTSVDVLCVT
AS**V**W**TLCALAVDRYLAVTNPLRYGALVTKRCARTAVVLVWVVSAAVSFAPIMSQWWRVG**
ADAEAQRCHSNPRCCAFASNMPYVLLSSSVSFYLPPLVMLFV**A**ARVFVVA**KRQLNIFEMLR**
DEGLRLKIYKDTEGYTIGIGHLLTKSPSLNAAKSELDKAIGRNTNGVITKDEAEKLFNQ
DVDAAVRGILRNAKLKPVYDSLDAVRAALINMVFQMGETGVAGFTNSLRMLQQKRW
DEAAVNLAKSRYNQTPNRAKRVITTFRTGTWDAYKFCLKEHRALCTLGLIMGTFTLCW
LPFFLANVLRALGGPSLVPGPAFLALNWLGYANSAM**NPLI**L**CRSPDFR**SAFRLLC**RCGRRLP**
PEP

- C-terminal truncation Δ372-408
- mutations E^{1.31}A, M^{2.53}V, I^{3.40}V, E^{3.41}W, Y^{5.58}A, F^{7.48}M and Y^{7.53}L

mβ3 adrenergic receptor (485 aa, 53022.0 Da)

MAPWPHENSSLAPWPDLPNTANTSGLPVGPW**A**AALAGALLALAVLATVGGNLLVIVA
IAWTPRLQTMNTNFVFTSLAAADLV**V**GLLVVPPAATLALTGHWPLGATGCELWTSVDVLCVT
AS**L**W**TLCALAVDRYLAVTNPLRYGALVTKRCARTAVVLVWVVSAAVSFAPIMSQWWRVG**
ADAEAQRCHSNPRCCAFASNMPYVLLSSSVSFYLPPLVMLFV**L**ARVFVVA**KRQLNIFEMLR**
DEGLRLKIYKDTEGYTIGIGHLLTKSPSLNAAKSELDKAIGRNTNGVITKDEAEKLFNQ
DVDAAVRGILRNAKLKPVYDSLDAVRAALINMVFQMGETGVAGFTNSLRMLQQKRW
DEAAVNLAKSRYNQTPNRAKRVITTFRTGTWDAYKFCLKEHRALCTLGLIMGTH**TLC**
WLPFFLANVLRALGGPSLVPGPAFLALNWLGYANSAM**NPLI**L**CRSPDFR**SAFRLLC**RCGRRLP**
LPPEP

- C-terminal truncation Δ372-408
- mutations E^{1.31}A, M^{2.53}V, I^{3.40}L, E^{3.41}W, Y^{5.58}L, F^{6.44}H, F^{7.48}M and Y^{7.53}L

acgtaaaccggccacaagttcagcgtgtccggcgagggcgaggcgatgccacctacggcaagctgacctgaagttcatctgaccaccggca
agctgcccgtgcctggcccaccctcgtgaccaccctgacctacggcgtgagtgcttcagccgtaccccgaccacatgaagcagcacgacttc
ttcaagtccgccatgcccgaaggctacgtccaggagcgcaccatcttctcaaggacgacggcaactacaagaccgcgccgaggtgaagttcg
aggcgacaccctggtgaaccgcatcgagctgaagggcaccgacttcaaggaggacggcaacatcctggggcacaagctggagtacaactaca
acagccacaactctatatcatggccgacaagcagaagaacggcatcaagggtgaactcaagatccgccacaacatcgaggacggcagcgtgca
gtcgcggaccactaccagcagaacaccccatcggcgacggccccgtgctgctgcccgaacacactacctgagcaccagtccaagctgag
caaagacccaacgagaagcgcgatcacatggctctgctggagttcgtgaccgcccgggatcactctggcatggacgagctgfacaaggcc
gcgggatccgcgtggagccaccacagttcagaaggagggtggaagcgggtggaggctcaggaggcagcgcattgggtcccacccccagttga
aaagggtcaggaggtagcgaagatctgACCGAGACCAGCCAGGTGGCCCCCGCCtaaaagcttaagtttaaaaggcc
ggatccgacgttaactgtttattgagcttataatggttacaataaagcaatagcaccacaaatffcacaataaagcattttttcactgcattctagttg
tggtttgtccaaactcatcaatgtatcttatcatgtctggatctactagttctagctagaagactctagggtgtagcttctgaagagaagaaggaagg
aagggtggaggttaggaaacagtgagtcggcctgtgggtctctctggtgatctgacagcttctgggtcagaactcggagtcaccacgacaact
gctctctgtctgacgacaggggtcaggcaagcttgggtgccagcggtgaggtcaggggtggggaagcccagggtggggattccccatctc
ctcagtttacttctgcacctaactgggtcaggtcctctgcccggacactgatgacgcgctggcaggtctcactatcattgggtggcgagattcca
ggagccaatcagcgtgccgcggagcgtggtataaagtcacgcaaccgcccggactcagacaccgggatctgatcaagagacaggatgag
gatcgtttcgcattgaaacagatggattgcacgaggttctccggccttgggtggagaggctattcggctatgactgggcacaacagacaat
cggctgctctgatccgccgtgtccggctgtcagcgcagggcgcccgggtctttttgcaagaccgacctgtccggtgccctgaatgaactgcag
gacgaggcagcgcggctatcgtggctggccacgacgggcgttcttgcgagctgtgctcgcaggtgctactgaagcgggaagggactggctgc
tattggcgaaagtgccggggcaggatctctctcactctaccttgcctctgcccgagaagatccatcatggctgatcaatggcgcggtgcatac
gcttgatccggctacctgccattcgaccaccaagcgaacatcgcacgagcagcagctactcggatggaagccgggtcttctgctcagggatg
atctggacgaagagcatcaggggctcgcgccagccgaactgttccagggctcaaggcgcgcatgccgacggcgaggatctcgtctgacc
atggcgatgctgcttgcgaatatcaggtggaatggccgcttttctggattcagctgactgtggccggctgggtgtggcgaccgctatcagga
catagcgttggctaccctgatattgtgaagagcttggcgccgaatgggtgaccgcttctctgctttacggctatcggctcccgattcgcagc
gcatcgccttctatgccttctgacgagttcttctgagcgggactctggggctcgaatgaccgaccaagcgcgccaacctgccatcacgagatt
tcgattccaccggccttctatgaaaggttgggcttgggaatcgtttccgggacgccggctggatgatctccagcgggggatctcatgctgga
gttcttcgccaccaactgtttattgagcttataatggttacaataaagcaatagcaccacaaatffcacaataaagcattttttcactgcattctag
ttgtggtttgtccaaactcatcaatgtatcttatcatgtctggatcctagaagatcatacactccgctatcgtactgactgggtcatggctgcccccg
acaccgccaacaccgctgacgcgcctgacgggcttctgctccccggcatccgcttacagacaagctgtgaccgtctccgggagctgcatgt
gtcagaggtttaccgctatcaccgaaacgcgcgagggcagctgtggaatgtgtcagttagggtgtggaagtcaccaggtccccagcaggc
agaagatgcaaagcatgcatctcaattagtcagcaaccaggtgtgaaagtccccaggtccccagcaggcagaagatgcaaagcatgcatct
caattagtcagcaaccatagtcgcccccctaacctccgccatcccgccctaacctccgccagttccgccattctccgcccatggctgactaattt
ttttattatgacagggccgagggcctcggcctctgagctattccagaagtagtgaggaggtttttggaggcctaggcttttgcaaaaagctgg
cgagatttcaggagtaaggaaagctaaaatggagaaaaaactactggatataaccaccgttgatatacccattggcagctgaaagaacattttgag
gcatctcagtcagttgctcaatgtacctataaccagaccgtcagctggatattacggccttttaagaccgtaaagaaaaataagcacaagtttatcc
ggcctttatcacattctgccgcctgatgaatgctcaccggaattccgtatggcaatgaaagacgggtgagctggtgatatgggatagttacc
ttgttacaccgtttccatgagcaaacgtgaaacgttttcatcgtctgagtgatgaaaccagcagattccggcagtttctacacataatctgcaagatgt
ggcgtgttacggtgaaaacctggcctatttcctaaagggttattgagaatattttctgctcagccaatccctgggtgagtttaccagtttgattta
aacgtggccaatatggacaacttctcggccccgtttaccatgggcaatattatacgaaggcgacaaggtgctgatccgctggcgattcagg
ttcatcatgccgtttgtgatggcttccatgtggcagaatgcttaatgaattacaacagctactgcgatgagtgagggcgggggcgtaatTTTTAagg
cagttattggtgcccttaaacgctggtgctacgctgaataagtataataagcggatgaatggcagaaatcggcgatctttgtgaaggaaactt
acttctgtggtgtgacataattggacaactacctacagattaaagctctaaggtaataataaaatttttaaggtataatgtgtaaactactgattct
aattgtttgtgatttttagattccaacctatggaactgatgaatgggagcagtggtggaatgccfttaatgaggaaaacctgtttgctcagaagaaatgc
catctagtgatgataggctactgctactctcaactctactcctcaaaaaaagaagagaaggtagaagacccaaggactttcctcagaattg
ctaagttttgagtcagctgtgttttagtaatagaactcttctgctttgctatttacaccacaaaggaaaaagctgactgctatacaagaaaattatgg
aaaaatattctgaacctttataagtaggcataacagttataatcataactgttttttctactccacacaggeatagagtgctgctattaataactat
gctcaaaaattgtgaccttttagcttttaattgtaaaggggtaataaggaatatttgatgtatagtccttgactagagatcataatcagccataccaca
tttagaggtttactgtcttaaaaaacctcccacacctccccgaacctgaacataaaaatgaatgcaattgttgttgaactgtttattgagctta
taattggttacaataaagcaatagcatcacaatttcacaataaagcattttttcactgcattctagttgtggtttgtccaaactcatcaatgtatctatc

atgtctggatcgatcttcggaacttggccaaatcgtaatcatgcatagctgttctctgtgaaattgftatccgctcacaattccacacaacatacga
gccggagcataaagtgtaaagcctgggggtgcctaataagtgagtgactaactcacattaattgcgttgcgctcactgcccgcttccagtcgggaaacc
tgcgtgccagctgcattaatgaatcggccaacgcgcggggagagggcggttgcgtattggcgctcttccgcttctcctcgtcactgactcgtgcg
ctcggctgctcggctcggcgagcgggtatcagctcactcaaaaggcggttaatacggttatccacagaatcaggggataacgcaggaaagaacatgt
gagcaaaaggccagcaaaaggccaggaaccgtaaaaaggccgcgttgcggttttccataggctccgccccctgacgagcatcacaaaa
tcgacgctcaagtcagaggtggcgaaccgacaggactataaagataaccaggcgttcccccctggaagctccctcgtgcgctcctctgttccgac
cctgccgcttaccggatacctgtccgccttctccctcgggaagcgtggcgcttctcatagctcacgctgtaggtatctcagttcgggtgtaggtcgtt
cgtccaagctgggctgtgtgacgaacccccgttcagcccagccgctgcgccttatccggtaactatcgtcttgagccaaccggtaagacac
gactatgccactggcagcagccactggtaacaggattagcagagcagggatgtagggcgtgctacagagtcttgaagtggggcctaactac
ggctacactagaagaacagatatttggatctgcgctctgtgaagccagttacctcggaaaaagagttggtagctcttgatccggcaacaaccac
cgctggtagcgggtggttttttgttgaagcagcagattacgcgcagaaaaaaaggatctcaagaagatccttggatcttctacggggtcgtgacgt
cagtggaacgaaaactcacgttaagggatttggctatgagattataaaaaggatctcacctagatccttttaataaaaatgaagttttaaataat
ctaaagtatatatgagtaaaactggctgacagttaccaatgcttaatcagtgaggcacctatctcagcgtctgtctatttctgtcaccatagttgctg
actccccgtcgtgtagataactacgatacgggagggccttaccatctggccccagtgctgcaatgataccgcgagaccacgctcaccggctccag
atttatcagcaataaaccagccagccggaaggccgagcgcagaagtggtcctgcaactttatccgctccatccagctattattgttccgggga
agctagagtaagtagttccagtttaatttgcgcaacgttggcattgctacagcattcgtggtgacgctcgtcgttggtaggttcattca
gctccggtccaacgatcaaggcgagttacatgatccccatgttgtgcaaaaaagcggtagctcctcggctcctccgacggtgacagaagtaag
ttggccgagtggtatcactcatggtatggcagcactgcataattcttactgtcatgccaatccgtaagatgcttttctgtgactggtgagtaactaac
aagtcattctgagaatagtgatgcggcgaccgagttgctcttcccggcgtcaatacgggataataccgcgccacatacagaactttaaagtgtc
atcattggaacgttctcggggcgaaaactctcaaggatctaccgctgtgagatccagttcgtgtaaccactcgtgacccaactgatctca
gcatctttactttcaccagcg

green: GFP, grey: 1D4 peptide (tag), dark grey: strep tag, red: tetO sequence, yellow: CMV promoter,
partial, pink: 3C precision protease, blue: NheI/ NotI cleavage site

REFERENCES

1. Pierce, K.L., R.T. Premont, and R.J. Lefkowitz, *Seven-transmembrane receptors*. *Nat Rev Mol Cell Biol*, 2002. **3**(9): p. 639-50.
2. Tautermann, C.S., *GPCR structures in drug design, emerging opportunities with new structures*. *Bioorg Med Chem Lett*, 2014. **24**(17): p. 4073-9.
3. Cherezov, V., et al., *High-resolution crystal structure of an engineered human beta2-adrenergic G protein-coupled receptor*. *Science*, 2007. **318**(5854): p. 1258-65.
4. Rasmussen, S.G., et al., *Crystal structure of the human beta2 adrenergic G-protein-coupled receptor*. *Nature*, 2007. **450**(7168): p. 383-7.
5. Stevens, R.C., V. Cherezov, V. Katritch, R. Abagyan, P. Kuhn, H. Rosen, and K. Wuthrich, *The GPCR Network: a large-scale collaboration to determine human GPCR structure and function*. *Nat Rev Drug Discov*, 2013. **12**(1): p. 25-34.
6. Venkatakrishnan, A.J., X. Deupi, G. Lebon, C.G. Tate, G.F. Schertler, and M.M. Babu, *Molecular signatures of G-protein-coupled receptors*. *Nature*, 2013. **494**(7436): p. 185-94.
7. Tate, C.G., *A crystal clear solution for determining G-protein-coupled receptor structures*. *Trends Biochem Sci*, 2012. **37**(9): p. 343-52.
8. Rajagopal, S., K. Rajagopal, and R.J. Lefkowitz, *Teaching old receptors new tricks: biasing seven-transmembrane receptors*. *Nat Rev Drug Discov*, 2010. **9**(5): p. 373-86.
9. Kobilka, B.K., *G protein coupled receptor structure and activation*. *Biochim Biophys Acta*, 2007. **1768**(4): p. 794-807.
10. Alexander, S.P., et al., *The Concise Guide to PHARMACOLOGY 2015/16: G protein-coupled receptors*. *Br J Pharmacol*, 2015. **172**(24): p. 5744-869.
11. Fang, Y., T. Kenakin, and C. Liu, *Editorial: Orphan GPCRs As Emerging Drug Targets*. *Front Pharmacol*, 2015. **6**: p. 295.
12. Xiang, J., E. Chun, C. Liu, L. Jing, Z. Al-Sahouri, L. Zhu, and W. Liu, *Successful Strategies to Determine High-Resolution Structures of GPCRs*. *Trends Pharmacol Sci*, 2016.
13. Kruse, A.C., et al., *Structure and dynamics of the M3 muscarinic acetylcholine receptor*. *Nature*, 2012. **482**(7386): p. 552-6.
14. Dror, R.O., A.C. Pan, D.H. Arlow, D.W. Borhani, P. Maragakis, Y. Shan, H. Xu, and D.E. Shaw, *Pathway and mechanism of drug binding to G-protein-coupled receptors*. *Proc Natl Acad Sci U S A*, 2011. **108**(32): p. 13118-23.
15. Gonzalez, A., T. Perez-Acle, L. Pardo, and X. Deupi, *Molecular basis of ligand dissociation in beta-adrenergic receptors*. *PLoS One*, 2011. **6**(9): p. e23815.
16. Manglik, A., et al., *Crystal structure of the micro-opioid receptor bound to a morphinan antagonist*. *Nature*, 2012. **485**(7398): p. 321-6.
17. Madabushi, S., A.K. Gross, A. Philippi, E.C. Meng, T.G. Wensel, and O. Lichtarge, *Evolutionary trace of G protein-coupled receptors reveals clusters of residues that determine global and class-specific functions*. *J Biol Chem*, 2004. **279**(9): p. 8126-32.
18. Rasmussen, S.G., et al., *Crystal structure of the beta2 adrenergic receptor-Gs protein complex*. *Nature*, 2011. **477**(7366): p. 549-55.
19. Deupi, X., P. Edwards, A. Singhal, B. Nickle, D. Oprian, G. Schertler, and J. Standfuss, *Stabilized G protein binding site in the structure of constitutively active metarhodopsin-II*. *Proc Natl Acad Sci U S A*, 2012. **109**(1): p. 119-24.
20. Jaakola, V.P., J. Prilusky, J.L. Sussman, and A. Goldman, *G protein-coupled receptors show unusual patterns of intrinsic unfolding*. *Protein Eng Des Sel*, 2005. **18**(2): p. 103-10.
21. Butcher, A.J., K.C. Kong, R. Prihandoko, and A.B. Tobin, *Physiological role of G-protein coupled receptor phosphorylation*. *Handb Exp Pharmacol*, 2012(208): p. 79-94.
22. Qin, K., C. Dong, G. Wu, and N.A. Lambert, *Inactive-state preassembly of G(q)-coupled receptors and G(q) heterotrimers*. *Nat Chem Biol*, 2011. **7**(10): p. 740-7.

23. Nobles, K.N., et al., *Distinct phosphorylation sites on the beta(2)-adrenergic receptor establish a barcode that encodes differential functions of beta-arrestin*. *Sci Signal*, 2011. **4**(185): p. ra51.
24. Brueckner, F., C.L. Piscitelli, C.J. Tsai, J. Standfuss, X. Deupi, and G.F. Schertler, *Structure of beta-adrenergic receptors*. *Methods Enzymol*, 2013. **520**: p. 117-51.
25. Malbon, C.C. and H.-y. Wang, *Adrenergic Receptors*, in *eLS*. 2001, John Wiley & Sons, Ltd.
26. Lands, A.M., A. Arnold, J.P. McAuliff, F.P. Luduena, and T.G. Brown, Jr., *Differentiation of receptor systems activated by sympathomimetic amines*. *Nature*, 1967. **214**(5088): p. 597-8.
27. Ahlquist, R.P., *A study of the adrenotropic receptors*. *Am J Physiol*, 1948. **153**(3): p. 586-600.
28. Berthelsen, S. and W.A. Pettinger, *A functional basis for classification of alpha-adrenergic receptors*. *Life Sci*, 1977. **21**(5): p. 595-606.
29. Bylund, D.B., D.C. Eikenberg, J.P. Hieble, S.Z. Langer, R.J. Lefkowitz, K.P. Minneman, P.B. Molinoff, R.R. Ruffolo, Jr., and U. Trendelenburg, *International Union of Pharmacology nomenclature of adrenoceptors*. *Pharmacol Rev*, 1994. **46**(2): p. 121-36.
30. Strosberg, A.D., *Structure, function, and regulation of adrenergic receptors*. *Protein Sci*, 1993. **2**(8): p. 1198-209.
31. Patel, C.B., N. Noor, and H.A. Rockman, *Functional selectivity in adrenergic and angiotensin signaling systems*. *Mol Pharmacol*, 2010. **78**(6): p. 983-92.
32. Golan, D.E., *Principles of pharmacology the pathophysiologic basis of drug therapy*. 3rd ed. Monographs in population biology. 2012, Philadelphia: Wolters Kluwer/Lippincott Williams & Wilkins. 954 S.
33. Baker, J.G., I.P. Hall, and S.J. Hill, *Agonist and inverse agonist actions of beta-blockers at the human beta 2-adrenoceptor provide evidence for agonist-directed signaling*. *Mol Pharmacol*, 2003. **64**(6): p. 1357-69.
34. Heidenreich, P.A., K.M. McDonald, T. Hastie, B. Fadel, V. Hagan, B.K. Lee, and M.A. Hlatky, *Meta-analysis of trials comparing beta-blockers, calcium antagonists, and nitrates for stable angina*. *JAMA*, 1999. **281**(20): p. 1927-36.
35. Morgan, T.O., A.I. Anderson, and R.J. MacInnis, *ACE inhibitors, beta-blockers, calcium blockers, and diuretics for the control of systolic hypertension*. *Am J Hypertens*, 2001. **14**(3): p. 241-7.
36. Port, J.D. and M.R. Bristow, *Altered beta-adrenergic receptor gene regulation and signaling in chronic heart failure*. *J Mol Cell Cardiol*, 2001. **33**(5): p. 887-905.
37. Moraes, I., G. Evans, J. Sanchez-Weatherby, S. Newstead, and P.D. Stewart, *Membrane protein structure determination - the next generation*. *Biochim Biophys Acta*, 2014. **1838**(1 Pt A): p. 78-87.
38. Rosenbaum, D.M., S.G. Rasmussen, and B.K. Kobilka, *The structure and function of G-protein-coupled receptors*. *Nature*, 2009. **459**(7245): p. 356-63.
39. Fredriksson, R., M.C. Lagerstrom, L.G. Lundin, and H.B. Schioth, *The G-protein-coupled receptors in the human genome form five main families. Phylogenetic analysis, paralogon groups, and fingerprints*. *Mol Pharmacol*, 2003. **63**(6): p. 1256-72.
40. Warne, T., M.J. Serrano-Vega, J.G. Baker, R. Moukhametzianov, P.C. Edwards, R. Henderson, A.G. Leslie, C.G. Tate, and G.F. Schertler, *Structure of a beta1-adrenergic G-protein-coupled receptor*. *Nature*, 2008. **454**(7203): p. 486-91.
41. Lebon, G., T. Warne, P.C. Edwards, K. Bennett, C.J. Langmead, A.G. Leslie, and C.G. Tate, *Agonist-bound adenosine A2A receptor structures reveal common features of GPCR activation*. *Nature*, 2011. **474**(7352): p. 521-5.
42. Dore, A.S., et al., *Structure of the adenosine A(2A) receptor in complex with ZM241385 and the xanthines XAC and caffeine*. *Structure*, 2011. **19**(9): p. 1283-93.
43. Rosenbaum, D.M., et al., *GPCR engineering yields high-resolution structural insights into beta2-adrenergic receptor function*. *Science*, 2007. **318**(5854): p. 1266-73.

44. Chun, E., et al., *Fusion partner toolchest for the stabilization and crystallization of G protein-coupled receptors*. Structure, 2012. **20**(6): p. 967-76.
45. Thompson, A.A., et al., *Structure of the nociceptin/orphanin FQ receptor in complex with a peptide mimetic*. Nature, 2012. **485**(7398): p. 395-9.
46. Hino, T., et al., *G-protein-coupled receptor inactivation by an allosteric inverse-agonist antibody*. Nature, 2012. **482**(7384): p. 237-40.
47. Rasmussen, S.G., et al., *Structure of a nanobody-stabilized active state of the beta(2) adrenoceptor*. Nature, 2011. **469**(7329): p. 175-80.
48. Caffrey, M., *Crystallizing membrane proteins for structure determination: use of lipidic mesophases*. Annu Rev Biophys, 2009. **38**: p. 29-51.
49. Bill, R.M., et al., *Overcoming barriers to membrane protein structure determination*. Nat Biotechnol, 2011. **29**(4): p. 335-40.
50. Kobilka, B. and G.F. Schertler, *New G-protein-coupled receptor crystal structures: insights and limitations*. Trends Pharmacol Sci, 2008. **29**(2): p. 79-83.
51. Jaakola, V.P., M.T. Griffith, M.A. Hanson, V. Cherezov, E.Y. Chien, J.R. Lane, A.P. Ijzerman, and R.C. Stevens, *The 2.6 angstrom crystal structure of a human A2A adenosine receptor bound to an antagonist*. Science, 2008. **322**(5905): p. 1211-7.
52. Siu, F.Y., et al., *Structure of the human glucagon class B G-protein-coupled receptor*. Nature, 2013. **499**(7459): p. 444-9.
53. Hollenstein, K., J. Kean, A. Bortolato, R.K. Cheng, A.S. Dore, A. Jazayeri, R.M. Cooke, M. Weir, and F.H. Marshall, *Structure of class B GPCR corticotropin-releasing factor receptor 1*. Nature, 2013. **499**(7459): p. 438-43.
54. Dore, A.S., et al., *Structure of class C GPCR metabotropic glutamate receptor 5 transmembrane domain*. Nature, 2014. **511**(7511): p. 557-62.
55. Wu, H., et al., *Structure of a class C GPCR metabotropic glutamate receptor 1 bound to an allosteric modulator*. Science, 2014. **344**(6179): p. 58-64.
56. Wang, C., et al., *Structure of the human smoothed receptor bound to an antitumour agent*. Nature, 2013. **497**(7449): p. 338-43.
57. Schlinkmann, K.M. and A. Pluckthun, *Directed evolution of G-protein-coupled receptors for high functional expression and detergent stability*. Methods Enzymol, 2013. **520**: p. 67-97.
58. Milic, D. and D.B. Veprintsev, *Large-scale production and protein engineering of G protein-coupled receptors for structural studies*. Front Pharmacol, 2015. **6**: p. 66.
59. Park, S.H., et al., *Structure of the chemokine receptor CXCR1 in phospholipid bilayers*. Nature, 2012. **491**(7426): p. 779-83.
60. Egloff, P., et al., *Structure of signaling-competent neurotensin receptor 1 obtained by directed evolution in Escherichia coli*. Proc Natl Acad Sci U S A, 2014. **111**(6): p. E655-62.
61. Tobin, A.B., *G-protein-coupled receptor phosphorylation: where, when and by whom*. Br J Pharmacol, 2008. **153 Suppl 1**: p. S167-76.
62. Zuckerman, D.M., S.W. Hicks, G. Charron, H.C. Hang, and C.E. Machamer, *Differential regulation of two palmitoylation sites in the cytoplasmic tail of the beta1-adrenergic receptor*. J Biol Chem, 2011. **286**(21): p. 19014-23.
63. Bertheleme, N., P.S. Chae, S. Singh, D. Mossakowska, M.M. Hann, K.J. Smith, J.A. Hubbard, S.J. Dowell, and B. Byrne, *Unlocking the secrets of the gatekeeper: methods for stabilizing and crystallizing GPCRs*. Biochim Biophys Acta, 2013. **1828**(11): p. 2583-91.
64. Parker, E.M. and E.M. Ross, *Truncation of the extended carboxyl-terminal domain increases the expression and regulatory activity of the avian beta-adrenergic receptor*. J Biol Chem, 1991. **266**(15): p. 9987-96.
65. Sonoda, Y., et al., *Benchmarking membrane protein detergent stability for improving throughput of high-resolution X-ray structures*. Structure, 2011. **19**(1): p. 17-25.

66. Hattori, M., R.E. Hibbs, and E. Gouaux, *A fluorescence-detection size-exclusion chromatography-based thermostability assay for membrane protein precrystallization screening*. *Structure*, 2012. **20**(8): p. 1293-9.
67. Drew, D.E., G. von Heijne, P. Nordlund, and J.W. de Gier, *Green fluorescent protein as an indicator to monitor membrane protein overexpression in Escherichia coli*. *FEBS Lett*, 2001. **507**(2): p. 220-4.
68. Drew, D., et al., *A scalable, GFP-based pipeline for membrane protein overexpression screening and purification*. *Protein Sci*, 2005. **14**(8): p. 2011-7.
69. Drew, D., M. Lerch, E. Kunji, D.J. Slotboom, and J.W. de Gier, *Optimization of membrane protein overexpression and purification using GFP fusions*. *Nat Methods*, 2006. **3**(4): p. 303-13.
70. Drew, D., S. Newstead, Y. Sonoda, H. Kim, G. von Heijne, and S. Iwata, *GFP-based optimization scheme for the overexpression and purification of eukaryotic membrane proteins in Saccharomyces cerevisiae*. *Nat Protoc*, 2008. **3**(5): p. 784-98.
71. Zhang, X., R.C. Stevens, and F. Xu, *The importance of ligands for G protein-coupled receptor stability*. *Trends Biochem Sci*, 2015. **40**(2): p. 79-87.
72. Liu, W., et al., *Structural basis for allosteric regulation of GPCRs by sodium ions*. *Science*, 2012. **337**(6091): p. 232-6.
73. Wang, C., et al., *Structural basis for molecular recognition at serotonin receptors*. *Science*, 2013. **340**(6132): p. 610-4.
74. Wacker, D., et al., *Structural features for functional selectivity at serotonin receptors*. *Science*, 2013. **340**(6132): p. 615-9.
75. Zhang, J., et al., *Agonist-bound structure of the human P2Y12 receptor*. *Nature*, 2014. **509**(7498): p. 119-22.
76. Wang, C., et al., *Structural basis for Smoothed receptor modulation and chemoresistance to anticancer drugs*. *Nat Commun*, 2014. **5**: p. 4355.
77. Tan, Q., et al., *Structure of the CCR5 chemokine receptor-HIV entry inhibitor maraviroc complex*. *Science*, 2013. **341**(6152): p. 1387-90.
78. Zhang, D., et al., *Two disparate ligand-binding sites in the human P2Y1 receptor*. *Nature*, 2015. **520**(7547): p. 317-21.
79. Yin, J., J.C. Mobarec, P. Kolb, and D.M. Rosenbaum, *Crystal structure of the human OX2 orexin receptor bound to the insomnia drug suvorexant*. *Nature*, 2015. **519**(7542): p. 247-50.
80. Yin, J., et al., *Structure and ligand-binding mechanism of the human OX1 and OX2 orexin receptors*. *Nat Struct Mol Biol*, 2016. **23**(4): p. 293-9.
81. Thal, D.M., et al., *Crystal structures of the M1 and M4 muscarinic acetylcholine receptors*. *Nature*, 2016. **531**(7594): p. 335-40.
82. Serrano-Vega, M.J., F. Magnani, Y. Shibata, and C.G. Tate, *Conformational thermostabilization of the beta1-adrenergic receptor in a detergent-resistant form*. *Proc Natl Acad Sci U S A*, 2008. **105**(3): p. 877-82.
83. Magnani, F., Y. Shibata, M.J. Serrano-Vega, and C.G. Tate, *Co-evolving stability and conformational homogeneity of the human adenosine A2a receptor*. *Proc Natl Acad Sci U S A*, 2008. **105**(31): p. 10744-9.
84. Steyaert, J. and B.K. Kobilka, *Nanobody stabilization of G protein-coupled receptor conformational states*. *Curr Opin Struct Biol*, 2011. **21**(4): p. 567-72.
85. Kobilka, B.K. and X. Deupi, *Conformational complexity of G-protein-coupled receptors*. *Trends Pharmacol Sci*, 2007. **28**(8): p. 397-406.
86. Maeda, S., et al., *Crystallization scale preparation of a stable GPCR signaling complex between constitutively active rhodopsin and G-protein*. *PLoS One*, 2014. **9**(6): p. e98714.
87. Lebon, G., T. Warne, and C.G. Tate, *Agonist-bound structures of G protein-coupled receptors*. *Curr Opin Struct Biol*, 2012. **22**(4): p. 482-90.

88. Alexandrov, A.I., M. Mileni, E.Y. Chien, M.A. Hanson, and R.C. Stevens, *Microscale fluorescent thermal stability assay for membrane proteins*. *Structure*, 2008. **16**(3): p. 351-9.
89. Deupi, X. and J. Standfuss, *Structural insights into agonist-induced activation of G-protein-coupled receptors*. *Curr Opin Struct Biol*, 2011. **21**(4): p. 541-51.
90. Palczewski, K., et al., *Crystal structure of rhodopsin: A G protein-coupled receptor*. *Science*, 2000. **289**(5480): p. 739-45.
91. Okada, T., I. Le Trong, B.A. Fox, C.A. Behnke, R.E. Stenkamp, and K. Palczewski, *X-Ray diffraction analysis of three-dimensional crystals of bovine rhodopsin obtained from mixed micelles*. *J Struct Biol*, 2000. **130**(1): p. 73-80.
92. Okada, T., M. Sugihara, A.N. Bondar, M. Elstner, P. Entel, and V. Buss, *The retinal conformation and its environment in rhodopsin in light of a new 2.2 Å crystal structure*. *J Mol Biol*, 2004. **342**(2): p. 571-83.
93. Edwards, P.C., J. Li, M. Burghammer, J.H. McDowell, C. Villa, P.A. Hargrave, and G.F. Schertler, *Crystals of native and modified bovine rhodopsins and their heavy atom derivatives*. *J Mol Biol*, 2004. **343**(5): p. 1439-50.
94. Salom, D., I. Le Trong, E. Pohl, J.A. Ballesteros, R.E. Stenkamp, K. Palczewski, and D.T. Lodowski, *Improvements in G protein-coupled receptor purification yield light stable rhodopsin crystals*. *J Struct Biol*, 2006. **156**(3): p. 497-504.
95. Standfuss, J., G. Xie, P.C. Edwards, M. Burghammer, D.D. Oprian, and G.F. Schertler, *Crystal structure of a thermally stable rhodopsin mutant*. *J Mol Biol*, 2007. **372**(5): p. 1179-88.
96. Murakami, M. and T. Kouyama, *Crystal structure of squid rhodopsin*. *Nature*, 2008. **453**(7193): p. 363-7.
97. Park, J.H., P. Scheerer, K.P. Hofmann, H.W. Choe, and O.P. Ernst, *Crystal structure of the ligand-free G-protein-coupled receptor opsin*. *Nature*, 2008. **454**(7201): p. 183-7.
98. Choe, H.W., Y.J. Kim, J.H. Park, T. Morizumi, E.F. Pai, N. Krauss, K.P. Hofmann, P. Scheerer, and O.P. Ernst, *Crystal structure of metarhodopsin II*. *Nature*, 2011. **471**(7340): p. 651-5.
99. Shimamura, T., K. Hiraki, N. Takahashi, T. Hori, H. Ago, K. Masuda, K. Takio, M. Ishiguro, and M. Miyano, *Crystal structure of squid rhodopsin with intracellularly extended cytoplasmic region*. *J Biol Chem*, 2008. **283**(26): p. 17753-6.
100. Warne, T., M.J. Serrano-Vega, C.G. Tate, and G.F. Schertler, *Development and crystallization of a minimal thermostabilised G protein-coupled receptor*. *Protein Expr Purif*, 2009. **65**(2): p. 204-13.
101. Warne, T., R. Moukhametzianov, J.G. Baker, R. Nehme, P.C. Edwards, A.G. Leslie, G.F. Schertler, and C.G. Tate, *The structural basis for agonist and partial agonist action on a beta(1)-adrenergic receptor*. *Nature*, 2011. **469**(7329): p. 241-4.
102. Moukhametzianov, R., T. Warne, P.C. Edwards, M.J. Serrano-Vega, A.G. Leslie, C.G. Tate, and G.F. Schertler, *Two distinct conformations of helix 6 observed in antagonist-bound structures of a beta1-adrenergic receptor*. *Proc Natl Acad Sci U S A*, 2011. **108**(20): p. 8228-32.
103. Lebon, G., K. Bennett, A. Jazayeri, and C.G. Tate, *Thermostabilisation of an agonist-bound conformation of the human adenosine A(2A) receptor*. *J Mol Biol*, 2011. **409**(3): p. 298-310.
104. Ujwal, R. and J.U. Bowie, *Crystallizing membrane proteins using lipidic bicelles*. *Methods*, 2011. **55**(4): p. 337-41.
105. Landau, E.M. and J.P. Rosenbusch, *Lipidic cubic phases: a novel concept for the crystallization of membrane proteins*. *Proc Natl Acad Sci U S A*, 1996. **93**(25): p. 14532-5.
106. Pebay-Peyroula, E., G. Rummel, J.P. Rosenbusch, and E.M. Landau, *X-ray structure of bacteriorhodopsin at 2.5 angstroms from microcrystals grown in lipidic cubic phases*. *Science*, 1997. **277**(5332): p. 1676-81.
107. Luecke, H., B. Schobert, H.T. Richter, J.P. Cartailler, and J.K. Lanyi, *Structure of bacteriorhodopsin at 1.55 Å resolution*. *J Mol Biol*, 1999. **291**(4): p. 899-911.
108. Kolbe, M., H. Besir, L.O. Essen, and D. Oesterhelt, *Structure of the light-driven chloride pump halorhodopsin at 1.8 Å resolution*. *Science*, 2000. **288**(5470): p. 1390-6.

109. Li, D., J. Lee, and M. Caffrey, *Crystallizing Membrane Proteins in Lipidic Mesophases. A Host Lipid Screen*. Cryst Growth Des, 2011. **11**(2): p. 530-537.
110. Caffrey, M. and V. Cherezov, *Crystallizing membrane proteins using lipidic mesophases*. Nat Protoc, 2009. **4**(5): p. 706-31.
111. Caffrey, M., *A comprehensive review of the lipid cubic phase or in meso method for crystallizing membrane and soluble proteins and complexes*. Acta Crystallogr F Struct Biol Commun, 2015. **71**(Pt 1): p. 3-18.
112. Caffrey, M. and C. Porter, *Crystallizing Membrane Proteins for Structure Determination using Lipidic Mesophases*. Journal of Visualized Experiments : JoVE, 2010(45): p. 1712.
113. Li, D., C. Boland, D. Aragao, K. Walsh, and M. Caffrey, *Harvesting and Cryo-cooling Crystals of Membrane Proteins Grown in Lipidic Mesophases for Structure Determination by Macromolecular Crystallography*. Journal of Visualized Experiments : JoVE, 2012(67): p. 4001.
114. Li, D., C. Boland, K. Walsh, and M. Caffrey, *Use of a Robot for High-throughput Crystallization of Membrane Proteins in Lipidic Mesophases*. Journal of Visualized Experiments : JoVE, 2012(67): p. 4000.
115. Aherne, M., J.A. Lyons, and M. Caffrey, *A fast, simple and robust protocol for growing crystals in the lipidic cubic phase*. J Appl Crystallogr, 2012. **45**(Pt 6): p. 1330-1333.
116. Hanson, M.A., V. Cherezov, M.T. Griffith, C.B. Roth, V.P. Jaakola, E.Y. Chien, J. Velasquez, P. Kuhn, and R.C. Stevens, *A specific cholesterol binding site is established by the 2.8 Å structure of the human beta2-adrenergic receptor*. Structure, 2008. **16**(6): p. 897-905.
117. Serrano-Vega, M.J. and C.G. Tate, *Transferability of thermostabilizing mutations between β -adrenergic receptors*. Molecular Membrane Biology, 2009. **26**(8): p. 385-396.
118. Ballesteros, J.A. and H. Weinstein, *[19] Integrated methods for the construction of three-dimensional models and computational probing of structure-function relations in G protein-coupled receptors*, in *Methods in Neurosciences*, C.S. Stuart, Editor. 1995, Academic Press. p. 366-428.
119. Miller, J.L. and C.G. Tate, *Engineering an ultra-thermostable beta(1)-adrenoceptor*. J Mol Biol, 2011. **413**(3): p. 628-38.
120. Dodevski, I. and A. Pluckthun, *Evolution of three human GPCRs for higher expression and stability*. J Mol Biol, 2011. **408**(4): p. 599-615.
121. Munk, C., et al., *GPCRdb: the G protein-coupled receptor database - an introduction*. Br J Pharmacol, 2016. **173**(14): p. 2195-207.
122. Isberg, V., et al., *GPCRdb: an information system for G protein-coupled receptors*. Nucleic Acids Res, 2016.
123. Warne, T., J. Chirnside, and G.F. Schertler, *Expression and purification of truncated, non-glycosylated turkey beta-adrenergic receptors for crystallization*. Biochim Biophys Acta, 2003. **1610**(1): p. 133-40.
124. Feroz, H., et al., *Concentrating membrane proteins using ultrafiltration without concentrating detergents*. Biotechnol Bioeng, 2016. **113**(10): p. 2122-30.
125. Eddy, M.T., T. Didenko, R.C. Stevens, and K. Wuthrich, *beta2-Adrenergic Receptor Conformational Response to Fusion Protein in the Third Intracellular Loop*. Structure, 2016.

Ziva Vuckovic Mueller curriculum vitae

PERSONAL DETAILS

Name: Ziva Vuckovic Mueller
Address: Albisriederstrasse 54
8003 Zurich
Switzerland
Mobile: +41 79 851 36 08
E-mail: ziva.vuckovic@psi.ch
Date of birth: 30 July 1987
Nationality Slovenian
Languages: Slovene (mother tongue)
English (fluent)
German (moderate)

EDUCATION

2013- present **PhD student in Structural Biology**
Department of Biology, Swiss Federal Institute of Technology Zurich
(ETHZ) and Paul Scherrer Institut

2006- 2012 **Master of Science in Biochemistry**, University of Ljubljana, Slovenia
Master thesis: "Introduction of automated cell counting procedure in
biotechnological processes and specific monoclonal antibody production
follow up."

RESEARCH EXPERIENCE

Apr. 2012- Jul. 2012 **Trainee**, Paul Scherrer Institut, Switzerland with Prof. Ballmer-Hofer
Producing co-crystallisation partners for vascular endothelial growth
factor receptor.

Jul. 2011- Mar. 2012 **Diploma final thesis work**, Blood Transfusion Centre of Slovenia,
Slovenia with Prof. Curin-Serbec

Sep. 2010- Mar. 2011 **Trainee**, Mawson Institute, Australia
Research project: Drug delivery from contact lenses.

Jun. 2007- Aug. 2007 **Summer student**, National Institute of Chemistry, Ljubljana
Protein purification support

Jun. 2006- Aug. 2006 **Summer student**, National Institute of Chemistry, Ljubljana
Protein purification support

SCHOLARSHIPS AND AWARDS

- Dec. 2015** **Conference travel grant from Life sciences society (LS2) Switzerland**
for attending the GPCR workshop
- Jan. 2013- present** **Marie Curie initial training network scholarship** (Nanomem)
- Sep. 2002- Sep. 2011** **Zois scholarship** for gifted students, awarded by Republic of Slovenia

POSTERS AND TALKS

- GPCR Workshop, USA, December 2015 (**Poster**)
- Retreat of Biomolecular Structure and Mechanism, Switzerland, June 2015 (**Poster**)
- Nanomem Mid-term meeting, Belgium, November 2014 (**Talk**)
- Retreat of Biomolecular Structure and Mechanism, Switzerland, August 2014 (**Poster**)

PUBLICATIONS

Heydenreich FM*, Vuckovic Z*, Matkovic M and Veprintsev DB (2015) **Stabilisation of G protein-coupled receptors by point mutations.** *Front. Pharmacol.* 6:82. doi: 10.3389/fphar.2015.00082

*joined first authors

INTERESTS

Running, climbing, paragliding, travelling